Universität Rostock

Traditio et Innovatio

Department of Waste Management and Material Flow

Rostock University

ELECTRICAL POWER GENERATION FROM RESIDUAL BIOMASS BY COMBUSTION IN EXTERNALLY FIRED GAS TURBINES (EFGT)

DISSERTATION

Submitted in the fulfillment of the requirements of

The Academic Board of Rostock University

Faculty of Agriculture and Environmental Sciences

For the Degree of DOCTOR of Engineering (Dr.-Ing.)

Mathhar A. A. Bdour

Born in Irbid 30.05.1987, Jordan

Rostock-Germany

2017

Gutachter:

1. Gutachter:

   Prof. Michael Nelles

   Universität Rostock, AUF, Inhaber des Lehrstuhls -Abfall-und Stoffstromwirtschaft

2. Gutachter:

   Dr.-Ing. Andreas Ortwein

   DBFZ Deutsches Biomasseforschungszentrum gemeinnützige GmbH, Bereich Thermo-chemische Konversion (TK), Arbeitsgruppenleiter Bedarfsgerechte Kraft-Wärme-Kopplung

3. Gutachter:

   Dr.-Ing. Mohammad Al-Addous

   The German Jordanian University, The School of Natural Resources Engineering and Management (SNREM, Energy Engineering Department

Datum der Einreichung: 13.03.2017

Datum der Verteidigung: 29.06.2017

Summary

As biofuels started to have an important position in the world, it is worth to investigate the more efficient and effective way to exploit this source in developing and even industrial countries. Thermochemical conversion of biomass is considered as the most common way of energy utilization. At the same time, externally fired gas turbine plants appear as a rising technology in energy utilization from solid fuels. Integrating both direct combustion as one of the thermochemical processes and externally fired gas turbine technology is implemented in this research.

Externally fired gas turbine technology application in providing energy as a distributed generation plants improves electrical grid. For instance, share in energy supply in peak periods, decrease transmission lines losses, and other technical aspects. Moreover, this type of energy has more reliability than some other traditional renewables, because it doesn't depend on the weather changes like wind and solar energy. The technology is capable to use several types of biomass including agricultural residues, thus allowing for a broad field of application.

However, its application in the small range is still not commercialized. To improve concept development, optimum design parameters, plant flexibility, and technical description are discussed for the very small range, considering also resulting efficiency losses.

Externally fired gas turbine plant has the advantage of solid fuel flexibility. However, its performance is highly dependable on the selection of components. High temperatures, high rotational speed, and pellets feeding mechanism as well as ash are important aspects that should be carefully managed. This adds extra cost on the total investment, the thing that affects plant competition.

Plant performance is tested under several conditions for better technical overview. Heat exchanger temperature difference (e.g. due to accumulated dirt) shows a considerable effect on the produced electrical power. This means a continuous cleaning is important to keep maximizing heat transfer though the heat exchanger, and turbine inlet temperature. It is also seen that the transient response of the plant is relatively slow, in addition to small fluctuations in steady state operation. This is related to the combustion behavior of solid fuel. Thus,

combustion process is currently the limiting factor for flexible operation of externally fired gas turbines.

Mechanical power delivered from turbine and consumed from compressor is highly depending on isentropic efficiencies of both units and on temperature values at turbine inlet. For the reference case, compressor to turbine power is 67%, this is an indicator that compressor consumes relatively high power which reduces the delivered net power from the cycle. Higher output electrical power could be achieved when dealing with higher efficiencies for these components, as well as the electrical generator efficiency.

Pressure and air mass flow through the clean cycle side are optimized to provide the maximum power. It is noticed that air mass flow is relatively small, around 0.02 kg/s for the reference case steady state. Such small mass flow requires small compressor and turbine sizes as well. Operating pressure ratio is registered to be around 3.5 for the reference case. Both values are mapped as a function of turbine inlet temperature.

To accomplish the concept of flexibility, hardware-in-the-loop (HiL) is integrated beside the real combustion process. It serves in being more flexible in tuning plant parameters for several values, for instance, heat exchanger temperature difference, compressor and turbine efficiencies, and pressure and mass flow values. In addition, complex control of the overall system can be researched.

Three different biomass types are tested: wood, straw, and torrefied pellets. Wood pellets combustion shows higher temperature values, while straw combustion shows the lowest one. By using this variation, the results of this study can be used for a broad range of agricultural and forestry residues.

Jordan is one of the countries that suffer from energy problem. Investigating biomass as a solution beside other renewables leads to more diversity and more reliability in energy supply. Olive processing residues is one of the major biomass types in Jordan. By applying the concept of externally fired gas turbine, olive residues can be used in distributed generation units. These units can be mounted in small scale (e.g. at the olive mills) and be used to feed into the electrical distribution network. The cost of installing such system is higher than traditional ones which use liquid or gas fuel, but totally this difference in cost is compensated to a certain degree by the low fuel cost. Since the main cost is only for installing these plants and maintenance. Other biomass types could be also taken into consideration since the plant

applies the concept of fuel flexibility, leading to higher annual operation hours and lower power generation costs.

Beside electrical generation, combined heat and power could be investigated with externally fired gas turbine plant. Exploiting heat energy at least partially compensates low electrical efficiency, and helps to reducing energy consumed for normal heating applications.

Zusammenfassung

Aufgrund der Bedeutung von Biomasse als Energieträger ist es von Interesse, den effizienteren und effektiveren Einsatz dieser Ressource in Entwicklungs- und Industrieländern zu untersuchen. Die thermo-chemische Konversion ist eines der verbreitetsten Verfahren zur Energiebereitstellung aus Biomasse. Extern befeuerte Gasturbinen (*Externally Fired Gas Turbine – EFGT*) haben sich zudem als vielversprechende Technologie zur energetischen Nutzung fester Brennstoffe gezeigt. In dieser Arbeit wird die Kombination des thermo-chemischen Prozesses der direkten Verbrennung mit der Technologie der extern befeuerten Gasturbine untersucht.

Der Einsatz von extern befeuerten Gasturbinen zur dezentralen Strombereitstellung kann stromnetzstabilisierend wirken, beispielsweise durch die gezielte Bereitstellung von Strom in Spitzenzeiten oder durch verringerte Übertragungsverluste. Darüber hinaus weist diese Energiequelle eine höhere Zuverlässigkeit als andere erneuerbare Energien auf, weil sie nicht von den Wetterveränderungen wie Wind und Solarenergie abhängt. Die Technologie kann eine Vielzahl von Biomassen einschließlich agrarwirtschaftlicher Reststoffe nutzen, so dass sie in einem breiten Einsatzfeld verwendet werden kann.

Allerdings ist die Anwendung im kleinen Leistungsbereich noch nicht kommerzialisiert. Zur Verbesserung der Konzeptentwicklung werden optimale Designparameter, Anlagenflexibilität und technische Beschreibung für diesen unter Berücksichtigung verringerter Wirkungsgrade diskutiert.

Extern befeuerte Gasturbinen haben grundsätzlich den Vorteil einer hohen Brennstoffflexibilität. Allerdings ist ihre Leistung sehr stark von der Auswahl der Komponenten abhängig. Hohe Temperaturen, hohe Drehzahl und die Pelletzuführung sowie die Ascheentfernung sind wichtige Aspekte, die berücksichtigt werden müssen und sich negativ auf die erforderliche Investition auswirken.

Eine technische Bewertung der Anlage erfolgt durch Variierung verschiedener Parameter. Wärmetauscher-Temperaturdifferenz (bedingt beispielsweise durch Verunreinigungen) zeigt einen erheblichen Einfluss auf die erzeugte elektrische Leistung. Dies bedeutet, dass eine kontinuierliche Reinigung wichtig ist, um die Wärmeübertragung durch den Wärmetauscher und die Turbineneintrittstemperatur zu maximieren. Es konnte zudem gezeigt werden, dass die Reaktion des Systems auf sprungartige Lastwechsel relativ langsam erfolgt, zusätzlich zu

kleinen Fluktuationen im stationären Betrieb. Dies hängt im Wesentlichen mit dem Verbrennungsverhalten von festem Brennstoff zusammen, d.h. dass der Verbrennungsvorgang derzeit der limitierende Faktor für die Flexibilität der extern befeuerten Gasturbine ist.

Die mechanische Leistung, die von der Turbine geliefert und vom Kompressor verbraucht wird, hängt sehr stark von der isentropischen Effizienz der beiden Komponenten sowie von der Turbineneintrittstemperatur ab. Für den Referenzfall beträgt das Verhältnis von Verdichter- zu Turbinenleistung 67%, dies ist ein Indikator dafür, dass der Kompressor eine relativ hohe Leistung verbraucht, wodurch die abgegebene Leistung deutlich reduziert wird. Eine höhere Ausgangsleistung kann durch Komponenten mit höheren isentropischen Wirkungsgraden sowie durch einen Generator mit höherem elektrischen Wirkungsgrad erzielt werden.

Betriebsdruck und Luftmassenstrom auf der Reinluftseite wurden bezüglich der maximalen Leistungsabgabe optimiert. Es wird festgestellt, dass der Luftmassenstrom mit etwa 0,02 kg/s für den Referenzfall im stationären Zustand relativ klein ist. Ein solcher kleiner Massenstrom erfordert auch kleine Kompressor- und Turbinengrößen. Das optimale Betriebsdruckverhältnis wurde für den Referenzfall auf etwa 3,5 berechnet. Beide Werte werden als Funktion der Turbineneintrittstemperatur abgebildet.

Um das Konzept bezüglich seiner Flexibilität zu untersuchen, wurde das Hardware-in-the-Loop-Konzept neben dem realen Verbrennungsprozess integriert. Es dient dazu, flexibler bei der Abstimmung von Anlagenparametern für mehrere Werte zu sein, zum Beispiel Wärmetauscher-Temperaturdifferenz, Kompressor- und Turbinenwirkungsgrade sowie Druck- und Massenstromwerte. Darüber hinaus ist es möglich, die komplexe Ansteuerung der Gesamtanlage zu untersuchen.

Drei verschiedene Biomassetypen werden getestet: Holz, Stroh und torrefizierte Pellets. Bei der Verbrennung von Holzpellets wurden höhere Temperaturwerte im Abgasstrom gemessen, während bei der Strohverbrennung die niedrigsten auftraten. Durch diese Variation konnte ein breites und praxisrelevantes Einsatzspektrum mit hoher Relevanz für die Nutzung verschiedener Agrar- und Forstreststoffe untersucht werden.

Jordanien ist eines der Länder, die unter Energieproblemen leiden. Die Untersuchung von Biomasse als Lösung neben anderen erneuerbaren Energien führt zu mehr Vielfalt und mehr

Zuverlässigkeit bei der Energieversorgung. Olivenverarbeitungsrückstände sind eine der wichtigsten Biomasse-Typen in Jordanien. Durch die Anwendung des Konzepts der extern befeuerten Gasturbine können Olivenreste in verteilten Erzeugungseinheiten eingesetzt werden. Diese Geräte können im sehr kleinen Leistungsbereich (z.B. in den Olivenmühlen) installiert und zur Einspeisung in das Verteilungsnetz eingesetzt werden. Die Kosten für die Installation eines solchen Systems sind höher als herkömmliche, die Flüssig- oder Gasbrennstoff verwenden, aber dieser Unterschied in den Kosten wird bis zu einem gewissen Grad durch die niedrigen Kraftstoffkosten kompensiert. Aufgrund der hohen Brennstoffflexibilität können auch andere Biomassearten berücksichtigt werden, so dass die Nutzungsgrade derartiger Anlagen erhöht und damit die Stromgestehungskosten reduziert werden können.

Neben der elektrischen Erzeugung konnte die Kraft-Wärme-Kopplung mit einer extern gefeuerten Gasturbinenanlage untersucht werden. Die Nutzung von Wärmeenergie kompensiert zumindest teilweise den relativ geringen elektrischen Wirkungsgrad und hilft bei der Reduzierung der Energie, die für normale Heizungsanwendungen verbraucht wird.

Table of Contents

Nomenclature

A	Area
AFR	Air to fuel ratio
BFB	Bubbling fluidized bed
C	Heat Capacity
CC	Capital cost
Cd	Coefficient of discharge
CFB	Circulating fluidized bed
CHP	Combined heat and power
c_p	Specific heat capacity at constant pressure
c_v	Specific heat capacity at constant volume
D,d	Diameter
EFGT	Externally Fired Gas Turbine
f	Friction factor
FBGGT	Fixed bed gasifier-gas turbine
FC	Fixed carbon
GCV	Gross calorific value
GT	Gas Turbine
H	Hydrogen concentration
h	Specific enthalpy
HE	Heat exchanger
HED	Heat exchanger difference
HiL	Hardware in the Loop
k	Ratio of specific heats
L	Length
M	Moisture
m	Mass
$\dot{m}$	Mass flow
NC	Non-Conventional
NHV	Net heating value
NTU	Number of Transfer Units
ORC	Organic Rankine cycle
P	Power
p	Pressure
PC	Plant capacity
PIX	Pellet index
PLC	Programmable Logic Controller
PR	Pressure ratio
Q	Heat
q	Specific heat
r	Radius
Re	Reynolds number
s	Dimensionless scale factor
T	Absolute temperature
t	time
TIT	Turbine Inlet Temperature
U	Heat transfer coefficient
u	Blade speed
v	Axial flow speed

VM	Volatile matter
u_{fg}	Internal energy of vaporization
W	Weight
w	work

Greek Letters

η	Efficiency
λ	Excess air factor
ρ	Density
ϵ	Effectiveness
θ	T (K)/1000

Subscripts

C,c	Cold stream
d	Dry
db	Dry basis
f	Feed stock
H,h	Hot stream
h,0	Dry basis higher heating value
I	input
l	Lower
O	output
p	Polytrophic
w	Mass related work
wb	Wet basis

List of figures

List of tables

1   Introduction and Problem Statement

The hazards of decaying natural (non-renewable) energy resources in the world started to appear on governments and citizens, especially in areas which suffer from fossil fuel storage or non-oil producing countries in general. The solution approach for such problem is to investigate other resources such as renewables, in addition to improve their implementation. So many questions rise in this sector, which led to extensive efforts in renewable energy investigation. In order to add further step, this research focuses on biomass utilization.

It's clearly known that renewable energy sources like solar and wind forms are clean and free of achieving, but they are not dependable since the non-regular occurrence of wind and the absence of sun in the night. Geothermal energy and energy from dams can be considered as continues types. However, their influence is geographically limited in certain places.

Biomass has interesting merits that encourage its exploitation. Along with reliable energy feeding, storage of raw material property enhances its investment. Agricultural crops residues, residues from processing agro-industrial plants, forests residues, and energy plants perform the main source of woody biomass.

Biomass or bioenergy could be defined as the residues of plants and animals that results from the bio processes. The main source of energy is plant, since it contains the basic organic materials, and the energy which gained from the photochemical or photosynthesis process [1]. Energy achieved from biomass is basically in the heat form. The major question come in how to design an efficient conversion plant for better energy investigation. Efficiency, control, emissions, cost, structure complexity, and energy achieved are the main factors in determining the way of energy production. Application requirements are also important for this selection. Thermochemical conversion processes are the most promising in energy utilization from solid fuels in general. It is divided into three categories, gasification, pyrolysis, and combustion [2].

Both gasification and pyrolysis require further installation before thermal energy form is achieved. Both conversion processes depend on producing gas to be combusted later. Direct combustion becomes more simple and direct for utilization. Noting that, the achieved energy from biomass is at the maximum when burned directly. Thus, direct combustion provides the maximum energy extraction with simple construction [1].

In spite of describing direct combustion as technically easier than gasification and pyrolysis, its selection still has further challenges. Especially when talking about designing a modern plant for energy generation. With technology development, many ideas were presented in this scope, gas turbines technology is one of the rising ideas.

Gas turbine influence in Externally Fired Gas Turbine (EFGT) cycle adds a competitive idea in the scope of energy utilization from solid biomass. This is mainly due to the separation of combustion process from moving parts inside the setup. Additionally, there is no need for water as a thermal fluid, the thing that serves areas where water shortage is another challenge beside energy, or places which are far from water supply. EFGT is not a novel study, but it performs a promising concept for using gas turbines.

Some point's pours in biomass based EFGT technology like seeking of biomass investigation by the means of efficiency, reliability, flexibility, and costly effective. In addition, smart grid and dealing with distributed generations push the development of micro scale generation plants. Finally, EFGT has the merit of energy extracting from solid fuels where dirty combustion is handled.

EFGT is presented mainly for medium and micro scale. Meanwhile, there is no exact definition for the ranges till now, researchers used to define their own limits. Unfortunately, there is no adequate technical coverage for very small sizes lower than $30 \, kW_{th}$. So the importance of this study comes from handling this range, for instance, $15 \, kW_{th}$.

Previous points storm the mind to the main challenge in this research, and that is developing a very small plant which deal with biomass and use the concept of EFGT. The problem of such small size (i.e. $15 \, kW_{th}$) is the lack of study provided from literature. There the technical analysis were concentrated on much more plants power ranges (i.e. around $100 \, kW_{th}$).

Previous researched concentrated on expecting efficiency values for such size. However, here more detailed overview of efficiency and energy production is presented. Several factors in plant design affect the operation and the ability of productivity like devices efficiencies (i.e. heat exchanger (HE), turbine, compressor, and burner). In addition, biomass type, pressure, and fluid flow. The discussion is not only about the previous aspects and parameters, it is also for optimizing plant design which adds an extra point in this research novelty.

Technical challenges accompanied with EFGT biomass based plant come from the high combustion temperatures, difficult direct combustion controlling, pressurized fluid (i.e. air),

turbomachinery coupling, and high rotational speed. So in order to compromise between mentioned challenges and providing a modern study, the idea of using Hardware in the Loop (HiL) is exploited. This merge between real setups and dynamically modeled ones returns in many benefits, mainly, avoiding difficulties in practical installation and provide flexible operation. HiL opens the door to go further in plant description and scientific analyzing. HiL in EFGT is a novel idea here, since dynamic model is presented in the real time, which is different from normal simulation. Furthermore, plant control using HiL could be easily performed to meet demands requirements.

Externally fired gas turbine cycle consists of some mechanical and thermal heat transfer devices, suitable sizes and common parameters are important. A major challenge in this research is determining those parameters to provide the optimum operation, and so the maximum output power.

Flexibility in dealing with several biomass types is another goal, this make a spread concept of externally fired gas turbine cycle based on biomass types. In addition, the effect on environment is enclosed by determining the emitted gases, and an economical evaluation of the proposed system.

Finally, integrating hardware in the loop concept in such plant is a pioneer idea. Applying this concept is a new confrontation in simulating real system in the real time operation. However, hardware in the loop increases the term of flexibility where better idea and wider tests become possible.

2 Theory

2.1 Biomass as a fuel

Biomass history began from thousands of years in the form of using wood as a source for heating applications. In spite of discovering fossil fuel during the industrial revolution, bioenergy still has a great interest especially in the third world.

Biomass concept means all organic materials that is maintained or produced basically from plants. Photosynthesis process in plant is responsible for producing plant material using sun light, water, and other components presented by soil. Energy gained from the biomass refers to the chemical bonds between molecules (oxygen, hydrogen, and carbon). These chemical bonds are from storing sun light as a chemical form in the plant. Energy is gained by breaking these bonds using oxidation such as in combustion systems (which will be discussed in this thesis), or by other processes like digestion or decomposition [1].

In general, biomass energy can be used in electricity generation, transportation and heating. Its processing in several applications serves the global warming as well. Since CO_2 emitted from burning biomass is already consumed by plants which forms biomass itself [3].

The spread types of chemical components in the plants are structural and nonstructural carbohydrates and other compounds. Take into consideration other materials like cellulose, hemicellulose, lignin, lipids, proteins, simple sugars, starches, hydrocarbons, and ash. For comparison with other fuels, biomass has high oxygen content between 30-40 wt %, while carbon is the main content with a value of 30-60 wt %, and hydrogen has a share of 5-6 wt % in dry case [4].

The three main compounds of biomass are cellulose, hemicellulose, and lignin. Cellulose forms the main component of biomass and occupies 40-55% in wood and agricultural straw. Hemicellulose can be described as a support material for the cellulose fibers and composed elementary as in cellulose. Finally, lignin which provides more strength for the wood fibers and forms 15-35% of biomass weight [5].

2.1.1 Biomass classification

The source of biomass generally determines the type of solid biofuel. Referring to European standard (EN14961-1), there are four sub-categories for solid biofuel classification [6]:

1- Woody biomass, which are from trees, bushes, and shrubs.

2- Herbaceous biomass, these plants are usually grows for one season and then die.

3- Fruit biomass, this type is from plant parts which hold seeds.

4- Blends and mixtures, which are biomass materials from different origins.

The main goal of classification of solid biofuels is to allow comparing and identifying raw materials depending on their origins with the largest amount of information. Using simple and flexible tables lead customers and producers to the suitable selection of biomass type that corresponds to the needed fuel quality.

2.1.2 Biomass properties

Biomass characteristics depend on plants nature from which it produced. For instance, woody plant species have slow growth rate behavior, and consist of tightly bound fibers that provide a hard external surface. Herbaceous plants are perennial in general. They are described to have more loosely bound fibers that mean a lower proportion of lignin which binds cellulosic fibers together. Both previous types are examples for long-chain natural polymers [1].

Biomass description is important for application. This is achieved by defining it with respect to its properties. The main properties of the material during subsequent processing as an energy source are related to [1]:

1- Moisture content

Moisture varies with high ranges between different biomass fuels, and it has a great effect on the combustion process. Moisture is classified in two definitions, dry basis moisture (M_{db}), and it is the mass of water in the feedstock per unit mass in the dry material. The wet basis moisture (M_{wb}), and it is the ratio of the water to the total mass (eq. 2-1)[4].

$$M_{db} = \frac{m_w}{m_{f,d}} \qquad M_{wb} = \frac{m_w}{m_{f,d}+m_w} \qquad M_{wb} = \frac{m_{db}}{1+m_{db}} \qquad M_{db} = \frac{m_{wb}}{1-m_{wb}} \qquad \textbf{(2-1)}$$

The lowest value of moisture is 2-3 wt % in char and paper as biomass based products. It could reach 98 wt % in primary material like sewage sludge [7].

2- Heating Value

Heating value is the amount of energy content in a certain material or heat value that can be achieved when burning the biomass material. Heating value is measured in term of energy content per unit mass or per unit volume (i.e. MJ/kg for solids, MJ/L for liquids and MJ/Nm^3 for gases). There are two forms for expressing the calorific value concept [8]:

a) Gross calorific value (GCV) or higher heating value (HHV), here it is important to mention the moisture content in the sample (see eq. 2-2) [4]:

$$HHV = HHV_{h,0}(1 - M_{wb})$$

(2-2)

And as shown it depends on the dry basis mater and the moisture content.

b) Net heating value (NHV) or lower heating value (LHV) (see eq. 2-3) [4]:

$$LHV = (1 - M_{wb})\left[HHV_{h,0} - u_{fg}\left(M_{db} + \frac{W_{H_2O}}{2W_H}H\right)\right]$$

(2-3)

And it depends on the higher heating value, hydrogen concentration, and moisture content.

The heat needed for water vaporization reduces the total output heat (see eq. 2-4):

$$Q_{residual}(\%) = 100\left[1 - \frac{u_{fg}M_{wb}}{(1 - M_{wb})HHV_{h,0}}\right]$$

(2-4)

3- Properties of fixed carbon and volatile matter

Those are two forms of chemical energy stored in the solid material, the volatiles content (volatile matter) and fixed carbon. Volatile matter is known as that portion driven off as a gas with moisture content when heating up to 950 ^{o}C for 7min. While the fixed carbon content is the remains solid particles after the volatiles is removed and the ash is not included [1].

As an example, volatile matter content reach around 85 wt % in wood Western hemlock and Douglas fir, while the rest is mostly fixed carbon [7].

4- Ash / residue content

In all processes that convert biomass into energy, there is a natural influence of residues or ash, which make extra cost on handling and overall process in general. Woody biomass has

lower ash content compared with coal which could reach more than 10 %. Nevertheless, it is important for plant designing to prevent or minimize slagging and fouling effects [9].

5- Bulk density

Volume decides the storage and transportation conditions like sizing. But in order to know the heat content for delivered fuel, weight is necessary. It is calculated by knowing the bulk density. This method could not be very accurate due to the estimation of volume and differences in biomass sizes and compression level especially for pellets [10].

Biomass has relatively low bulk density. The thing that causes some disadvantages like low heat content per unit volume, large storage area needed, and non-effective consumption investment specially when transporting for far places [11][12][13].

In general, the energy density of the biomass is law. Due to this point, deferent technologies should be used for effective energy production. Thus, different parameters of biomass should be determined [13] (Table 2-1).

Table 2-1. Bulk density, calorific value, and energy density of different biomass samples **[10]**

Biomass type	Moisture (wt% w.b.)	GCV (MJ kg^{1-} d.b.)	NCV (MJ kg^{-1} w.b.)	Bulk density (kg.m^{-3})	Energy density (MJ.m^{-3})
Wood pellets	10.0	19.8	16.4	600	9840
Wood chips (hardwood)	50.0	19.8	8.0	450	3600
Grass (high pressure bales)	18.0	18.4	13.7	200	2740
Straw (wheat, high pressure bales)	15.0	18.7	14.5	120	1740

Plants that can be used for bioenergy are spread around the world since the possibility of their growth in deferent conditions. But the most suitable plants are those which can be harvested easily by conventional methods. Because developing special machines is an expensive choice. Some examples on widely used energy crops are coppiced wood species

(such as willow, poplar, and eucalyptus), miscanthus and canary reed grass. For future, energy crops can vary the pattern of using energy since it can be expanded for large scale not like other forms of other biomass resources[14].

Energy crops are those plants that convert solar energy into biomass form with an efficient way. For example, high yielding vegetative grasses, short rotation forest crops, and C_4 crop plants that grow in a commercial scale. They can produce over 400 GJ/ha/yr in case of good growing conditions, and for achieving higher energy species should be selected correctly for meeting site conditions like weather and soil type [14].

Ultimate and proximate analyses summarize biomass description for normal using. Here main components are presented in addition to heating values, so consumer can decide the suitable type for his requirements (Table 2-2).

ISO 9001 quality management consists of quality planning, quality control, quality assurance and quality improvement [15]. EN 15234 standard covers fuel quality assurance and quality control is EN 15234 [6]. The goal of quality assurance is to insure that steady quality is continually achieved in accordance with customer requirements.

Supplier should issue the quality of biofuel for the end user and his records should stands for at least one year regarding to EN 14961 [6].

Table 2-2. Ultimate and proximate analysis of various biomass fuels (dry basis) **[5]**

Name	Proximate analysis (wt%)			Ultimate Analysis (wt%)					Higher Heating Value (MJ/kg)	
	FC[a)]	VM.[b)]	Ash	C	H	O	N	S	Measured MJ kg^{-1}	Calculated MJ kg^{-1}
Woody biomass										
Black locust	18.3	80.9	0.8	50.73	5.71	41.93	0.57	0.01	19.71	20.12
Ponderosa pine	17.2	82.5	0.3	49.25	5.99	44.36	0.06	0.03	20.02	19.66
White oak	17.2	81.3	1.5	49.48	5.38	43.13	0.35	0.01	19.42	19.12
Processed Biomass										
plywood	15.8	82.1	2.1	48.13	5.87	42.46	1.45	0	18.96	19.26

Agricultural										
Walnut shells	21.2	78.3	0.6	49.98	5.71	43.35	0.21	0.01	20.18	19.68
Almond prunings	21.5	76.8	1.6	51.3	5.29	40.9	0.66	0.01	20.01	19.87
Cornobs	18.5	80.1	1.4	46.58	5.87	45.46	0.47	0.01	18.77	18.44
Wheat straw	19.8	71.3	8.9	43.2	5	39.4	0.61	0.11	17.51	16.71
Sugercane Bagasse	15	73.8	11	44.8	5.35	39.55	0.38	0.01	17.33	17.61
Rice hulls	15.8	63.6	21	38.3	4.36	35.45	0.83	0.06	14.89	14.4
Charcoal										
Charcoal	89.3	9.67	1	92.04	2.45	2.96	0.53	1	34.39	34.78
Oak char (565°C)	55.6	27.1	17	64.6	2.1	15.5	0.4	0.1	23.05	23.06
Coconut shell Char (750°C)	87.2	9.93	2.9	88.95	0.73	6.04	1.38	0	31.12	31.21
Eucalyptus Char (950°C)	70.3	19.2	10	76.1	1.33	11.1	1.02	0	27.6	26.75

a) FC: fixed carbon.

b) VM: volatile matter.

2.1.3 Ash melting point

Ash is produced due to the physical and chemical processes that happened to the inorganic mineral matter and elements during the combustion process [16]. The produced ash particles are important in designing aspects for heat exchanging surfaces and combustion chamber. In addition, the melting point of ash is necessary to avoid deposition problems. Once ash melts, the tendency to stick on the walls of heat exchanger and boiler increases, thus, ash should be dry and powdery [17].

Potassium, sulfur, chlorine, and silica elements are important for ash characteristics, since their properties affect the melting point [18]. Potassium is existed in biomass as an organic form that vaporized and decomposed during combustion process, which results in forming oxides, hydroxides, chlorides, and sulfates. These compounds have low melting temperatures which cause a sticky layer on the walls due to the condensing of their vapor [18]. Sulfur affects depositing depending on the presence of other elements. For example, in woods that contain a high amount of calcium and potassium and low amount of sulfur, the production of deposits is low when burning alone. On the other hand, when the burning happens for mixed sulfur with other spices like manure or straw, the deposits will have a high amount of K_2SO_4 and $CaSO_4$ [18]. Chlorine determines from experience the total amount of alkali vapor products, both of them are important in predicting the deposits properties [18]. Finally, silica, that melts alone at $1700^{o}C$. But when being with alkali metals like potassium and sodium as oxides, hydroxides or metal-organic compounds then it will form a low melting eutectics [18].

Ash melting is an important phenomenon for two main reasons. Firstly, it causes the formation of sinter layers on the grate, the bubbling fluidized bed (BFB), or circulating fluidized bed (CFB). Secondly, to obviate forming of deposits on the walls of the furnace or heat exchanger due to ash slagging. The existence of some elements like calcium and magnesium increases the melting temperature. On the other hand, some elements like potassium and sodium do the opposite by decreasing the melting temperature. If it is combined with silicon then low-melting silicates will be formed in fly-ash particles. A general view about ash melting temperatures is shown in table 2-3 [19].

Table 2-3. Ash melting temperatures of various biomass samples [19]

Sample number	Biomass	Fusibility (^{o}C)[a)]			
		Initial deformation	Sphere	Hemisphere	Fluid
1	Pine	1190	1200	1220	1280
2	Poplar	>1400	>1400	>1400	>1400
3	Wheat straw	850	1040	1120	1320
4	Rice straw	860	980	1100	1220
5	Olive stones	1030	n.d.	1090	1160
6	Orujillo	1260	n.d.	1320	1330

a)   n.d.: not detected.

2.1.4 Olive processing residues

An interesting type of biomass is olive processing residues. It has a good energy property that supports its influence. Thus, olive residues are an interesting and promising source of biomass [20]. Recently, olive production is registered to be 2,742,500 tons for the year 2015/2016 worldwide. Mediterranean countries share this production with a very high percentage, approximately 97%. This concentration in Mediterranean countries encourage investment of olive residues to benefit in both removing solid wastes and energy utilization [21][22].

Drawing out oil from olive is usually performed by both traditional pressing and two or three phase schemes centrifugation method [23]. Solid residues percentage depends on process used, for instance it is approximately 40% from pressing, 30-50% and 60-70% for three and two phases respectively, those residues have a high water content [24][25].

Water produced after processing includes organic acids, lipids, alcohols, and phytotoxic materials. Organic matter along with nutrients is useful for soil fertilizing. On the other hand, other contents perform a dangerous effect on environment [26].

A compromised estimation of 25% could be used to expect the amount of dry residues from the total processed olive mass [27]. So referring to the total production, solid residues from olive could be estimated to be around 685,625 tons worldwide in 2015/2016, most of them in Mediterranean countries.

Other treatment technologies like aerobic/anaerobic biological treatment, incineration, and gasification are associated with olive mill residues rather than direct combustion. Those processes could be ineffective technically or costly [28].

As byproducts, olive residues removing or treatment adds further cost related to the local availability with large areas [11]. In addition, Low bulk density makes it non-effective for far consumption investment. However, processing residues for energy utilization serves in reducing local wood consumption from forests.

2.2 Combustion

The most common thermochemical energy conversion processes used for solid biomass combined heat and power production are direct combustion (which is the used method in this research), pyrolysis and gasification of biomass [2][29]. Combustion appears with the advantage of non-selective fuel type compared with other processes [30]. Unfortunately, low

thermal efficiency, instability of heat load and slagging which are considered as challenges in biomass processing in combustion applications [2][31].

Combustion process could be defined as an energy extracting from fuel by burning in the presence of oxygen. Whatever the fuel form, energy is stored as chemical bonds. This process is simple in gaseous and liquid fuels, but it gets more complicated for solid ones [16]. Energy produced could be used for direct heating or commonly in power plants where steam is produced for electrical power generation [32].

The overall combustion process consists of partial steps for the right and complete burning. These steps are drying, pyrolysis, and ignition, combustion of volatile matter, and combustion of the residual char (figure 2-1). In drying process, moisture is released at the beginning burning process. Better combustion performance could be performed by heating biomass up before burning. Since water could be easily adhere to the pellets from the surrounding medium, or it could be existed from manufacturing process. In pyrolysis, the organic material decomposes forming a gaseous product in heating stage, this step happens at a higher temperature than drying. After that, the ignition process starts the combustion, and the temperature is above the value at which the combustion evolves independently. Due to thermal equilibrium, temperature stays constant after ignition. Combustion of volatile matter is characterized by a very high reaction velocity, and so the burning time is achieved by their release and mixing with air. Finally, the combustion of the residual char happens for the remains after the volatile matter released, the remains consists of carbon and ash. Carbon at high temperatures is oxidized by oxygen, in general the combustion of solid char is slower than the homogeneous volatile matter combustion [16].
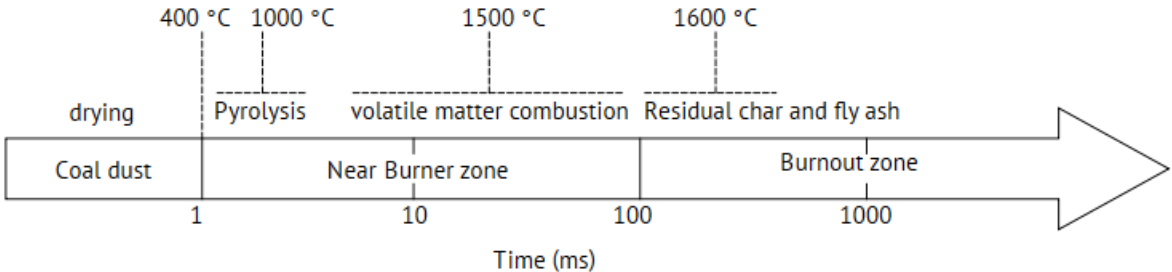
Figure 2-1. Combustion process in pulverized fuel firing[16]

Another presented method of energy conversion is gasification. With gasification process, the combustion system deals with gaseous fuel. This gas is produced from solid biomass by non-

complete combustion, then filtered, cooled, and finally combusted. This system needs further equipment's which could add extra cost. Also produces gases are with lower heating value than the direct combustion [33][34].

Biomass combustion beside coal is a good way for reducing emissions of NO_x and SO_x, reducing cost, and soil pollution [35].

2.3 Biomass (pellets) global potential

Biomass has fairly good potential in covering the basic or primary energy requirements in some developing countries. Energy achieved is basically used for normal heating or cooking, in addition to the investigation for electricity supply as a promising solution in developing countries for future [36]. Biomass cover around 10-15% of the primary energy requirements [36][37].

Biomass is registered to be the fastest growing sector in renewables. For example, from 2010-2012, biomass productivity has increased by 2320 PJ. On the other hand, photovoltaic and wind energy supply increases by 234 PJ and 645 PJ. World bioenergy association estimated the agricultural energy potential in the range between 13.1-122 EJ [38].

Being more specific with pellets production, we can see the increment profile since 2000 in figure 2-2. After 2014, wood pellets production increased fast to more than 25 million tons [39].

The estimated production in 2015 shows production sharing as well. Europe occupies the largest percentage with around 20 million tons, followed by North America, and Asia [39].

Experts expect that additional supply of woody biomass could reach 400 million tons by 2020, this is due to the renewable energy policy EU 2020 and the industrial pellets producers growth as well. Germany is considered as the largest European pellets producer so far. In 2015, pellets price average was 0.233 Euro/kg. Prices in 2015 are registered by the Nordic Pellet Index (PIX) to be 132.5 Euro per ton for industrial and commercial use, and 128.9 Euro per ton for commercial use according to the Pellet Price Index PPI 06 [40]. Wood pellets consumption is to be between 50-80 million tons by 2020 [41].
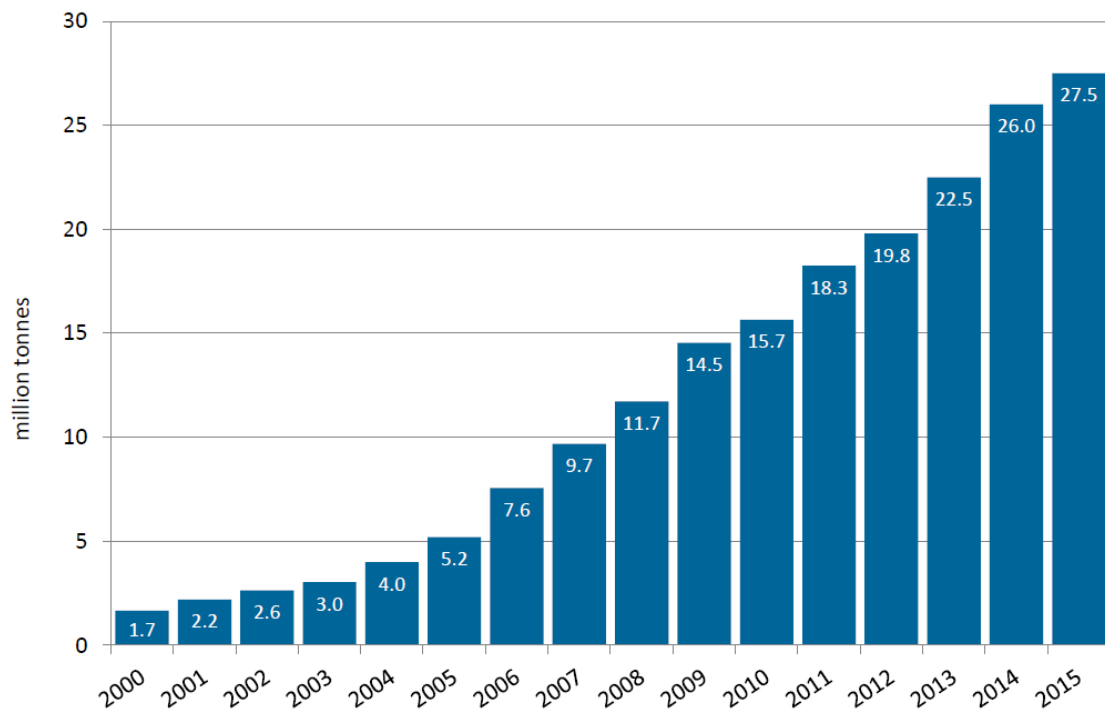
Figure 2-2. Global wood pellets production [39]

2.4   EFGT technology

Gas turbine could be defined as an energy transformation device, which is from flowing fluid form to rotating mechanical one. The rotational power form is needed for leading electrical generator [42]. For analyzing the thermal operation of gas turbine cycle, Brayton concept is used due to the presence of gaseous working fluid (air). Air is compressed and then expanded by the operation of the gas turbine after heat addition from the combustion process [43][44]. The continues improvment on gas turbines efficiencies present them as a competitive electrical generation units due to high power achievement from small sizes, lower initial cost, fuel flexibility, and it is not necessary to use water for cooling [45]. Further advantages are added to EFGT like low operational cost, high life time and reliability, relatively high energy efficiency even for small sizes [46][34].

The first registered closed-cycle gas turbine was in 1935 for Prof.Keller – Zurich with 2 MW_{el} and turbine inlet temperature (TIT) of 660 °C, efficiency reached more than 30% when TIT reaches 700 °C. This starting is followed by many plants that use air as working fluid. Mainly, in the period between 1960 and 1982 Oberhausen I closed cycle plant worked in Germany with 14 MW in combined heat and power system [47]. Several studies, plants and test

14

facilities handles currently EFGT concept summarized by Z.A. Zainal et al. [48], like the biomass fueled 50 kW$_{el}$ (800 °C Turbine Inlet Temperature (TIT)) developed by Talbott, UK [49].

The extrapolation of TIT trend improvement generated by McDonald in figure 2-3 still acceptable, it shows a significant increase after 1995 especially for open gas turbine cycles. This trend is fairly limited for closed cycle due to the material of heat exchanger technological availability [47][50].

F. Jurado et al. [51] provided a comparison between Fixed Bed Gasifier-Gas Turbine (FBG-GT) and EFGT for electrical generation along with heat, it was based on olive tree leaves and prunings. System capability is about 30 kW$_{el}$, the proposed system model shows that it is possible to reach 30 kW$_{el}$ and 60 kW$_{th}$, the achieved electric efficiency and overall efficiency for EFGT are (19.1% and 59.3%), which was higher than gasification system (12.3% and 45.4%). Further study provided on the effect of pressure ratio, inlet air temperature for preheating, and hot side temperature difference on efficiency.
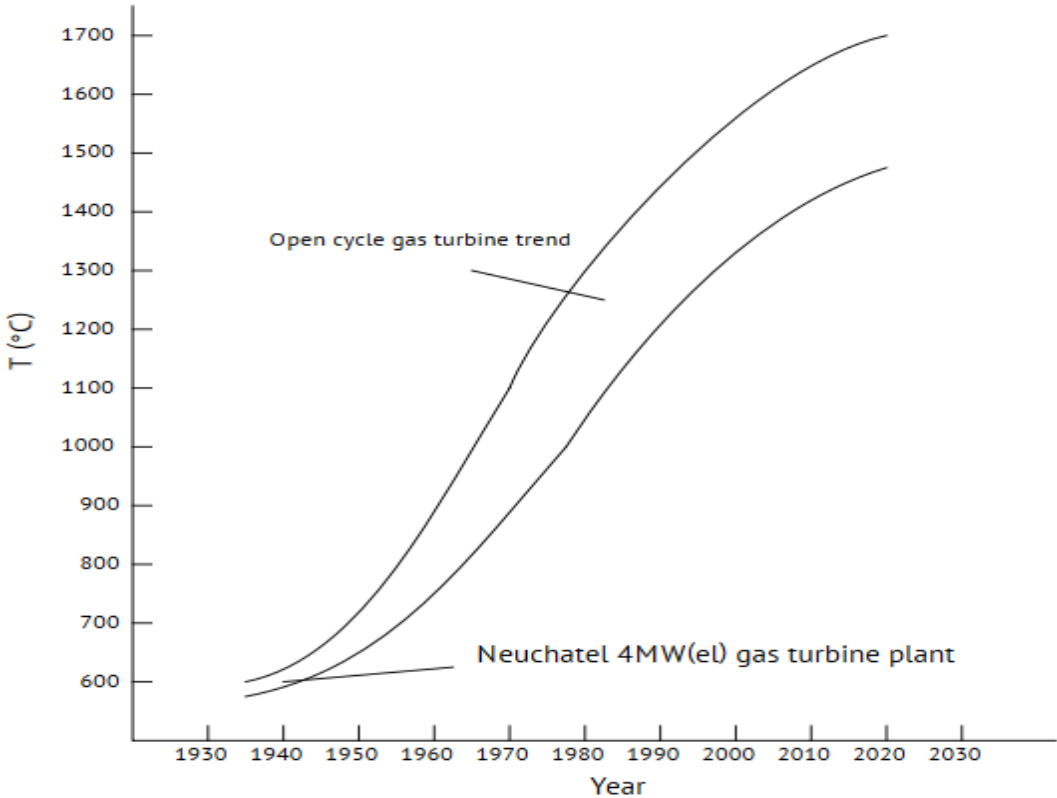
Figure 2-3. Gas turbine inlet temperature trend [47][50]

J. Karl in [52] provided the efficiency related to common power machines. Gas turbines in general have efficiency of around 20% to 38% for power sizes of 20-200 MW. But when moving to micro sizes, their efficiencies will be even lower than 20%. Combined heat and power systems have higher efficiencies, for instance, a plants more than 200 MW can have 60%.

EFGT has merits that make it more competitive than other systems, mainly, flexible fuel option, low maintenance and cleaning costs [53][54]. Also it comes a good choice in places which have water shortage, that is due to independent operation of water use for cooling [55]. Using gaseous medium instead of liquid one add further point in EFGT advantages, that is faster start-up and shut-down operations. So combustion process controls mainly or dominant [56].

Several studies were provided on EFGT especially micro scale. M. Kautz et al. [57] discussed the effect of gas-air heat exchanger performance on cycle efficiency and power generated which was about $100 \, kW_{el}$. The maximum electrical efficiency reached 44% for more than 1250 K TIT and at lowest temperature difference in the heat exchanger and TIT. Pressure drop influence a slight effect on the electrical efficiency when variating from 0 to 0.2 bar. Additionally, it is concluded that the design and material the heat exchanger is important especially for high temperature values, in spite of high cost of such design, the using of waste biomass will compensates extra costs.

A.M. Pantaleo et al. [34] provided a thermo-economic assessment of EFMGT fired by natural gas and biomass, he discussed the dual mode by ranging sharing percentage to 100% for both fuels. The suggested plant is in the range of $100 \, kW_{el}$, it shows an electrical efficiency of 30% for 100% natural gas fuel share and 19.2 % for 100% biomass fuel share.

The performance of stainless steel high temperature heat exchanger was also discussed by Z.A. Zainal et al. [58] which is placed in an EFGT cycle were a biomass gasifier combustor is used for thermal power. The effectiveness of the heat exchanger decreases from 68% to 60% with air temperature increasing from 210 °C to 450 °C, the same behavior applied with changing air mass flow from 0.095 to 0.099 kg/s.

Z.A. Zainal et al. [53] also discussed the startup operation of turbocharger in EFGT mode using gasification method in his project. Two configurations of starting up are tested, the first one is by using air blowers (5.5 kW and 7.5 kW), and the second one is by using the

compressor of the turbocharger. Air blowers method provided higher mass flow but lower pressure than the compressor in the second method. It is concluded that compressor using in the second method is not sufficient for starting up EFMGT and the only proven method is by using a high speed mechanical motor at the beginning.

Table 2-4. Overview on previous studies on biomass-fueled EFGT [64].

Reference	TIT (K)	Pressure Ratio	Fuel	Power	Efficiency	HED	RPM
Z. A. Zainal et al. [48] and original research is in [65] [49]	1073	4.5	Biomass	50 kW$_{el}$	15% elect.	n.a	n.a
Z. A. Zainal et al. [48] and original research is in [66]	1073	n.a	Biomass	500 kW$_{el}$	14% elect.	n.a	n.a
Traverso et al. [67]	1023	n.a	n.a	15-50 kWel	n.a	n.a	68,000
Pantaleo et al. [34]	1173 max	n.a	Biomass	66 kW$_{el}$	19% elect.	n.a	n.a
Kautz and Hansen [57]	1173	2–8	Biomass (gasification)	100 kW$_{el}$	16% and 30% with recuperator	10–150	n.a
Z. A. Zainal et al. [58]	967	n.a	Biomass (gasifier)	57 kW$_{th}$ transferred by the HE	n.a	n.a	n.a
Cocco et al. [55]	1223	3.5	Biomass	100 kW$_{el}$	22%–33% using drier	50–200	n.a
Vera et al. [68]		2–6	Olive tree prunings and leaves	30 kW$_{el}$	19.1% elect.	50–200	n.a
Detta et al. [69]	1050–1350 K	2–8	Biomass (gasifier)	100 kW	16%–34% thermal	200–300	n.a
De Mello and Monterio [70]	1223	4.5	Biomass	100 kW$_{el}$	20%–30% elect.	n.a	n.a

Typical systems that follow Organic Rankine Cycle (ORC) and EFGT have efficiencies in the range between 10-20%. It is also possible to have higher efficiency for EFGT cycles, approximately 25% [59]. A general expectation of such cycle's efficiency for the range up to 250 kW$_{th}$ could be made between 10-20%. For this research size lower values could be achieved [59] [60][61][62] [63].

Main previous researches are grouped in table 2-4, where efficiency, power, pressure, and the inlet turbine temperatures are the main values for comparison and validation later.

EFGT is a promising choice for the developing of medium and small ranges of generation, this is mainly due to its ability to handle various fuel types, including ones with suboptimal combustion properties [48][67]. Literature concentrates mainly on technical and economic aspects of EFGT for the range more than 100 kW. Also previous studies discussed EFGT in heat recovery for higher efficiency and high temperature heat exchanger with their thermal analysis [69][71][48][67][55][33][72][57].

The general concept of EFGT cycle is not a novel study. However, development and improvements are handled in design and considerations regarding each device. Also it comes in the envelope of optimum total design for maximum benefit. So the discussion in the following sections is about elements design and their operational conditions, in addition to determining common parameters.

2.4.1 Gas turbine technology

Gas turbine is a term also for the combination of compressor, combustor, and turbine. The combustion process is performed internally when dealing with gaseous and liquid fuel (clean combustion). Previously, it was not efficient for electrical generation compared with other systems like steam turbines power plants. The improvements steered the efficiency to be 18% at the beginning of commercial versions (1939 Neuchatel gas turbine) [56]. Due to its importance, it worth's to have a look on turbine application and its development in further applications.

The increasing dependence on gas turbine in electrical generation sector is due to several points. Firstly, increase natural gas production serves majorly in introducing gas turbine technology. Second, gas turbines can share positively in CO_2 reduction, the thing that serves in global warming problem solving, and policies influence on industrial countries regarding this point [60].

The use of gas turbine in combined heat and power (CHP) has many advantages compared with other technologies. Produced waste heat is relatively high in a way could be investigated in second loop of generation or domestic heating for efficiency improvement, lower weight for the same power compared with others, lower maintenance and capital costs, relatively flexible and reliable with short starting and transient time, possibility of handling dual fuel, rugged operation, and once again, more friendly for the environment especially CO_2 emissions compared with liquid and solid fuels [73].

Some turbines are designed to operate with different fuels, a good example is Capstone gas turbines. In addition to natural gas, liquid fuel, and biogas could be used. This enhances the exploitation of renewable concept from waste biomass. An overview of gas turbine construction is shown in figure 2-4 [74]
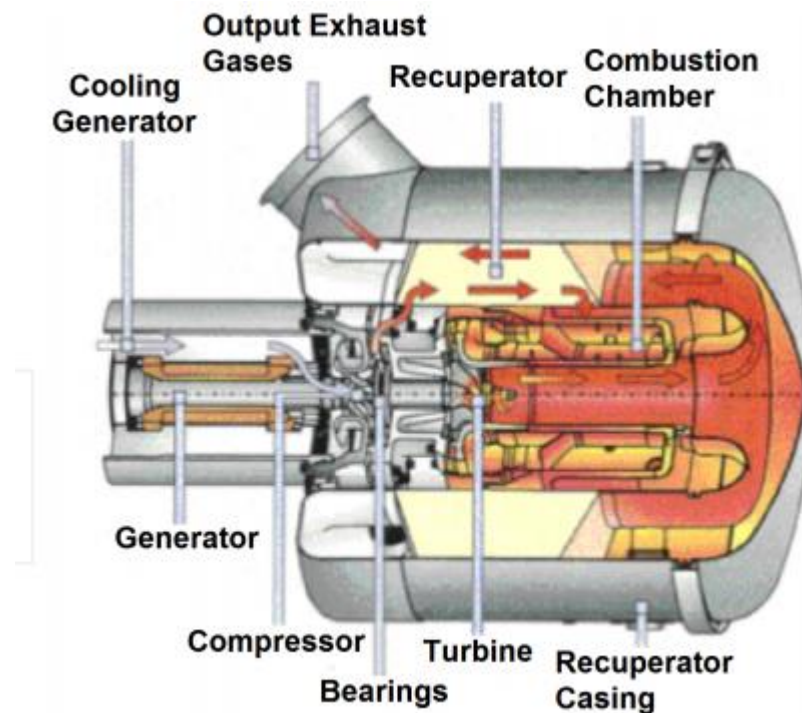
Figure 2-4. Open overview of Capstone gas turbine [74]

2.4.2 EFGT cycle

In contrast with normal gas turbine cycle, in which combustion is performed internally, EFGT performs the combustion process separately from the moving parts inside the cycle (see figure 2-5). EFGT is considered to be a promising option for small- to medium-scale plant sizes [48][67].
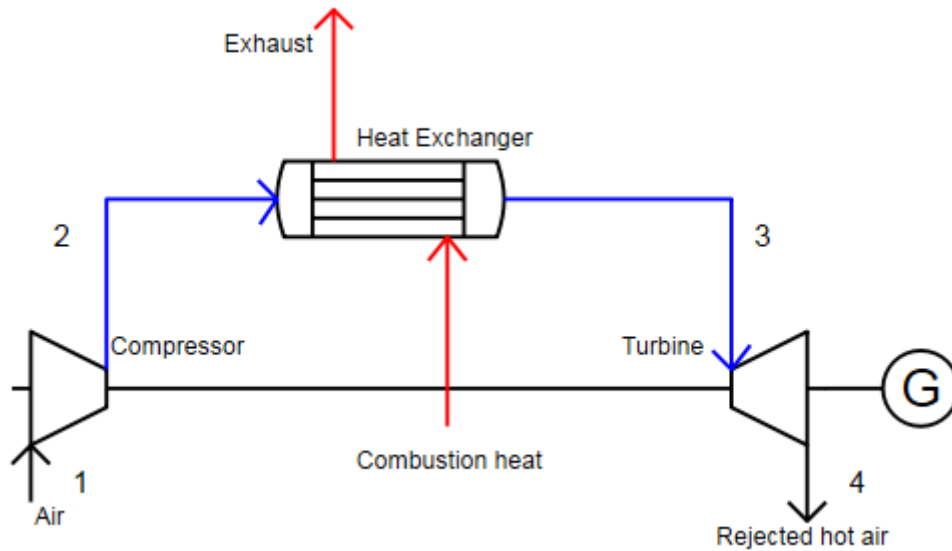
Figure 2-5. The schematic diagram of EFGT cycle

The thermal concept could be explained as the following. Thermal power is converted with a certain percentage to electrical or mechanical one. At this point, turbine is the related device for this conversion. Obviously, the power delivered from the turbine should cover the compressor need and an abundant power to the generator.

Heat addition system design depends on fuel type, for instance, liquid, and gaseous fuels are simpler than solid ones. Furthermore, solid fuel shape also should be considered, for example pellets is easier than woody ships or cakes. Since this research is interested in biomass fuel, pellets are the selected shape, a detailed description will be discussed in the related sections.

It is possible to have two design configurations of EFGT, open and closed loops (figure 2.6). In closed loop, the turbine hot stream output is cooled and re-entered to the compressor. Cooling is done simply by another heat exchanger, heat transferred in this case could be continued to be exploited in recovery stage or heating purposes.

Closed loop is common in Rankine cycle where water is the working fluid. This closed path increases the cycle efficiency by increasing the benefit of the rejected heat amount. In open loop, compressor entrance air is independent from the hot rejected air. It is easily to be applied for Brayton cycle since air amounts are not restricted for the use in general.
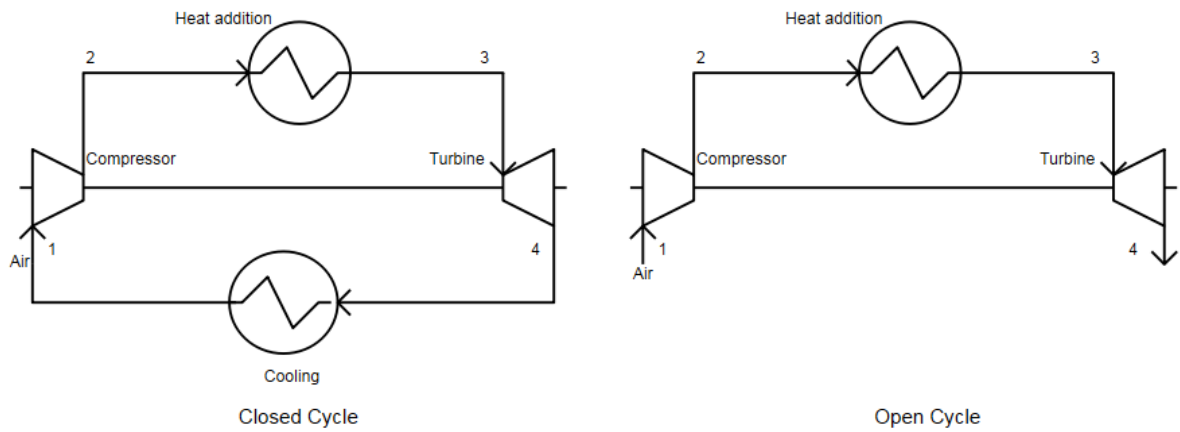
Figure 2-6. Open and closed loop Brayton cycles
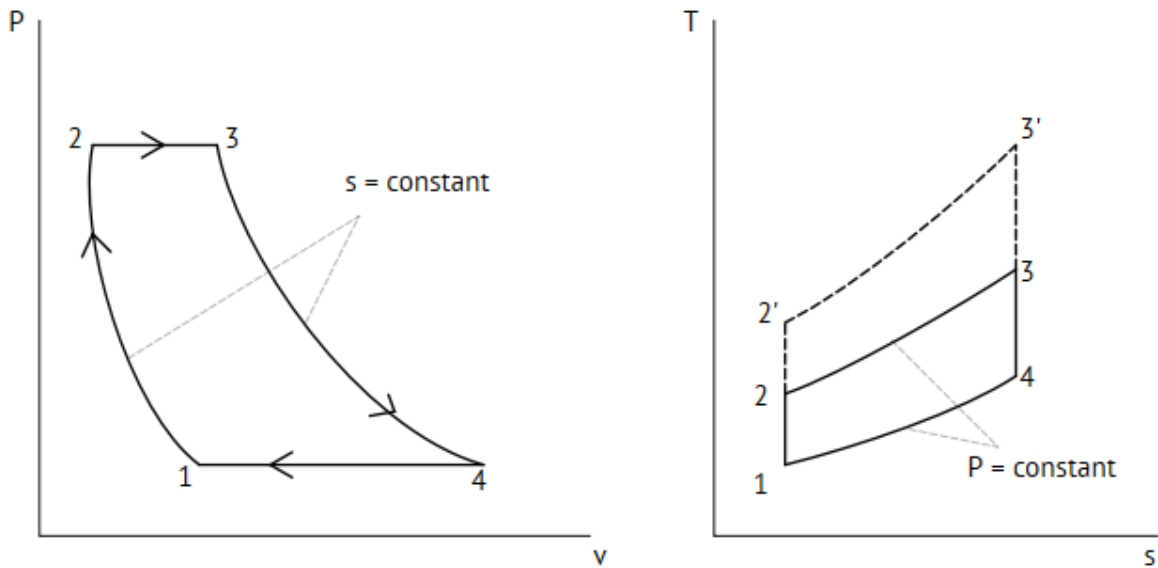
Figure 2-7. The standard Joule Thomson (Brayton) cycle[75].

Referring to the cycle relations and T-S diagram in figure 2-7 compressor performs an isentropic operation from 1-2, the same thing applied on turbine from 3-4. On the other hand, heat addition and rejection in 2-3 and 4-1 respectively are isobaric processes. If the ideal gas is assumed to be the working fluid in cycle, then the amount of heat enters and leaves the cycle is [16]:

$$q_{in} = h_3 - h_2 = c_p(T_3 - T_2)$$ (2-5)

$$q_{out} = h_4 - h_1 = c_p(T_4 - T_1)$$ (2-6)

Where:

q : the specific heat (J/kg)

h : the specific enthalby (J/Kg)

c_p : the specific heat capacity at constant pressure $(\frac{KJ}{KgK})$

T : the absolute temperature (K)

The work done by the compressor during 1 to 2 is:

$$w_{12} = h_2 - h_1 \qquad\qquad (2\text{-}7)$$

The work gained from the turbine during 3 to 4 is:

$$w_{34} = h_4 - h_3 \qquad\qquad (2\text{-}8)$$

And the net achieved work from this cycle is:

$$|w| = |w_{34}| - w_{12} \qquad\qquad (2\text{-}9)$$

The efficiency for Joule – Thomson process is:

$$\eta_{th} = \frac{|w|}{q_{in}} = 1 - \frac{(T_4 - T_1)}{(T_3 - T_2)} = 1 - (\frac{p_1}{p_2})^{\frac{k-1}{k}} \qquad\qquad (2\text{-}10)$$

It is clearly seen that the efficiency of the gas turbine plant depends on the difference in pressure ratio, any variation on the pressure ration affects the temperature T_2 in a direct proportion. Once the efficiency calculated by pressure values, the input heat by the operation of the combustion chamber can be easily calculated by:

$$q_{in} = \frac{|w|}{\eta_{th}} \qquad\qquad (2\text{-}11)$$

But for the real process of the gas turbine, irreversibility leads to a deviation from the ideal cycle. This irreversibility applies on the combustion chamber and on the turbine as well, the deviation is also caused by the flow passages and combustion chamber or in the heat exchanger in case of the closed cycle [75], see figure 2-8 where the real T-s Joule Thomson cycle.
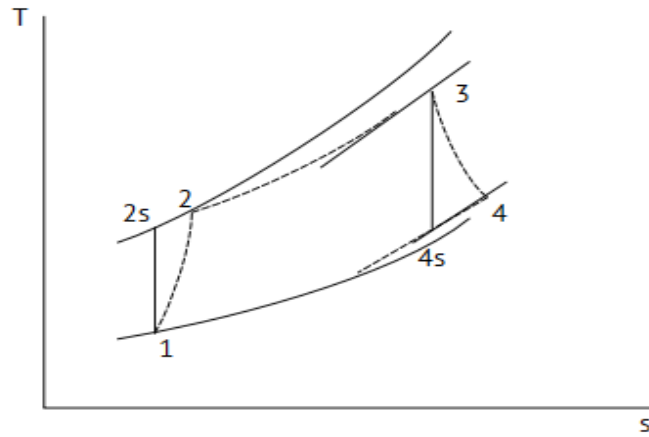
Figure 2-8. Effect on inefficiencies on the gas-turbine cycle [16]

The achieved isentropic compressor and turbine efficiencies are [16]:

$$\eta_{i,comp} = \frac{\left(h_{2,ideal} - h_1\right)}{\left(h_2 - h_1\right)} \tag{2-12}$$

$$\eta_{i,turbine} = \frac{\left(h_3 - h_4\right)}{\left(h_3 - h_{4,ideal}\right)} \tag{2-13}$$

2.4.3 Heat exchanger

Heat exchanger (HE) is important for the thermal heat transferring. Due to the influence of high temperature values of the combustion, it is important for the heat exchanger to stand at these values. So many researchers coincide the use of ceramic heat exchanger [76][77][55][67][78]. Pressure drop and effectiveness are considered to be the main points in designing the heat exchanger [57]. But later it is seen that pressure drop doesn't have a great effect on the electrical output power. On the other hand, effectiveness has a great effect on the output power. This could be improved by increasing the heat exchanger area [70].

Heat exchangers are widely used in the industry since the heat presence in manufacturing, power generating, heating, and cooling. For that, it is worth to mention the several types and classes of heat exchangers. The wide variety is due to the applications conditions like temperature levels and pressure, the shape and separation between streams are also important for fluid flow (table 2-5)[79].

Table 2-5. Heat exchangers classifications [79]

Classification according to construction	1. Tubular	1.1 Double pipe	
		1.2 shell and tube	1.2.1 Cross flow to tubes
			1.2.2 Parallel flow to tubes
		1.3 Spiral tube	
		1.4 Pipe coils	
	1. Plate type	2.1 Plate Heat Exchanger	2.1.1 Gasketed
			2.1.2 Welded
			2.1.3 Brazed
		2.2 Spiral	
		2.3 Plate coil	
		2.4 Printed circuit	
	3 Extended surface	3.1 Plate fin	
		3.2 Tube fin	3.2.1 Ordinary separating wall
			3.2.2 Heat pipe wall
	4 Regenerative	4.1 Rotary	
		4.2 Fixed matrix	
		4.3 Rotating hoods	
Classification according to flow arrangements	1 Single pass	1.1 Counter flow	
		1.2 Parallel flow	
		1.3 Cross flow	
		1.4 Split flow	
		1.5 Divided flow	
	2 Multi pass	2.1 Extended surface	2.1.1 Cross counter flow
			2.1.2 Cross parallel flow
			2.1.. Compound flow
		2.2 Shell and tube	2.2.1 Parallel counter flow
			m- shell passes
			n- tube passes
			5.2.2.2 split flow
			5.2.2.3 Divided flow
		2.3 Plate	Fluid 1 m passes
			Fluid 2 m passes

HE is a key component in EFGT biofuel based plant, that is due to the high combustion temperature (in combination with elevated pressure) and the aggressive behavior of the flow gases that cause oxidation, surface corrosion and erosion [80]. From several classifications and types of heat exchangers, shell-tube HE is selected for the application of this research as in [57][53]. Shell-tube type is the most suitable one due to its ability to operate in high

temperature conditions, the design can withstand fouling caused by combustion, and its thermal stress reluctance [58].

The suitable heat exchanger for EFGT operation should meet several demands for the right operation. The drawn particles from air, ash fractions, and other dirt are considerably dominant with time, especially for narrow HE streams. This problem appears by blocking the gas flow which affects the generated power. On the other hand, if the streams are separated by large distances, then the amount of heat transferred will decreases because of the increments in flow speed. Also, when high temperature is reached, the material became weak. The solution is by increasing the thickness of the material or by establishing a special room for thermal expansion. As previously mentioned, the most suitable type for this work is shell-tube type since it provides a complete insulation between the exhaust gases and air, also it can be designed to fit the flow, high temperature, fouling and blocking problems, which for example the plate type can't meet, and regenerator type as well, see figure 2-9 [58].

Figure 2-9. Shell – tube heat exchanger [53].

Two configurations related to shell-tube HE, parallel and counter flow. Each has temperature behavior, and the selection depends on the application. For instance, TIT in our research should be as maximum as possible, so countercurrent or counter-flow applies this requirement, and that is since (t_2) is as near as possible from the flue gas (T_1) (figure 2-10). This difference between T_4 and T_1 is defined here be Heat Exchanger Difference (HED).
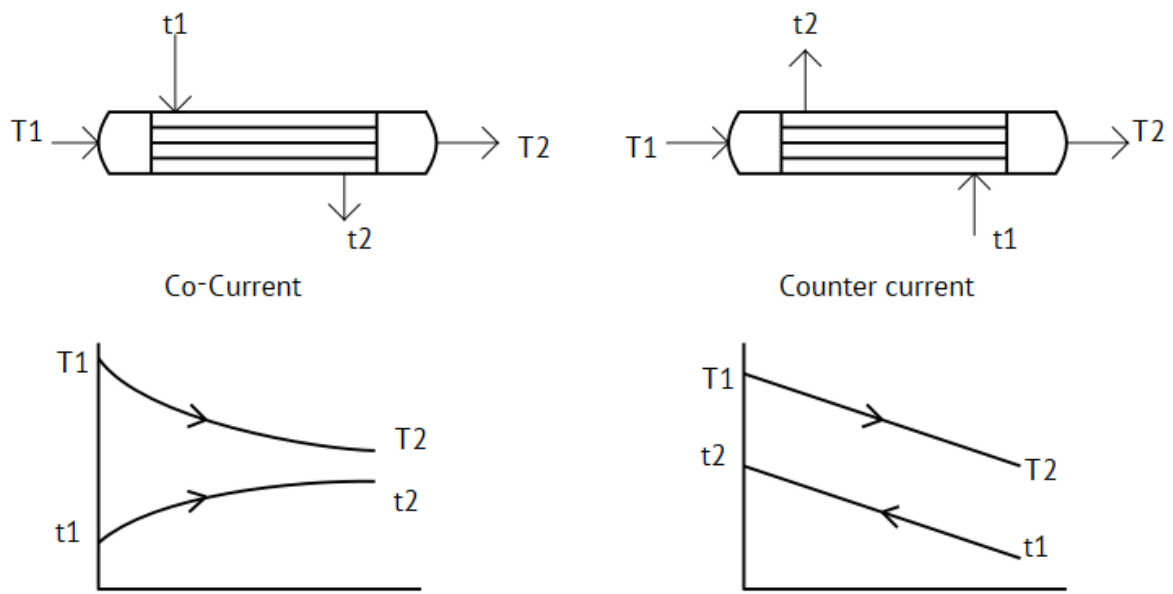
Figure 2-10. Countercurrent and Co-current operation for a shell and tube heat exchanger [81]

From the basic definition of the total heat transfer coefficient and mean temperature, the local heat transfer rate in the exchanger is as in eq. (2-12) [79]:

$$q = UA\Delta T_m \tag{2-14}$$

Where:

q: total or local (whatever appropriate) heat transfer rate in an exchanger.

U: overall heat transfer coefficient.

ΔT_m: The mean temperature deference.

A: Total flowing area

$$\Delta T_m = \frac{\Delta T_2 - \Delta T_1}{\ln \Delta T_2 / \Delta T_1} \tag{2-15}$$

Where $\Delta T_2 = T_{h,o} - T_{c,i}$ and $\Delta T_1 = T_{h,i} - T_{c,o}$
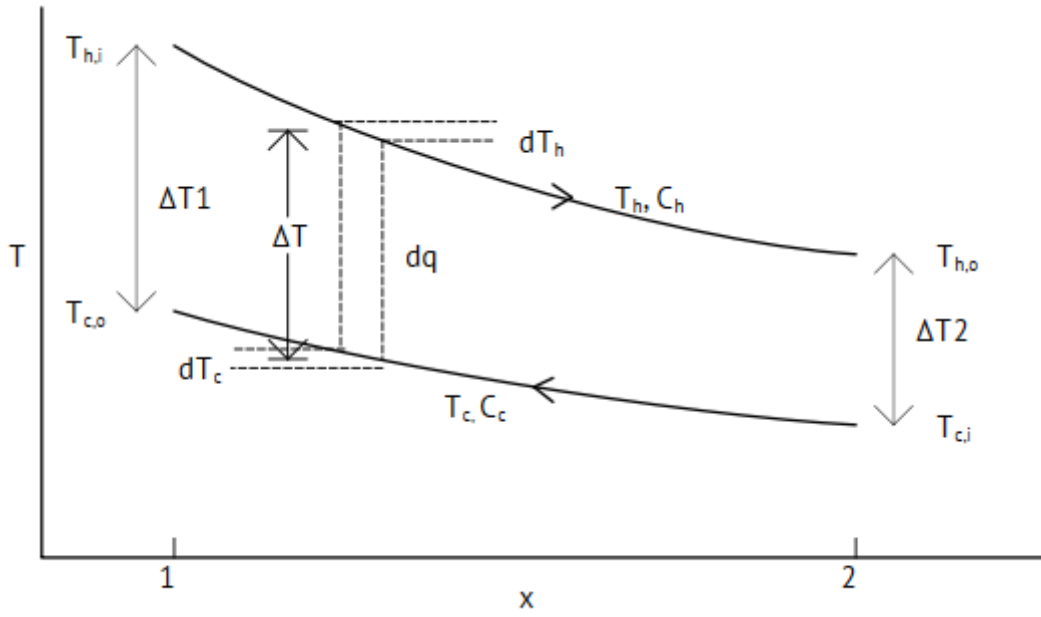
Figure 2-11. Counter flow HE temperatures [82]

Number of transfer units (NTU) method depends on relation between effectiveness and NTU, each HE configuration has special relation, for instance, shell-tube HE NTU and effectiveness are given in eq. 2-13,14 [82].

$$\epsilon_1 = 2\left\{1 + C_r + (1 + C_r^2)^{1/2} * \frac{1 + \exp\left[-(NTU)_1(1 + C_r^2)^{1/2}\right]}{1 - \exp\left[-(NTU)_1(1 + C_r^2)^{1/2}\right]}\right\}^{-1} \qquad \textbf{(2-16)}$$

$$\epsilon = \left[\left(\frac{1 - \epsilon_1 C_r}{1 - \epsilon_1}\right)^n - 1\right]\left[\left(\frac{1 - \epsilon_1 C_r}{1 - \epsilon_1}\right)^n - C_r\right]^n \qquad \textbf{(2-17)}$$

The next step is to find heat capacity for both hot and cold streams, depending on mass flow ($\dot{m}_c, \dot{m}_h$) and specific heats.

$$C_c = \dot{m}_c c_{p,c}$$

$$C_h = \dot{m}_h c_{p,h}$$

Then using the minimum heat capacity we can find the maximum possible heat to be transferred, where then the actual heat transferred is calculated. Finally, both outlet temperatures are calculated heat transferred equation.

$$q_{max} = C_{min}(T_{h,i} - T_{C,i}) \tag{2-18}$$

$$q = \epsilon q_{max}$$

$$T_{h,o} = T_{h,i} - \frac{q}{\dot{m}_h C_{p,h}}$$

$$T_{c,o} = T_{c,i} + \frac{q}{\dot{m}_c C_{p,c}}$$

Heat in the steady state operation is transferred from the hot side to the colder one by convection. Heat transferred by conduction happened through the wall, after that, subsequent convection from the wall to the cold fluid. It is a normal phenomenon of forming a fouling film on the heat exchanger walls during long time operation. These accumulated deposits from the fluid or from the chemical reaction products, or rust formation between the fluid and the wall has a high thermal resistivity. Thus, they affect the rate of heat transferred and the overall efficiency. This film taken into consideration in calculations by representing it by fouling factor $r_f = 1/h_f$, where h_f is the heat transfer coefficient from fouling [79].

2.4.4 Compressor

Compressor type selection is related to the application. Thus, in case of high flow rate is required, axial flow compressors are used. On the other hand, high pressure applications with relatively low flow rate (as for our case), centrifugal compressors are the suitable ones for this purpose [83].

Compressor efficiency is an important factor in cycle modeling. The instantaneous isentropic efficiency varies with pressure ratio, as in eq. (2-16), as well as the specific heat ratio.

$$\eta_c = \left[\left(\frac{P_2}{P_1}\right)^{\left(\frac{k-1}{k}\right)} - 1\right] / \left[\left(\frac{P_2}{P_1}\right)^{\left(\frac{k-1}{\eta_p k}\right)} - 1\right] \tag{2-19}$$

Compressor efficiency decreases with pressure ratio increase, it is also noticed that it is highly reduced at high pressure values. See figures 2-12 for different polytrophic efficiencies.
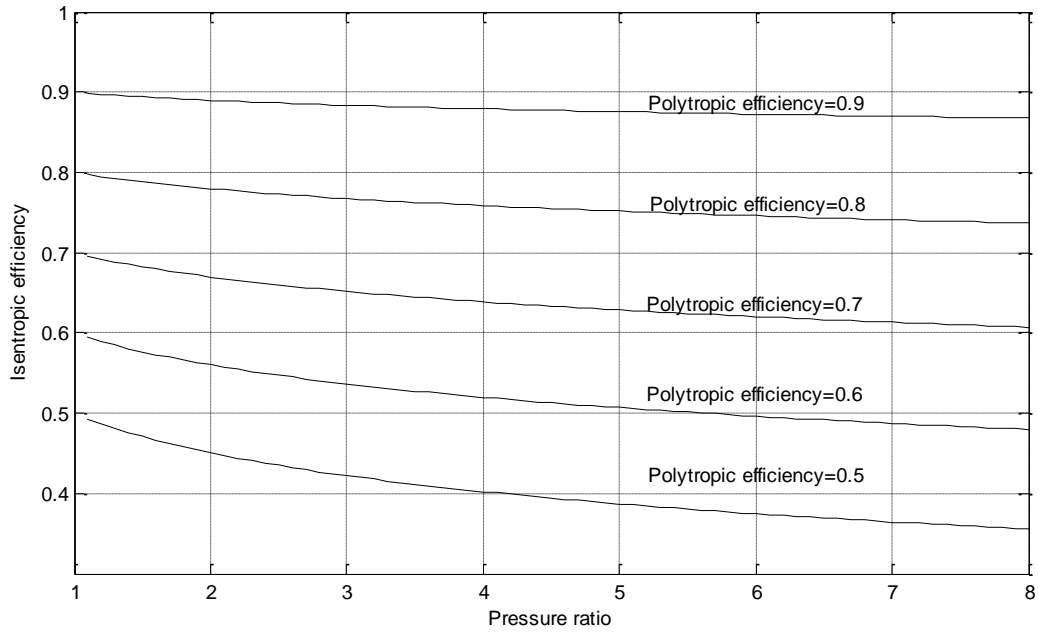
Figure 2-12. Compressor efficiencies

For practical application, compressor efficiency is determined from literature. This step is important for estimating the real value in the desired model (table 2-6).

Table 2-6. Compressor efficiencies from literature

Compressor efficiency %	Reference
62	Pritchard,D. [49], Matthiat Betsch [84]
87	Datta et al. [69]
70	Baina, F. et al.[85]
80	Al-Attab, Zainal [53]
76.8	Kautz et al. [57], de Mello et al. [70]
79	Vera D. et al. [86]
80 (polytropic)	Cocco,D. et al. [55]
74	Vidal, A. et al. [87]
87	Tahmasebi, A. et al[88]

Compressor design depends on its operational circumstances. In addition, the geometry selection is important to meet the desired pressure and mass flow that are suitable for plant size. The required compressor power is a function of pressure ratio, input temperatures, mass flows, and specific heats [89].

$$P_C = \frac{\dot{m}_C c_p T_1}{\eta_C} \left[\left(\frac{P_2}{P_1}\right)^{\left(\frac{k-1}{k}\right)} - 1 \right]$$

(2-20)

And c_p comes as a function of temperature, an average value could be taken in the middle point of HE. The same thing applied on cv and k as well see eq. 2-18 and graph 2-13 [75]

$$c_p = C_0 + C_1\theta + C_2\theta^2 + C_3\theta^3$$

(2-21)

Where $\theta = T(K)/1000$, constants from table A.6 [75]
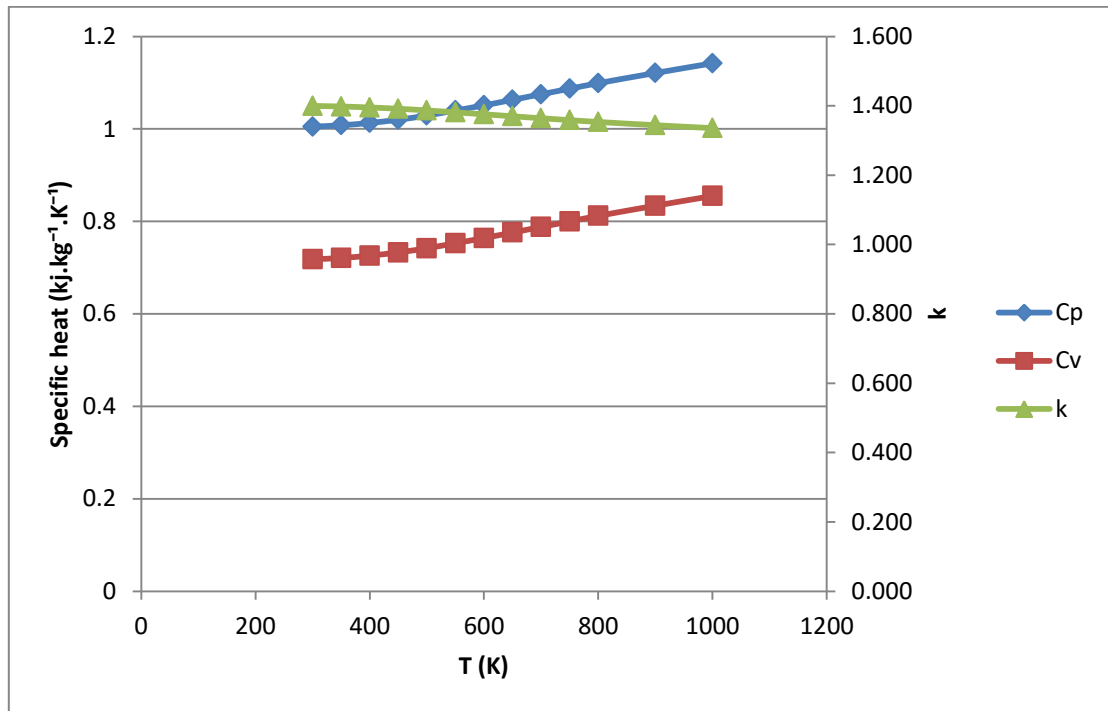
Figure 2-13. Specific heats variation with temperature

2.4.5 Turbine

Radial flow turbines are suitable for low flow rates rather than axial ones [83]. It is important for realistic operation that turbine parameters are carefully adjusted. As for compressor, turbine isentropic efficiency is a function of pressure ratio and specific heats ratio (eq. 2-19) [90].

$$\eta_t = \left[1 - \left(\frac{P_2}{P_1}\right)^{\left(\frac{\eta_p(k-1)}{k}\right)} \right] / \left[1 - \left(\frac{P_2}{P_1}\right)^{\left(\frac{k-1}{k}\right)} \right]$$

(2-22)

30

In contrast with compressor, turbine isentropic efficiency increases with pressure ratio increase (figure 2-14). It is noted that turbine efficiency is affected slightly lower than compressor efficiency at high pressure ratio values.
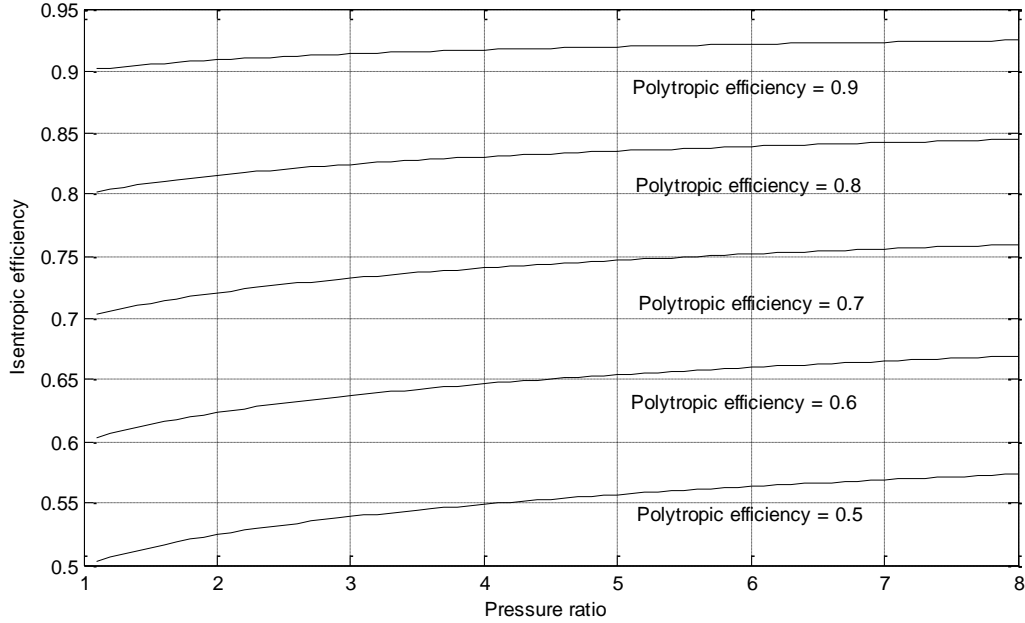
Figure 2-14. Turbine efficiencies

Efficiencies that are handled in literature are summarized in table 2-7, it is noted that turbines can have relatively high efficiency values.

Mechanical power generated from turbine is dependable on its efficiency, flow rate, TIT, pressure ratio, and specific heats ratio as well [89].

$$P_T = \eta_T \dot{m}_T c_p T_3 \left[1 - \left(\frac{P_4}{P_3} \right)^{\left(\frac{k-1}{k} \right)} \right] \tag{2-23}$$

In turbine modeling, it is important to find out the rotational speed. As mentioned previously, the expected speed for such range could exceed 100,000 rpm. For practical application, radial flow turbine is the suitable type (figure 2-14).

The specific work provided by the turbine could be given as a function of blade speed and axial flow speed [83]:

$$w = \frac{1}{2} (V_2^2 - V_3^2) + \frac{1}{2} (u_2^2 - u_3^2) + \frac{1}{2} (W_3^2 - W_2^2) \tag{2-24}$$

This is also given by the typical expression as the following:

$$w = u_2 V_{u2} - u_3 V_{u3}$$

(2-25)

Table 2-7. Compressor efficiencies from literature

Turbine efficiency %	Reference
80	Pritchard,D. [49], Matthiat Betsch [84]
89	Datta et al. [69]
77	Baina, F. et al.[85]
82	Al-Attab, Zainal [53]
82.6	Kautz et al. [57], de Mello et al. [70]
80	Vera D. et al. [86]
85 (polytropic)	Cocco,D. et al. [55]
89	Vidal, A. et al. [87]
89	Tahmasebi, A. et al[88]

Having a look on velocity vectors shown in figure 2-15, u_2 and v_2 must be large. On the other hand u_3 and v_3 must be small as possible, and this is achieved by turbine outlet design. As a result for that the exit swirl could be neglected and u_2 is approximately equals v_2, so the work becomes in eq. 2-22:

$$w = u_2 v_2 = u_2^2$$

(2-26)

The fan velocity u is a function of the angular peed and the mean radius of the fan.

$$u = \omega r$$

(2-27)
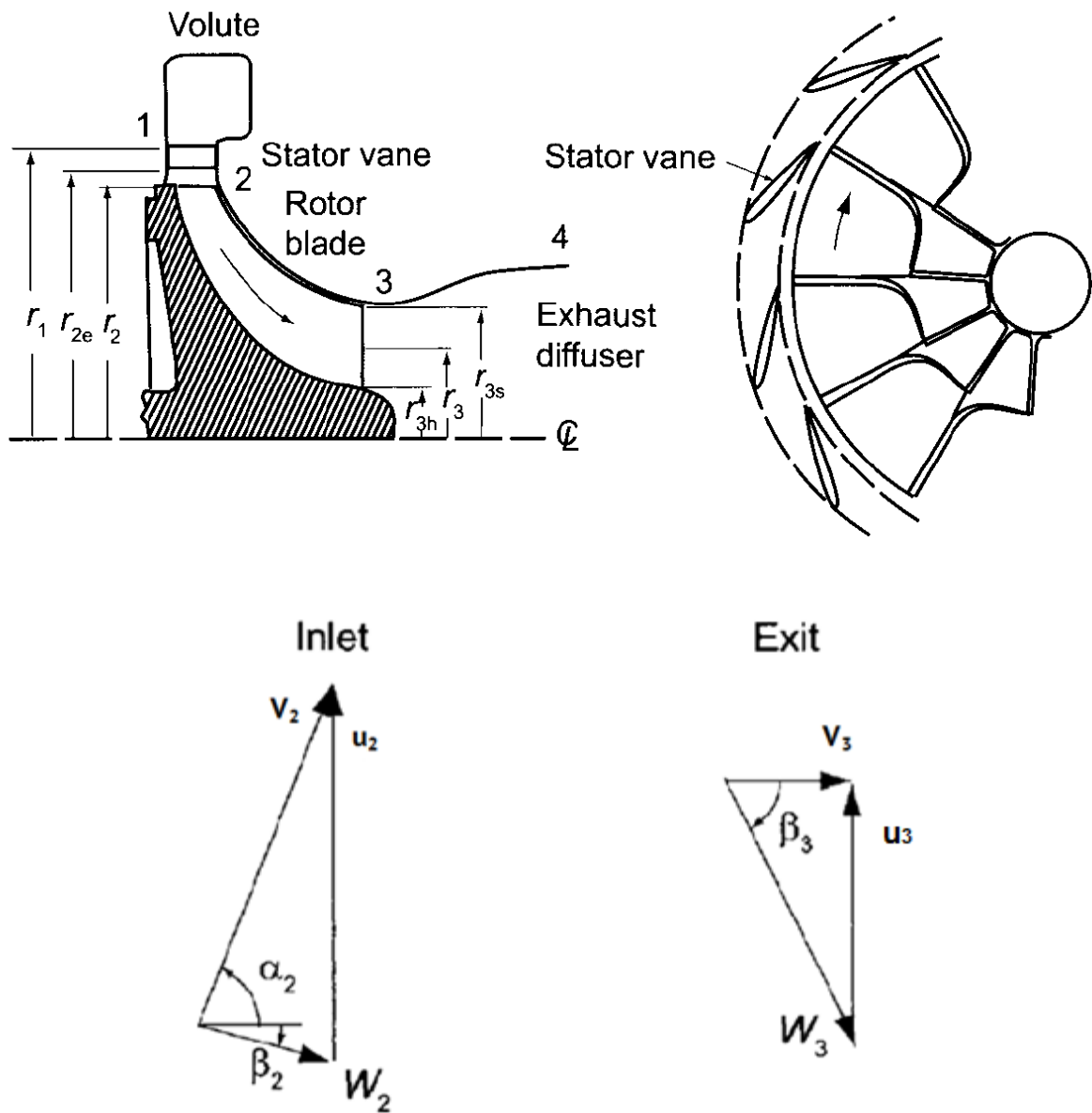
Figure 2-15. Radial flow turbine and velocity diagrams [83].

2.4.6 Turbocharger

Turbochargers have a great interest recently, especially in diesel engines performance developing aspects. This importance comes from their rule in achieving more power from lower engine sizes [91]. Normally 30-40% of the energy provided by the fuel for the combustion in diesel engines goes in the exhaust as waste, so the idea from the Turbocharger usage is to improve the engine efficiency by exploiting the exhaust gases and transfer it to mechanical or electrical energy [92].

For instance, it is known that the combustion process inside the engine is highly dependent on the amount of air enters inside for burning. The normal pressure outside is near 1 bar (for sea level), while the least value of the pressure needed to push the air should be higher than that. Enhancing breathing operation is obtained by installing the turbocharger which operate as a compressor to increase the inlet air depending on the exhaust energy [93].

A cutaway shown in figure 2-16 illustrates the main components of the turbocharger, it operates as a turbine, and a compressor in the same time connected with one shaft. Turbine is connected to the exhaust of the engine, once the hot gases enter the turbine, the housing is filled with the exhaust gas leading to a static pressure moves to the tip of the blades on the wheel, the movement from high pressure area to a lower one drives the turbine to rotate [93]. On the opposite side is the compressor which is connected mechanically with the turbine and rotates with it while the exhaust gases are flowing. The compressor function is to absorb fresh air by the compressor wheel and accelerate it to leave with higher pressure and speed for better engine feeding [93].
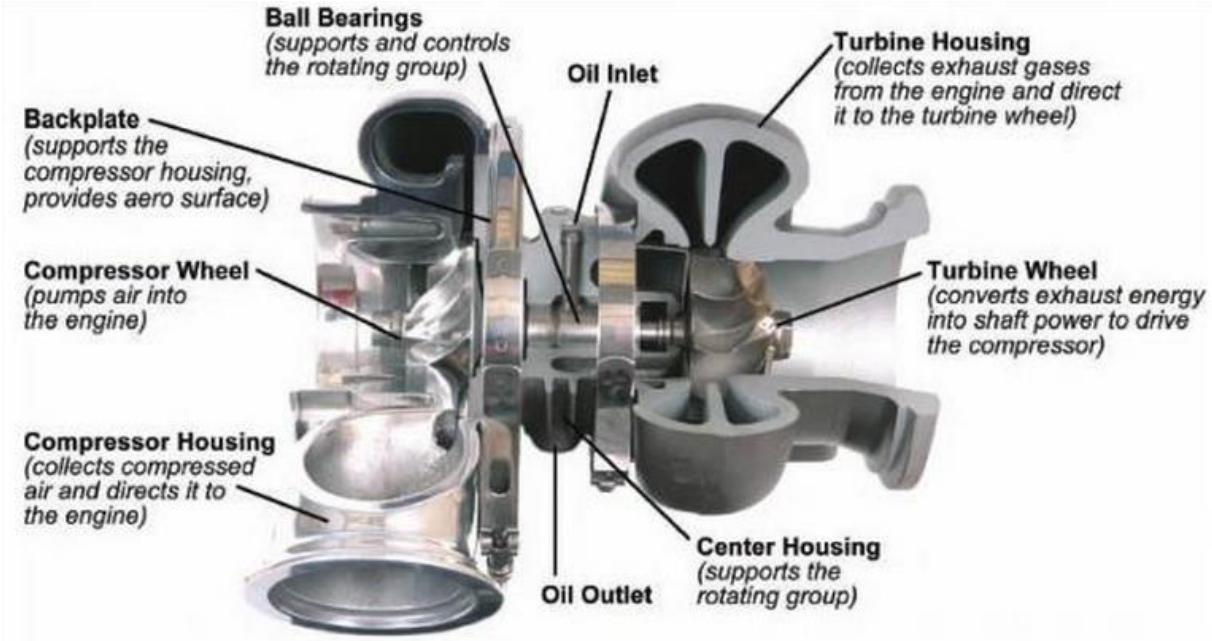
Figure 2-16. Cutaway photo of the turbocharger [93]

It is important to have the right turbine -to - engine size to avoid the mismatch between the both parts, since the lower size of the turbine could lead to a high boost pressure or on the other hand could cause an excessive back pressure, also higher size will not rotate on the desired demand so it would be useless [93].

Turbines in turbochargers are either radial flow or axial flow. Axial turbines are used in applications where large flow is needed, as in marine applications, it weight about 15-35 kg and has a rotational speed up to 35,000 rpm. On the other hand, radial flow turbines are used in automotive applications, where lower air flow values are existed. A typical weight around 1 kg of radial flow turbines with rotational speeds more than 100,000 rpm [94].

After having a look on turbocharger principle, it could be a good investment in EFGT cycle biomass based plants. By this configuration, compressor absorbs mechanically the needed power for generation from turbine instead of using a separate compressor.

Turbocharger employment adds further efforts technically, it need to be started by extra motor (i.e. the generator itself could be used in this case as a motor in the beginning) or blowers, compressor and turbine operations should be synchronized considering each performance map, and high rotational speed.

It is useful to note that in case of dealing with turbocharger configuration, its efficiency is the ratio between both compressor and turbine powers (eq. 2-23) [53]

$$\text{Turbocharger eff.} = \frac{P_C}{P_T} * 100\%$$

(2-28)

2.5 Hardware in the Loop (HiL)

Hardware-in-the-Loop (HiL) is a new concept developed in order to overshoot complexity and time in industry or scientific research. It means to replace some setups in the system by their model. Thus, it is a kind of simulation in the real time with the mathematical representation of the replaced setups, see figure 2-17 [95].
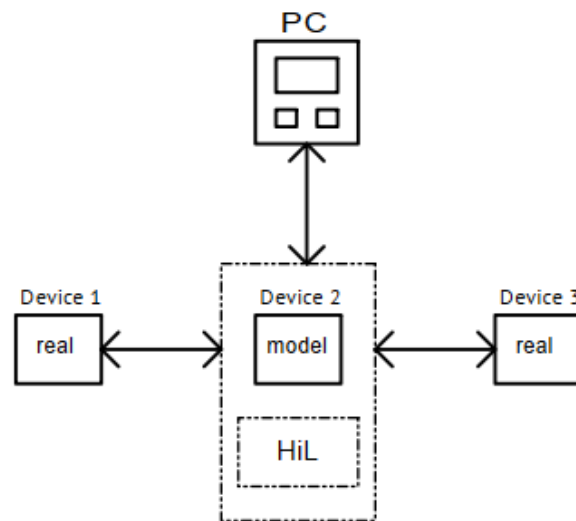
Figure 2-17. HiL position in a system

Inaccurate results are considered as one backward of normal simulation. In contrast with that, HiL interaction with real system provides more reliability due to real time operation. This emulation of replaced parts helps in avoiding risks if the real parts are installed, so it gives the feature of determining safe operational conditions. Another benefit is performing complete control on the rest system [96].

For the purpose of this research, HiL is used to replace some devices like compressor and gas turbine. And since the purpose is not discussing the deep aspects of both devices, HiL comes as the best solution to provide a complete study of the plant. The main parameters of both devices are introduced so any real research can handle those results for optimum compressor and turbine design. High rotational speed, electrical generator coupling, high frequency current, and vibration are considered the main difficulties concerned with real compressor-turbine operation.

Additionally, high temperatures are expected from dealing with biomass pellets combustion, also high fouling effect. The reasons that need a special heat exchanger design that also capable to deal with pressurized fluid. HiL implementation in modeling heat exchanger overcomes the previous challenges. Not only that, operational conditions could be easily presented, and we can see the effect of changings during operation like accumulated dirt's on the total plant power productivity.

3   Methodology

The total system discusses technically a micro scale EFGT plant for electrical power generation as a distributed (on-load) plant. Electrical power, temperatures, emissions, efficiency, and response to load changing are mainly presented by the means of flexibility and optimum operation. In addition to testing another pellets for wider knowledge on the effect of dealing with different biomass types.

Three types of pellets will be tested experimentally, wood, torrefied wood and straw pellets in order to have a better view on the plant behavior for different biomass types. Wood pellets are used as a reference case since it is the common type, torrefied wood and straw have high and law heating values respectively, the thing that makes other types within expected results.

Additionally, transferability of research on the specific Jordan context has been researched by using olive processing residues characteristics in Aspen plus model (figure 3-1).

3.1   Flow sheet simulation

In order to have a clear idea for the complete process and specify the optimum operational parameters, it is important to model the whole process. Aspen plus simulation tool is used for this purpose, see figure 3-1[1].

Aspen plus is a flow sheet simulation tool in process engineering where chemical and mechanical processes are modeled. Further information on flow sheet simulation and power can be found in literature [97][98][99]. Biomass is defined as a non-conventional (NC) material where both ultimate and proximate analyses are used as entries, in addition to the combustion yields. The produced heat continue to be exploited in energy production by the turbine model after heat transfer process that done by HE model, details will be discussed in each relative part.

---

[1] For consistent content, streams abbreviations will be used as subscripts in the whole document. CO could be mentioned as TIT as well.
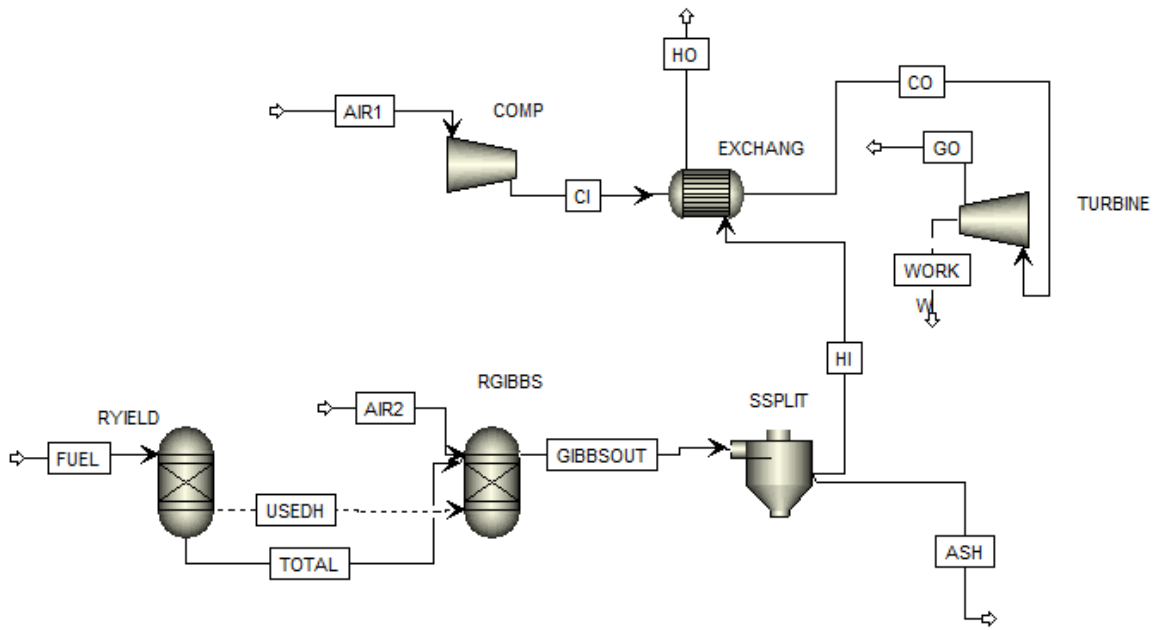
Figure 3-1. Complete model in Aspen plus

It is necessary to notice that Aspen plus power analyzing approach is used for mapping generation, also plant optimizing. Results may vary a little from experimental results, which refer to using advanced approach in Aspen for some parameters like gases specific heats and densities. Thus, temperature shifting of 10-20 K can happened on HE, in other words, changing the heat exchanger difference (HED) a little bit by the program itself to prevent temperature crossing can cause errors.

3.1.1 Combustion

The stoichiometric reaction is the first step in combustion discussion. Theoretically, the reaction formula of biomass combustion can be achieved as the following when burning stoichiometry [100]:

$$CH_aO_bN_cS_d + e(O + 3.76N_2) \xrightarrow{yields} CO_2 + pH_2O + rN_2 + qSO_2 \tag{3-1}$$
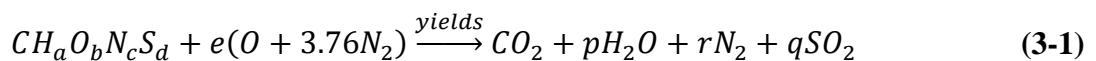
Where:

$$P = \frac{a}{2}$$

$$q = \frac{d}{2}$$

$$e = 1 + \frac{a}{4} + \frac{d}{2} - \frac{b}{2}$$

$$r = \frac{1.88a - 3.76b + 3.76d + f + 7.52}{2}$$

And for each biomass type, the following equations describe the related combustion equation:

Olive

$$CH_{1.6046}O_{0.5627}N_{0.014}S_{0.0016} + 1.1206(O + 3.76N_2) \xrightarrow{yields} CO_2 + 0.8023H_2O + 4.2205N_2$$
$$+ 0.0008SO_2$$

Wood

$$CH_{1.4719}O_{0.621}N_{0.002} + 1.0575(O + 3.76N_2) \xrightarrow{yields} CO_2 + 0.7359H_2O + 3.9772N_2$$

Straw

$$CH_{1.3814}O_{0.7679}N_{0.0137}S_{0.0018} + 0.9623(O + 3.76N_2) \xrightarrow{yields} CO_2 + 0.6907H_2O + 3.6251N_2$$
$$+ 0.0009SO_2$$

Torrefied wood pellets 275°C

$$CH_{1.2859}O_{0.5372}N_{0.0091}S_{0.0003} + 1.053(O + 3.76N_2) \xrightarrow{yields} CO_2 + 0.6429H_2O + 3.964N_2$$
$$+ 0.0002SO_2$$
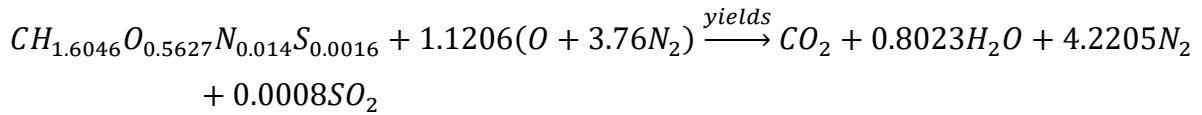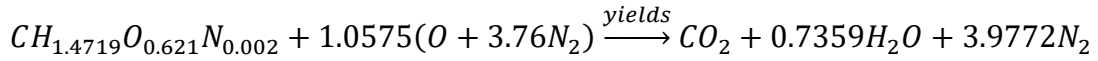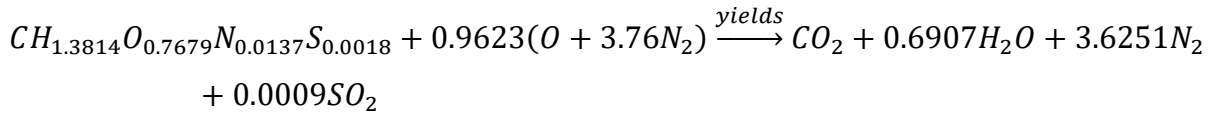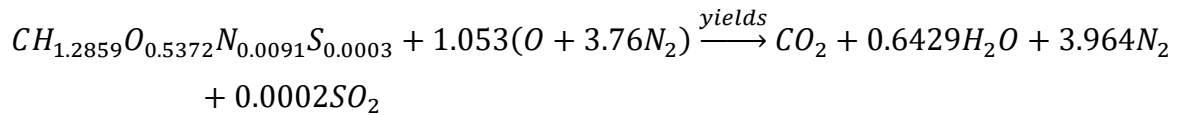
From the previous equations, the general frame of the products is clear, but solid fuels in general contains inorganic matter that doesn't react with a high percentage, oxidize, or becomes liquid as a shape of fouling or slag [34][33][34][33][34][34][35][26]. CO produced mainly in two cases, first, not enough oxygen during combustion, second, low temperature provided to the reaction where CO→ CO_2. As SO_2 is produced, it is possible to be oxidized to SO_3, or it could perform sulfuric acid which can cause some problems to the combustion system. Additionally, NO represents the major component in NO_x compounds (NO, NO_2, N_2O), the formation of NO_x is due to nitrogen oxidization (which either existed in the fuel or from combustion air) at high temperatures [32].

Wood combustion process passes throw stages, starting from drying, pyrolysis, combustion of evolved gases, and finally carbon dioxide oxidation. Table 3-1 shows the four stages and the temperature ranges for each one [8].

Table 3-1. Temperature ranges in combustion stages [8]

Stage	Temperature
Drying	288 – 373 K
Pyrolysis	373 – 475 K
Combustion of evolved gases	475 – 775 K
Oxidation of carbon	Above 775 K

Noting that for the range from 553 K to 775 K heat is produced from gases reactions, at this stage carbon dioxide and water vapor are highly produced followed by flame ignition. After all gases and tars are withdrawn, carbon (or charcoal) remains to be combusted after that [8].

Char combustion or gasification happens following group of reactions summarized by H. Hurt and M. Calo in [101], and for heterogeneous reaction with water vapor and carbon dioxide et al. Y. Haseli [102] and [103]:

$$C + O_2 \rightarrow CO/CO_2 \quad (Global\ power - law) \tag{3-2}$$

$$C + CO_2 \rightarrow 2CO \tag{3-3}$$

$$C + H_2O \rightarrow CO + H_2 \tag{3-4}$$
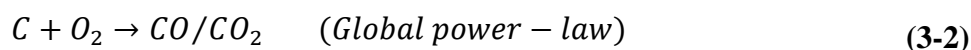
Water is produced mainly from the following reactions [104]:

$$CO_2 + H_2 \rightarrow CO + H_2O \tag{3-5}$$

$$CO + 3H_2 \rightarrow CH_4 + H_2O \tag{3-6}$$

$$H_2 + 1/2\ O_2 \rightarrow H_2O \tag{3-7}$$

Thermal formation of NO could be represented using the following reactions [105]:

$$O + N_2 \leftrightarrow NO + N \tag{3-8}$$

$$N + O_2 \leftrightarrow NO + O \tag{3-9}$$

$$N + OH \leftrightarrow NO + H \tag{3-10}$$

The stoichiometric equation is obtained from ultimate and proximate analysis and the heat produced as well, see table 3-2.

Table 3-2. Biomasses proximate and ultimate analysis

Chemical component	Value % Wood	Value % Straw	Value % Olive (Jordanian sample)	Value % Torrefied wood pellets 275°C
Proximate analysis(dry)				
Fixed carbon	15.5	18.27	17.4	22.75
Volatile matter	84.2	72.5	77.3	75.6
Ash	0.3	9.23	5.33	1.65
Total	100	100	100.03	100
Ultimate analysis				
Carbon	51.2	46.3	52.5	54.5
Hydrogen	6.28	5.33	7.02	5.84
Oxygen	42.394	47.407	39.39	39.034
Nitrogen	0.12	0.74	0.86	0.58
Sulfur	0.006	0.223	0.23	0.046
Total	100	100	100	100
HHV (MJ/kg)	20.380	17.75	21.66	21.58
LHV (MJ/kg)	19.06	16.62	20.15	20.35

In Aspen Plus, the combustion part is performed by using two reactors, RYield and RGibbs as shown in figure 3-2.
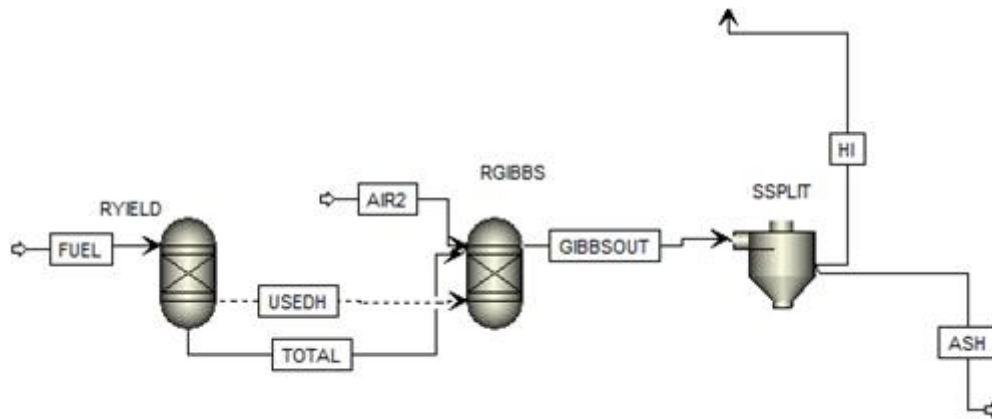
Figure 3-2. Combustion model in Aspen

Ryield reactor used when the stoichiometric reaction is not known, the reactance's, and the products are given without any need for the kinetics. RGibbs reactor performs the chemical equilibrium by minimizing the Gibbs free energy. Since biomass is considered as a nonconventional component, RGibbs reactor can't do the energy calculations, as a solution the RYield reactor is placed before RGibbs to convert biomass to constituent elements [106]. The residues components yields (mass basis) in are shown in table 3-3 for RYield reactor.

Table 3-3. RYield reactor components yield values

Components	Olive	Wood	Straw	Torrefied
N_2	0.00756945	0.0011409	0.0067747	0.00544167
O_2	0.34847505	0.40306	0.4340108	0.3662245
H_2O	0.0655	0.0464	0	0.0463
C	0.4644465	0.48678285	0.42387622	0.51132956
S	0.0020559	0.00005704	0.00204156	0.00043158
H_2	0.06214425	0.05970696	0.04879612	0.00544167
Ash	0.04980885	0.00285224	0.0845006	0.01548062
Sum	1	1	1	1

The flue gas components are performed by specifying the expected products in RGibbs reactor, the components are ($C_{pure\ solid}$, CO_2, N_2, H_2O, O_2, H_2, CO and SO_2). Heat stream is necessary between both reactors to transfer the heat of reaction to RGibbs. Finally, by adding SSPLIT the ash component is separated from the flue gas stream.

Air stream is necessary to complete the reaction in RGibbs, it is adjusted in order to keep a specified value of combustion temperature (i.e. controlling air to fuel ratio AFR or combustion lambda)

The excess air factor (λ) can be calculated by eq. 3-11 [4]:

$$\lambda = \frac{Air/Fuel}{(Air/Fuel)_{Stoichiometry}} \qquad \textbf{(3-11)}$$

3.1.2 Modeling parameters

To study the cycle behavior with deferent parameters values, it is necessary to have a reference case. By using the sensitivity tool in Aspen, it is possible to make a kind of optimization by replacing a single value with a range with steps. For instance, pressure (*p*) is variated from 1.4 to 8 bar with a step of 0.3 bar, air mass flow through the compressor ($\dot{m}_{air}$) is also variated from 0.001 to 0.045 with a step of 0.001. At each mass flow step pressure is variated with the given range. This process is at one TIT, the maximum power is registered, and the complete process is repeated for another TIT values.

Table 3-4. Reference case parameters [64]

General Parameters	
Ambient temperature	300 K
Operating pressure	4 bar
Air1	0.017 kg/s (for reference case)
Thermal power input	15 kW
Compressor isentropic efficiency	0.78 (approximated from [57])
Turbine isentropic efficiency	0.82 (approximated from [57])
Electrical generator efficiency	0.90 [68]
Temperature of HE terminals diff. (HED)	(20 K for reference case)

Considering the reference case parameters (table 3-4), mechanical output power is calculated from Aspen model, compressor and turbine performance is affected by $\dot{m}_{air}$ through the HE and p as well. Compressor and turbine behave in an increasing path with increasing air mass flow (noting that the power is delivered from the turbine and consumed from the compressor). At 0.017 kg/s turbine curved its path to a lower slope causing a decrease in the net power. At this point, the maximum output mechanical power is registered. It is important to note that the variation in figure 3-3 happens at constant pressure. On the other hand, and at a constant

$\dot{m}_{air}$, mechanical power behaves exponentially when p is variated, the maximum output power happens at $p = 4$ bar as in figure 3-4.
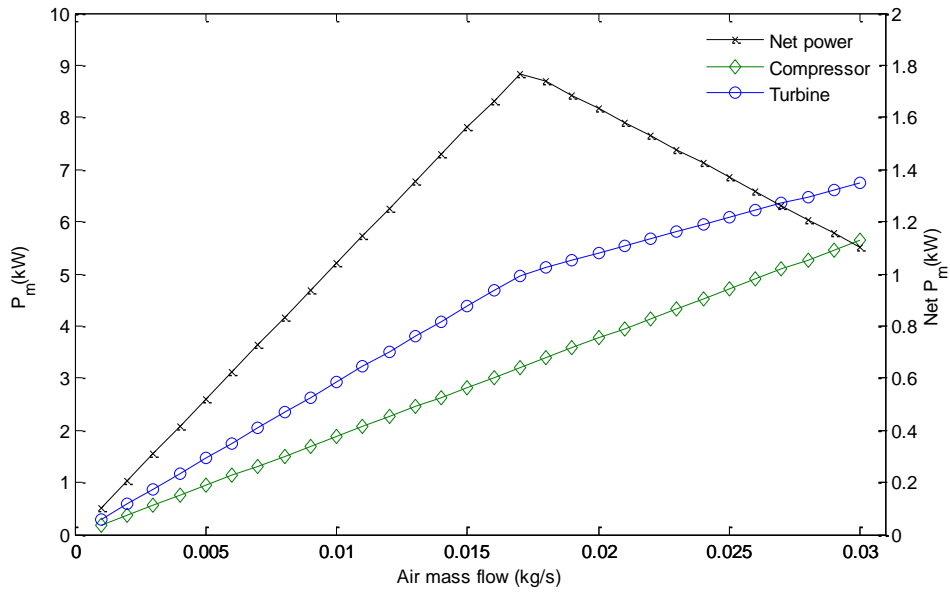
Figure 3-3. P_m variation with $\dot{m}_{air}$ [64]
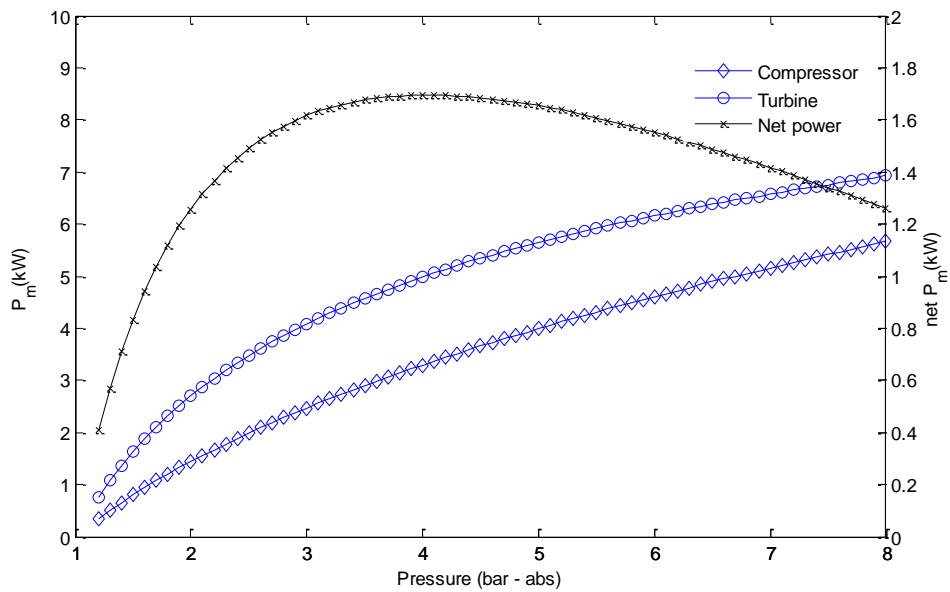
Figure 3-4. P_m variation with p [64]

As seen, the maximum net P_m is approximately 1.7 kW, this value happens at a single air mass flow. Furthermore, both figures are at 1062 K TIT with HED about 20 K. To be more general, both p and $\dot{m}_{air}$ should be assigned at different pressure and mass flow values, different TIT and HED, and power provided (thermal) as well.

Mapping of both p (and in other words pressure ratio - *PR*) and $\dot{m}_{air}$ flow through the compressor is generated by using Aspen Plus sensitivity tool. But before that, electrical efficiency is optimized at each turbine inlet temperature referring to the model shown in figure 3-1. The maximum electrical efficiency is achieved by changing both *PR* and $\dot{m}_{air}$.

The range of $\dot{m}_{air}$ in sensitivity is between 0.001 and 0.045 kg/s, with a step of 0.001. While *PR* range is from 1.4 to 8, low values are expected to be suitable for the operation [34]

TIT have maximum and minimum limits, the maximum is selected not more than 1100 K, and with a lower value of 600 K. Those considerations are due to limitations in on material firmness at high temperatures and inefficient operation at low temperatures. But in simulation results, TIT values are considered till more than 1800 K in order to make this mapping valid for high temperature standing material.

Flue gas temperature is controlled by air2 stream in figure 3-1, high temperature values can be reached by adjusting λ to 1, normal λ values are between 2-3. Previous steps resulting in a general mapping for *PR* and $\dot{m}_{air}$, (figures 3-5 a,b).

(a)

At HED = 100 K

(b)
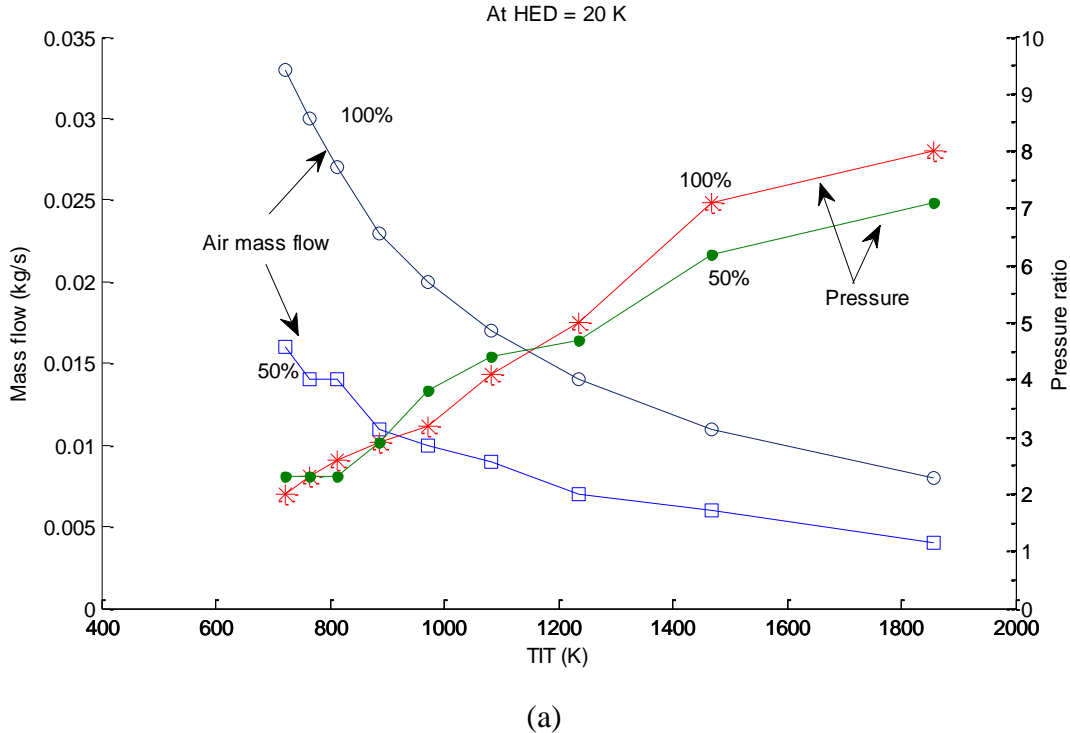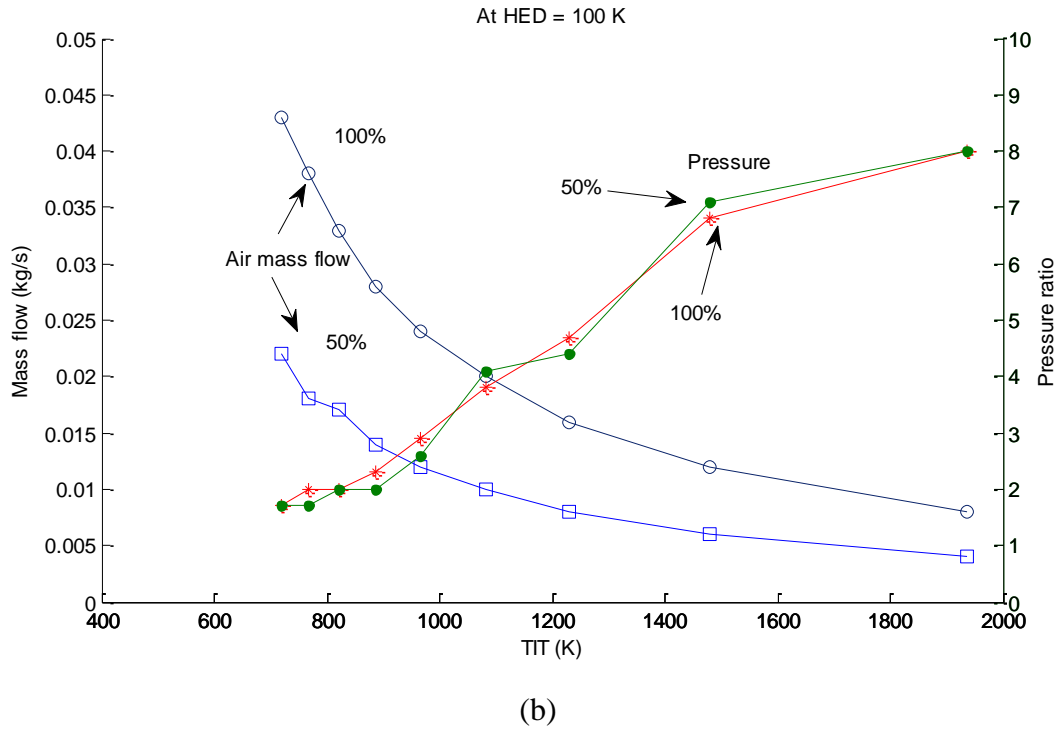
Figure 3-5. a) p and $\dot{m}_{air}$ mapping at 20 K HED. b) p and $\dot{m}_{air}$ at 100 K HED [64]

Optimized pressure values seem to be unaffected with input fuel power and HED, so a general linear variation with TIT could be concluded from the graph in figure 3-5 for pressure mapping. On the other hand, $\dot{m}_{air}$ at 100% of the fuel feed differs from 50%, and even for both HED values. $\dot{m}_{air}$ should be decreased exponentially with increasing TIT, the difference between 100% and 50% at low TIT values is higher than the difference for high TIT values.

Moreover, $\dot{m}_{air}$ curve for 100% of the fuel feed at 20 K HED has a lower offset than the same curve at 100 K HED. This indicates that lower HED means more heat transferred to the compressed air, so lower air mass flow, and lower power consumed from the compressor, and as a result higher efficiency.

We can estimate the relative equations from mapping, for instance, $\dot{m}_{air}$ follows the exponential equation 3-12 for 100% operation (i.e. 15 kW$_{th}$) and HED = 100 K.

$$\dot{m}_{air} = a * \exp(b.TIT) + c * \exp(d.TIT) \tag{3-12}$$

a =   0.7999   b = -0.005971   c =   0.04153   d = -0.0009077

while pressure is represented by the linear equation 3-13.

$$PR = 0.0058\,TIT - 2.0636$$ **(3-13)**

3.2 HiL model

Practically, a 15 kW$_{th}$ Pyro-Man pellets burner is installed along with a typical water heating boiler for the combustion stage. While the rest components are performed as an integrated model by using HiL. HiL part is implemented by Wago Programable Logic Controller (PLC), this PLC handle data logging, monitoring, and complete plant controlling at the same time.

Codesys software is used to model compressor, turbine, and HE in WAGO$^{®}$ PLC. Referring to IEC 61131, codesys supports both Structure Text (ST) and Function Block Diagram (FBD) which are used here. In addition to other languages like Instruction List (IL), Sequential Function Chart (SFC), the Continuous Function Chart Editor (CFC), and Ladder Diagram (LD). The Visualization in Codesys improves the complete model presentation, parameters variation for several operational cases, data monitoring, and devices controlling [107]. Figure 3-7 shows the complete project performed in Codesys visualization. This visualization performs the model for EFGT components except the burner, entitled in the dashed line in figure 3-6.In addition, it handles measuring and controlling combustion process that performed by the burner.
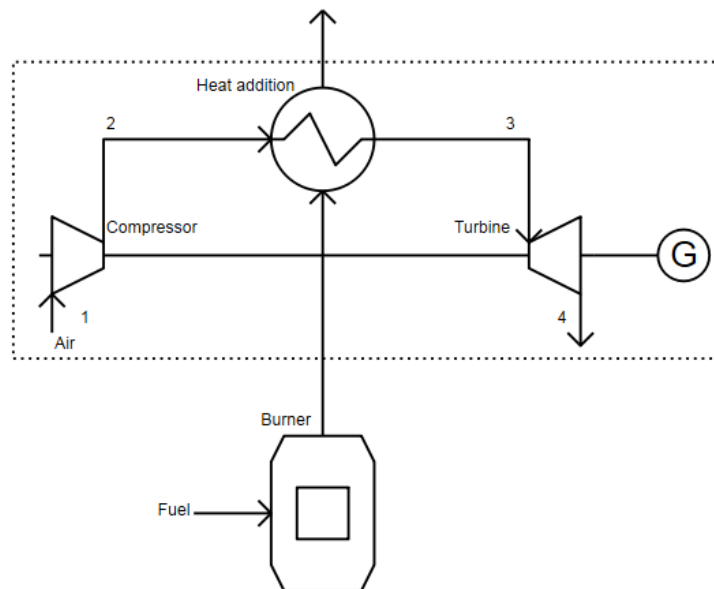

Figure 3-6. Open EFGT cycle.
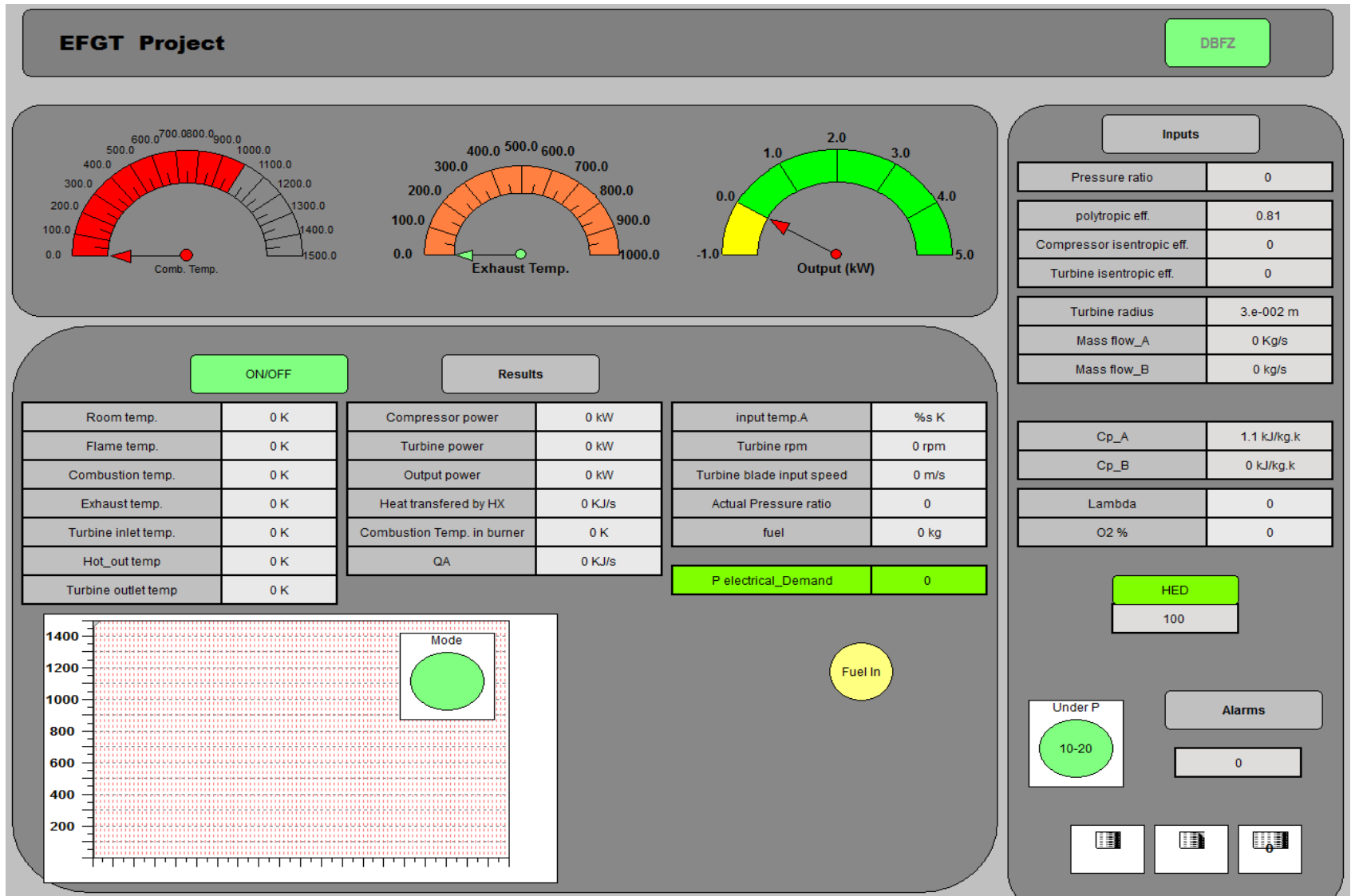
Figure 3-7. Visualized system.

3.2.1 Heat exchanger model

As estimated from literature, shell-tube heat exchanger is the optimum choice for the proposed system due to combustion criteria (e.g. dirty biomass combustion products). Since heat exchanger is responsible for energy transfer from the combustion, it is important to be designed to transfer as much heat as possible from combustion to the fluid (i.e. air) inside. In addition to meet combustion type conditions like slagging and high temperature.

Heat exchanger could be modeled dynamically either by logarithmic mean temperature difference or number of transfer units (NTU). Logarithmic mean temperature difference is used when temperatures on heat exchanger terminals (outlet and inlet) are known, while NTU when only the inlet temperatures are known.

Another practical and common method in modeling heat exchanger is using heat exchanger temperature difference method (HED), this value comes from experiencing such exchangers in the practice. Typical values taken in literature are between 20 –300 K, lower HED means better performance (i.e. higher turbine inlet temperature (TIT)). Detailed values are included in results for comparing and validation.

Heat exchanger could be geometrically calculated by using operational conditions in this research (table 3-5). Since heat exchanger is used as a model in HiL, geometrical design is useful for further researches but not considered as a main discussion in this study.

Table 3-5. Geometrical design parameters (subscriptions referring to figure 3-1)

Parameter	Value
T_{HI}	1500 K
T_{CI}	487 K (at 4 bar)
P_{th}	15 kW
$U_{average}$	20 W/m^2.K [108]
$\dot{m}_h$	0.014 (average value depending on the fan) kg/s
$\dot{m}_c$	0.015 kg/s
$c_{p,1500\,K}$	1.23 Table A4 [109]

Substituting values from table 3-5, both outlet temperatures, and ΔT_m are calculated:

$$T_{h,o} = 687\ K$$

$$T_{c,o} = 1500\ K$$

$$\Delta T_m = 168$$

Using information from table 3-5 we get the heat exchange area (A) of about A=4.46 m^2, take safety factor 1.4, the heat exchange area becomes 6 m^2. Several design assumptions could be ordered depending on available area. For instance, considering shell-tube HE, with length of 1.5 m, 20 mm outer tube radius, the calculated number of tubes in the heat exchanger is 32.

The design of HE should meet the maximum operating conditions like heat transfer amount, terminals temperatures, and available space. Other important aspects like temperature firmness, pressurized fluid, and cost should be taken into consideration for the physical operation.

The geometric design of the heat exchanger is concerned with combustion type, for biomass combustion, slagging is one of the disadvantages or challenges that should be overcome. This means enough space between tubes to avoid blocking flue gas path through some parts with time, since such case would maximize the heat resistivity so less heat is transferred. Additionally, cleaning and maintenance procedures should be included in design considerations.

Pressure value at outlet terminals would not be practically as inlet value, this means an additive factor in total efficiency detraction, where the pressure drop (Δp) decreases the ideal area in T-s diagram presented previously, pressure drop comes as a function of friction, tube length and diameter, and fluid mass flow (eq. 3-14) [82]:

$$\Delta p = f\,\frac{\rho u_m^2}{2D}\,L \qquad\qquad \textbf{(3-14)}$$

$$u_m = \frac{4\dot{m}}{\rho \pi D^2}$$

Friction factor (f) implies the roughness of tube material, smoother surface implemented by low values, and it increases with roughness increasing. Starting from Reynolds number (Re)

$$Re = \frac{4\dot{m}}{\pi D \mu} \qquad\qquad \textbf{(3-15)}$$

And from table A.4 in [82], then assuming $\bar{T} = 700\ K$ so $\mu = 338.8 \times 10^{-7} N.s/m^2$, D = 0.02 m, $\bar{\dot{m}} = 0.017$, Re becomes:

$$Re = \frac{4*0.017}{\pi*0.02*338.8\times10^{-7}} = 31943.73$$

The friction factor (f) then is calculated by the correlation which is suitable for smooth surfaces in the form of.

$$f = 0.184 Re_D^{-1/5} = 0.023 \qquad\qquad Re_D \geq 2 \times 10^4 \qquad\qquad \textbf{(3-16)}$$

3.2.2   Turbine model

Turbine performs a major rule in energy conversion. Proper geometric consideration should fit flow and power amounts. It is possible to consider the turbine radius for the purpose of geometry design.

Turbine rotor radius (r) is an important factor in determining the rotational speed, for instance, a radius of 10 cm can reaches 40000 rpm turbocharger rotational speed, 2 cm can reach around 200000 rpm [83].

For better overview, it is possible to use the model approximation (section 2.4.5) to find the rotational speeds as a function of TIT (figure 3-8). Assuming 2 cm rotor radius, rotational speed will start from 150000 rpm at approximately 700 K TIT, higher TIT values produce more than 300000 rpm for around 1200 K. Higher radius values decreases the rotational speed, for this research purpose a radius of 3 cm is considered.
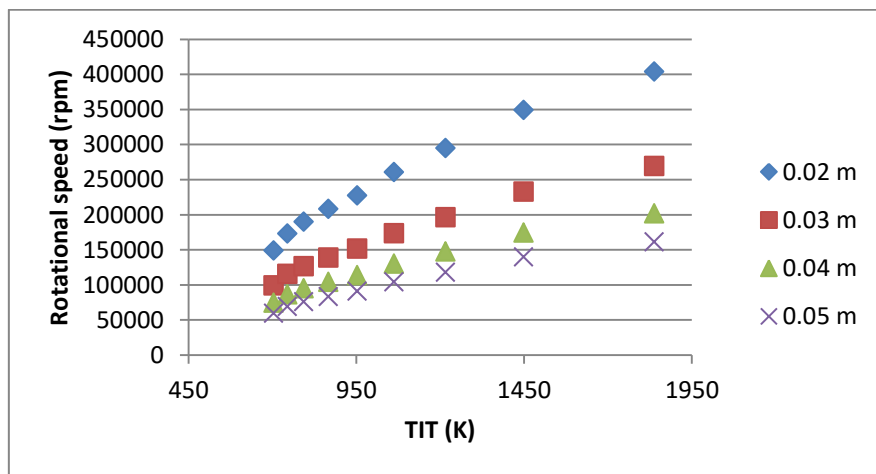
Figure 3-8. Turbine rotational speed at selected turbine rotor radius values

3.3 Setups and measurement system

To perform an adequate study, the practical part is selected to be combustion process. Biomass combustion is a main core of this study. A complete combustion system is prepared for this purpose as in figure 3-9.

Figure 3-9. Complete combustion system

3.3.1 Burner and combustion chamber

Direct pellets combustion system performs the heat addition part in EFGT cycle. These pellets are stored in a suitable tank to be fed later to Pyro-Man burner. Feeding system is a simple motor that is usually controlled from the burner itself to meet load demands (i.e. when used for normal heating). For experimental operation, it can be controlled from an external signal to meet the electrical power demands.

Figure 3-10. Open view of the Pyro-Man burner.

An open view of the burner shown in figure 3-10, the fan is responsible of delivering air to the combustion. Air enters combustion chamber from sides and from pellets feed tube. An important condition should be considered is pellets level in the combustion chamber, for safe operation, maximum pellets level in the pellets pipe should not exceed 20 cm from the combustion bed. Otherwise, the entered air will not be sufficient to a complete combustion, and a noticeable increase in CO level in the flue gas leading to flame extinguishing.

Along with the burner, the boiler comes in the second stage for heat transfer. For our system, the installed boiler is capable to deal with up to 20 kW_{th} for normal house water heating. There are actually no measurements installed for its operation (i.e. water heating), it is only provided with a recycling pump in a closed cycle water loop. A radiator for water cooling is installed within this loop in order to keep the temperature inside the boiler limited.

Pyro-Man burner can deal with pellets diameter from 6-8 mm as seen in figure 3-11, many other conditions should be satisfied to guarantee the proper operation. For instance, cleaning combustion chamber, see figure 3-12, and keep a good primary and secondary air values.

Figure 3-11. Pellets in storage tank
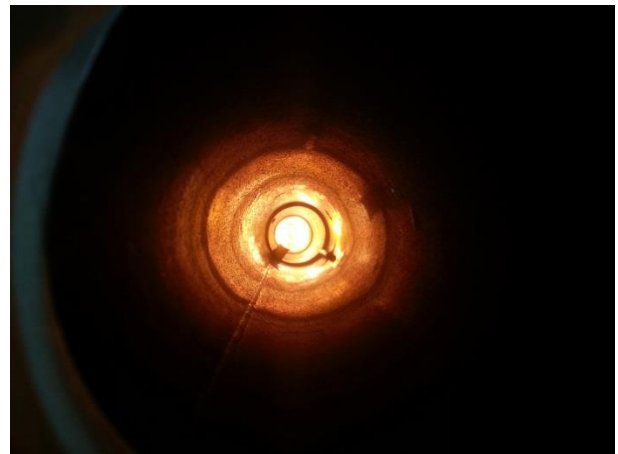
Figure 3-12. Combustion chamber

It is important to adjust pellets feed into the burner during starting and normal operation, since the motor feed is separated from the burner self-control board. Pellets feed motor is controlled by the PLC (which is also used as a HiL and measurement device as in the next section). Control strategy is as near as possible to the self-program in the burner, and that is estimated from practicing and noting the behavior. Feeding signal consists of ON and OFF positions in a periodic manner. In ON period the motor starts feeding and OFF it stops, time relevant to each period is important to guarantee enough feeding, and the same time prevent continues

accumulation of pellets in the feed pipe. For instance, ON period is 20 sec, and OFF period is 160 sec for full thermal power. Before reaching the steady operation, a delay of 20 min is made for the starting. Starting signal is 45 sec ON (the first period) and 4 min 30sec OFF, and then continue to be 20 sec ON with the same OFF period. PLC module signal is amplified to meet the relay coil switching voltage and power using transistor circuit shown in figure 3-13.

Figure 3-13. Switching amplifying circuit

3.3.2 Measurement system

The setup is equipped with a measurement system in several points, it comes as a connecting devices between the practical setups and HiL, in addition to complementing the control process. The data to be measured are basically temperatures, pressure, O_2 percentage in the flue gas, pellets weight, and flue gas flow. All readings are collected by the Wago PLC shown in figure 3-14 which also performs the devices model (i.e. HiL device which performs the rest of Brayton cycle components as mentioned previously).
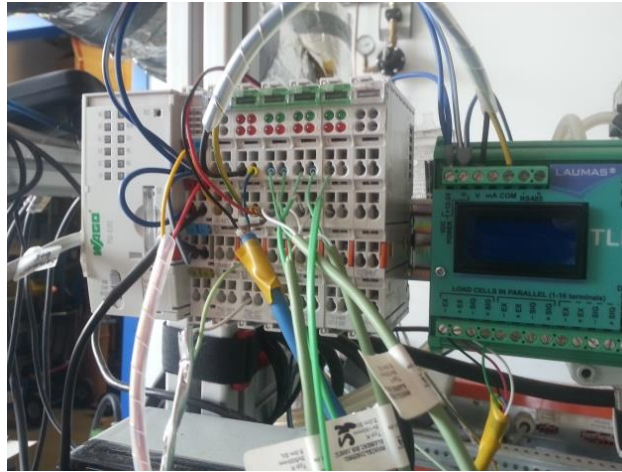
Figure 3-14. Wago PLC with its modules.

Temperature points are mainly taken for the flame at a distance of 12 cm from the burner flame pipe, the temperature sensor is installed inside a pipe as an indirect measuring in order to smooth flame instability, and this sensor is considered as the hot stream inlet temperature for the heat exchanger.

Figure 3-15. Temperature sensors in boiler

O_2 measuring performs two jobs, firstly to find out the combustion λ, secondly, as a safety indicator for the burner operation. The installed Pyro-Man burner needs enough input air for performing a good combustion. We notice a flame extinguishing once the O_2 in the flue gas

decreases beyond 8%, and unstable combustion for lower than 10%, so for safe combustion the O_2 should not be less than 10% in the flue gas where CO content is approximately 20 ppm.

Figure 3-16. Lambda probe

The flow of the flue gas (i.e. HE hot stream inlet) is measured by Orifice-blade concept. Here a blade of diameter 4 cm placed in the flue gas pipe as figure 3-17, then the pressure difference is measured (by taking two points before and after the blade). In addition, the temperature of the flue gas to assign density value.

The mass flow is given by [110]:

$$\dot{m} = \frac{C\varepsilon}{\sqrt{1 - \beta^4}} \frac{\pi d^2}{4} \sqrt{2\rho_1 \Delta p}$$

(3-17)

And coefficient of discharge is [111]:

$$Cd = 0.5959 + 0.0312\beta^{2.1} - 0.184\beta^6 + 2.286 \frac{\beta^4}{D_o(1 - \beta^4) - \beta^4} - 0.856 \frac{\beta^3}{D_o}$$

$$\beta = \frac{d}{D_1}$$
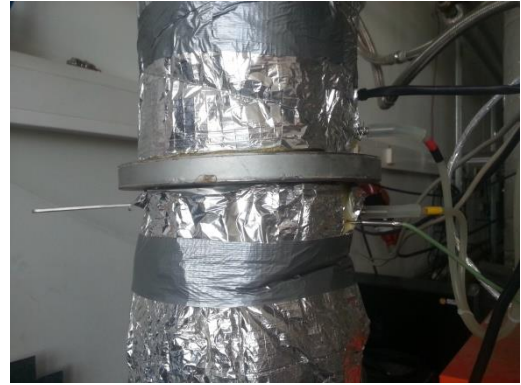
Figure 3-17. Orifice plate

The under pressure inside combustion chamber should be maintained between 10-20 Pa, high value could cause flame extinguishing due to the large amount of drained air, thus an under pressure sensor is necessary for safe operation.

Figure 3-18. Under pressure sensor

It is worth to mention that this controls the flue gas, and keeps approximately fixed flow of the total amount which consist both air and other gases produced from combustion. So if the fuel amount is reduced, the gases from combustion are reduced and the rest is compensated by increasing normal air in the mixture. That leads to the assumption of considering natural flow of combustion flue gases.

Additional balance is built in order to register fuel mass flow, figure 3-19.

Figure 3-19. Balance

Finally, gas emissions like CO_2, CO, O_2 are measured by gas analyzer (Eheim, Visit 02, PM-B-2,4, und 7). It is also useful for safety operation, especially for O_2 level and CO as mentioned previously.

Figure 3-20. Flue gas gases measurement

4 Results and discussion

The complete system is summarized in the schematic diagram (figure 4-1). In HiL all necessary inputs from combustion process, in addition to those common for the cycle are stated due to previous discussion in methodology. In addition, burner control with respect to load demands is in the scope of the setup.
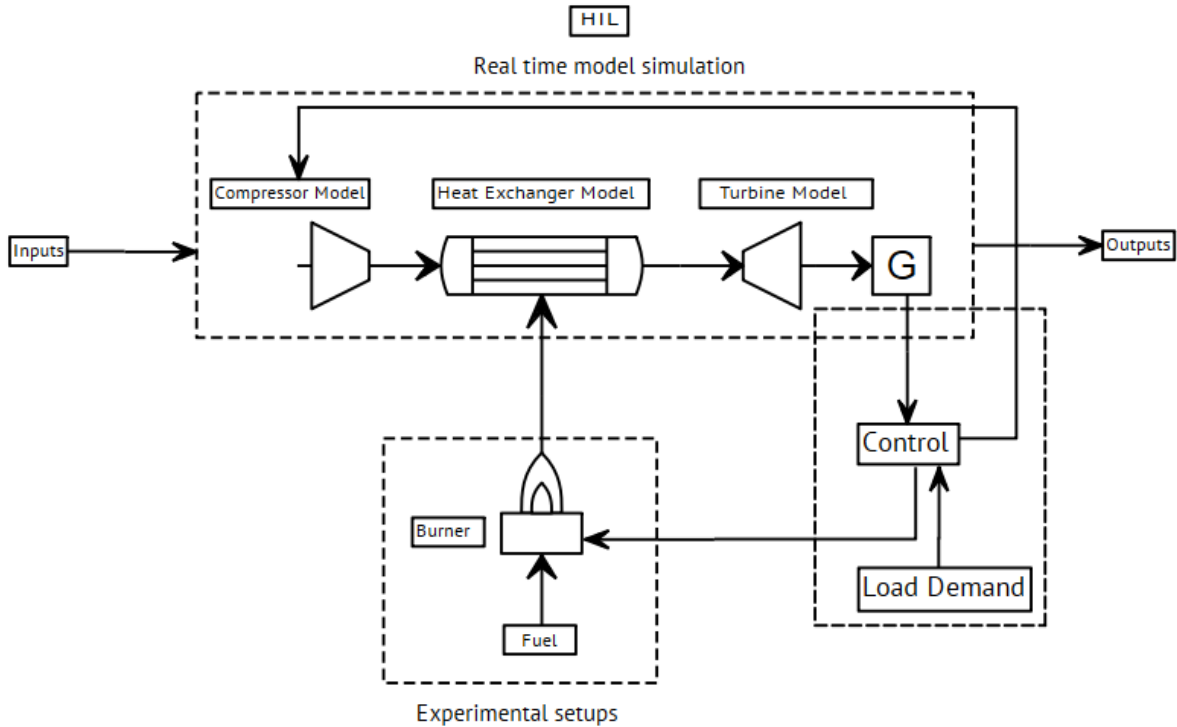
Figure 4-1. Complete system

Experimental In order to have logical results, it is necessary to set parameters to acceptable values. At the same time there is no exact consideration for complete system parameters, especially for the size in this research. Along with Aspen results that done previously, main researches grouped in table 2-4 are taken into consideration, where TIT, efficiencies, and HED are presented. This is also helpful in validating results from both Aspen and Codesys.

Parameters in table 3-5 are considered, additionally, for the flexibility requirements, further results are included even for parameters changing. A little difference is considered in the practical results than what presented. For instance, HED is considered to be 100 K, polytropic efficiency for both compressor and turbine is 81% in order to make real isentropic value with time.

4.1 HiL dynamic results

4.1.1 Validation with Aspen

Starting with results from the published paper in [64], the presented graph in figure 4-2 show the electrical power as a function of the hot inlet temperature stream (T_{HI}). In addition to full and half thermal power provided from the combustion process at two HED values.
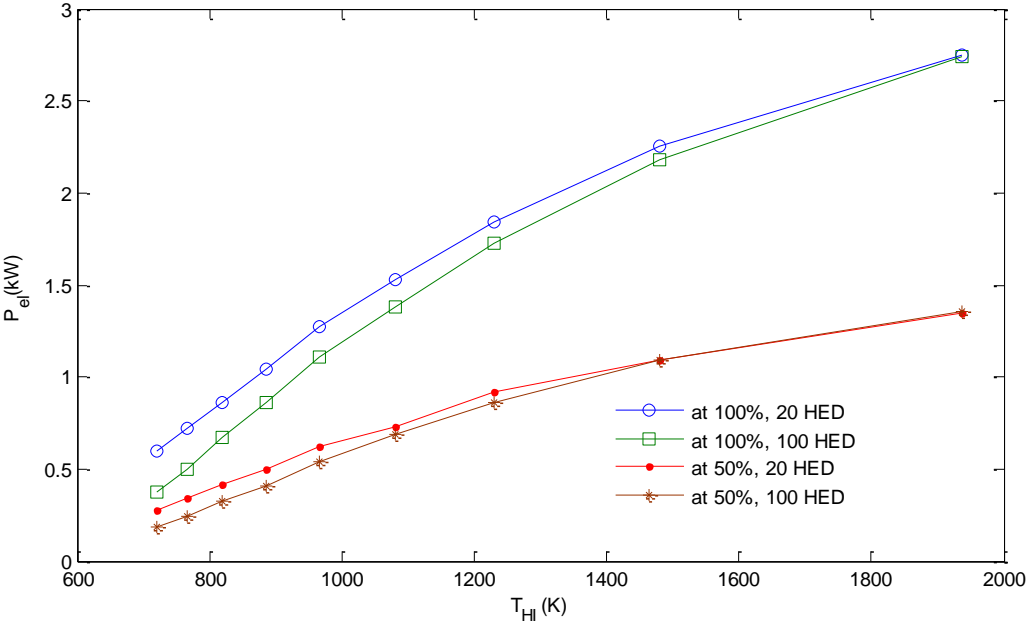
Figure 4-2 . Electrical power as a function of the turbine flue gas temperature for different HED [64]

Since the considered HED is 100 K for Codesys model, TIT could be considered in x-axis for power variation. Practically, TIT has a value of 950 K approximately, this results in having an electrical power between 1.3-1.4 kW. HiL values are near to Aspen model, which is a good starting validation (see figure 4-3).

Both *PR* and $\dot{m}_{air}$ are adjusted following maps mentioned previously. At the same TIT, we can see that the plant adjust both values to be 3.5 and 0.02 for *PR* and $\dot{m}_{air}$ respectively. From time 0 – 6 min it is considered as a transient period.
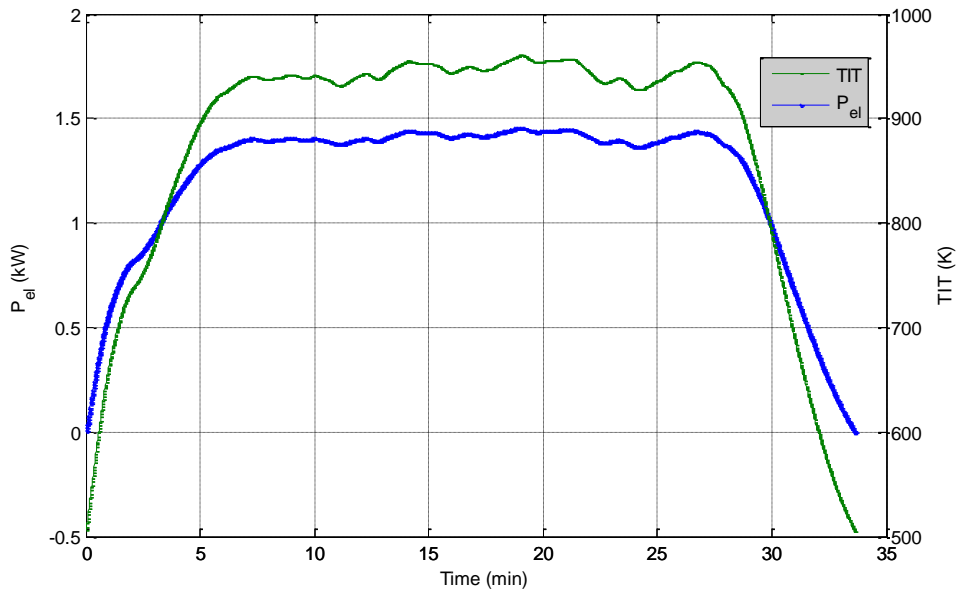
Figure 4-3. Electrical power and TIT
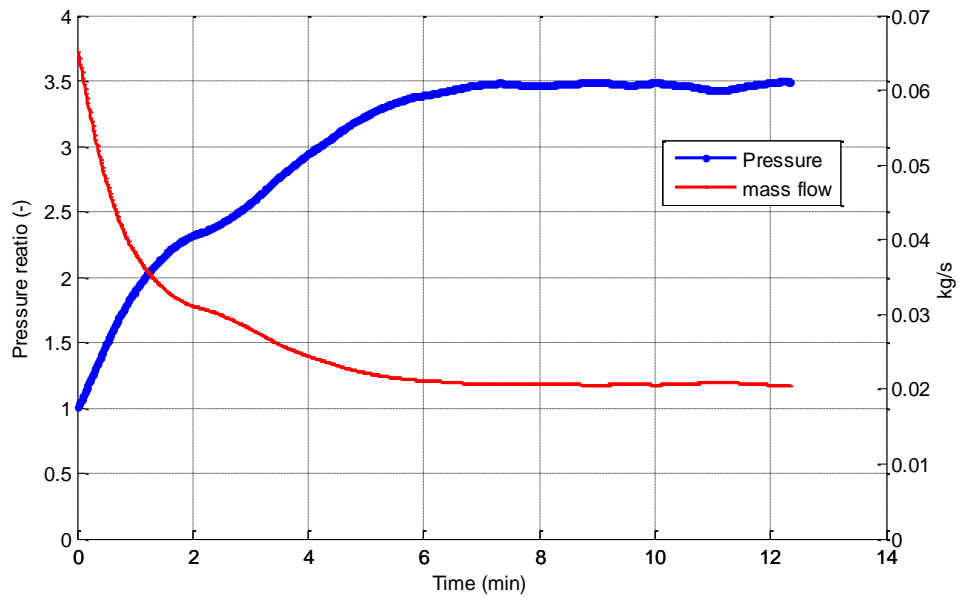
Figure 4-4. PR and $\dot{m}_{air}$ for the reference practical case

The behavior of electrical power from figure 4-5 and using the transient period in figure 4-4 is increasing with *PR* and the opposite with $\dot{m}_{air}$.
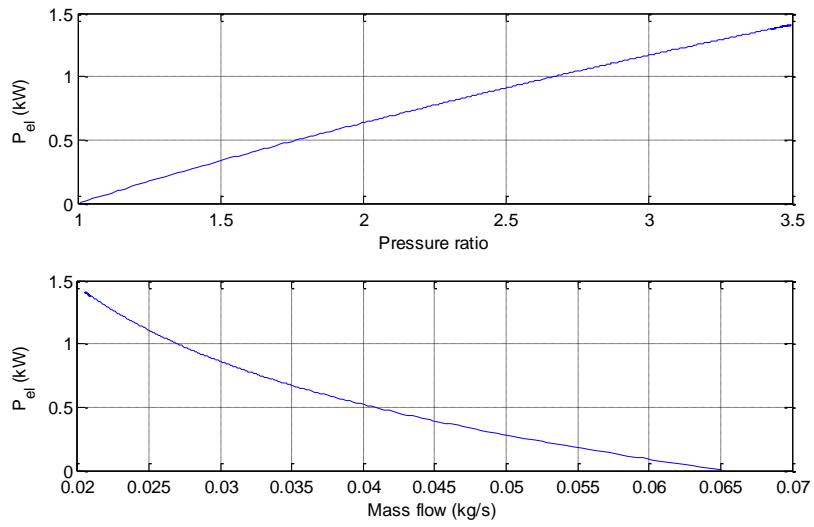
Figure 4-5. Electrical power with p and $\dot{m}_{air}$

Electrical efficiency calculated from HiL seems to be very near to Aspen results, we can say that the normal operation efficiency is around 9% when dealing with 950 K TIT. See both figures 4-6,7.
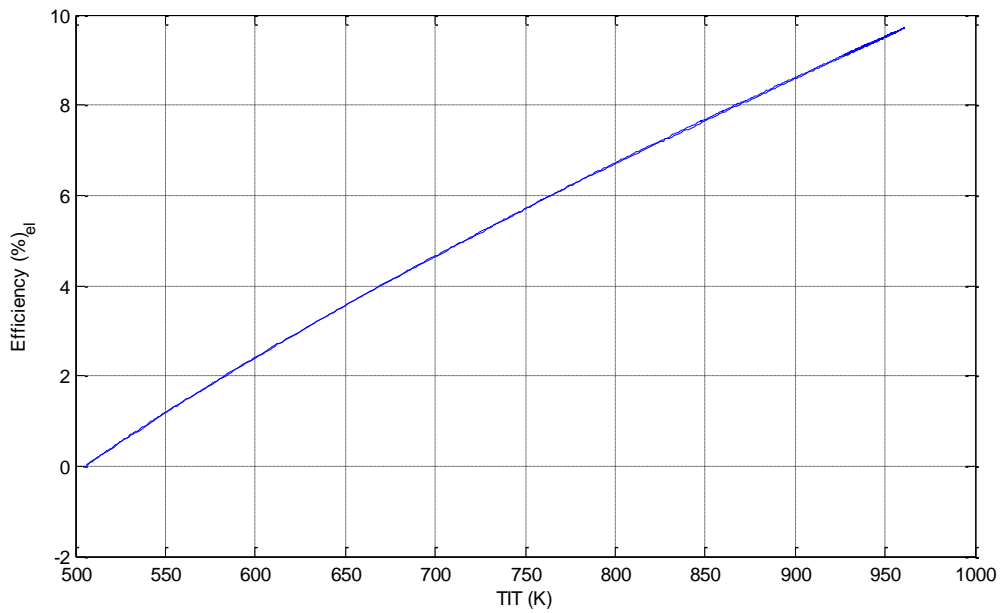
Figure 4-6. Reference case efficiency as a function of TIT
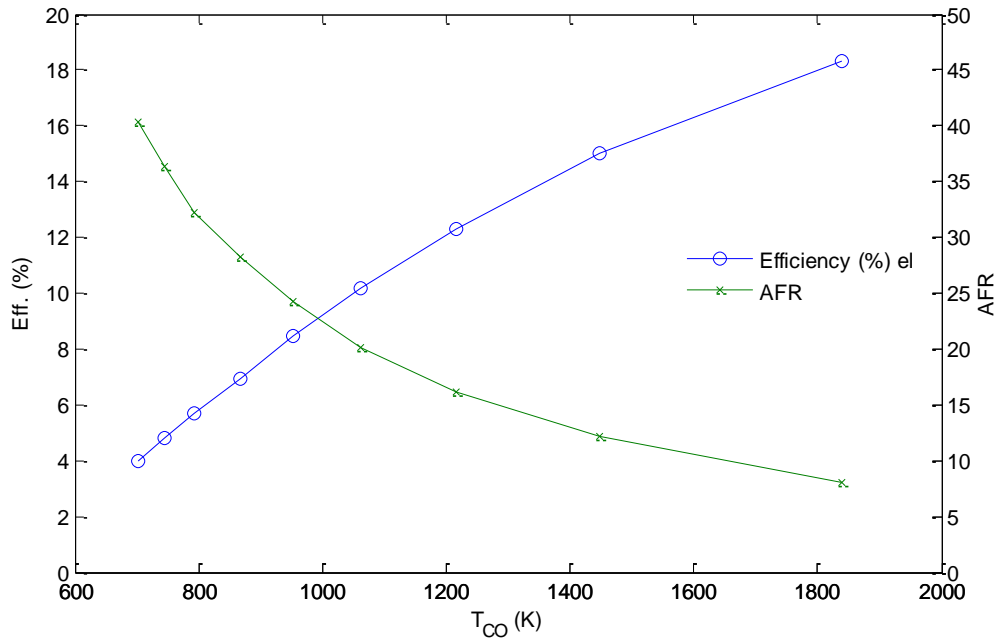
Figure 4-7. Efficiency and air to fuel ratio with TIT [64]

Simple differences between Aspen and Codesys refer to the slight change of polytropic efficiency. TIT can highly increase the efficiency when reaching very high values, however burner design should be capable for this, as well as the heat exchanger and turbine material. We can see clearly that the dynamic model deals with more precise efficiency rather than Aspen simulation. Aspen has a fixed isentropic efficiency of 0.78 and 0.82 for compressor and turbine. Those values are said to be lower than 0.78 and more than 0.83 as in figure 4-8.
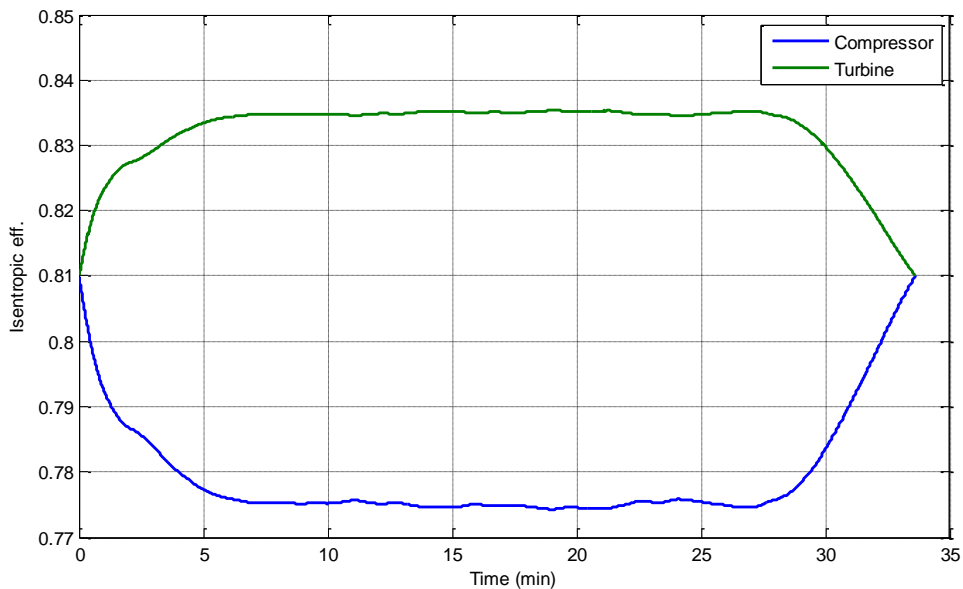
Figure 4-8. Compressor and turbine isentropic efficiencies

Other factors cause difference between simulation and HiL like flame instability and specific heat change with temperature. Those differences are normal by such comparison since they are with a very small error range. It is important to note that the flame temperature has a great effect on the performance. It is linked with other conditions like burner cleaning, humidity in pellets and under pressure. So we can see later that flame temperature could not be around 1050 K as mentioned in this section. Experiments are separately handled and differences mentioned are applicable in this situation.

Referring to literature efficiency values, and moving to the size of 15 kW$_{th}$, in addition to the comparison done in this section, we can say that electrical efficiency achieved here for the normal operation is acceptable.

For the reference case, we could summarize the T-s diagram with its four stages in figure 4-9.
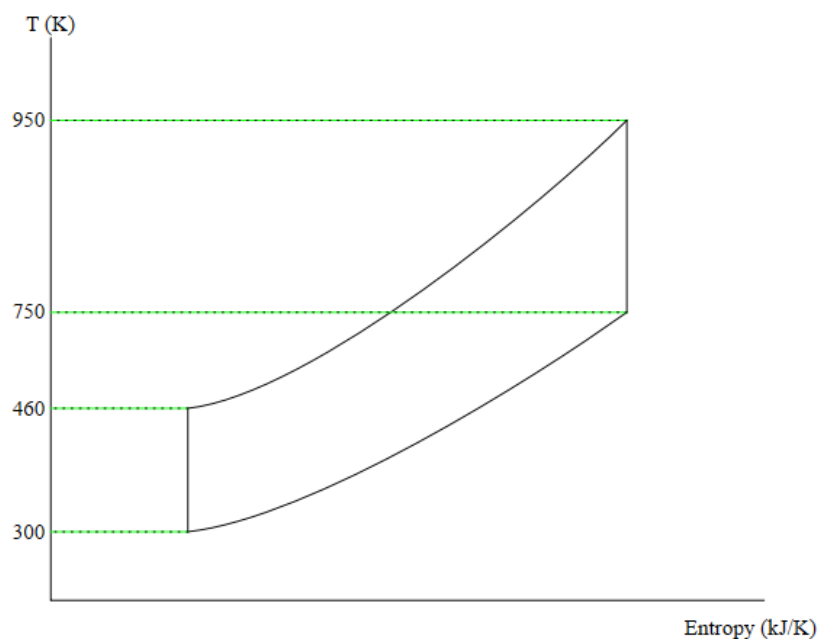
Figure 4-9. Ts diagram

The operating pressure is 3.5 bar, a small pressure drop value through the clean stream (CO) is registered to be 1.5 Pa. This value is dependable on the heat exchanger design and material used. High pressure drop values reduces the total efficiency since the mechanical power provided from the turbine is directly related to the pressure ration (However, its influence in this research is very small).

4.1.2 Thermal heat exchange

Heat exchanger temperature difference (HED) influence plays an important role in power extraction efficiency, higher HED mean lower turbine inlet temperature and output electrical power as well. HED is an indicator for the heat transfer ability from in the heat exchanger, which is affected by accumulated slag during operation. We can see that electrical power around 1.3 KW_{el} for HED 50 K as shown in figure 4-10, going over than 150 K HED leads to have beyond 1 KW_{el} for the steady state operation.
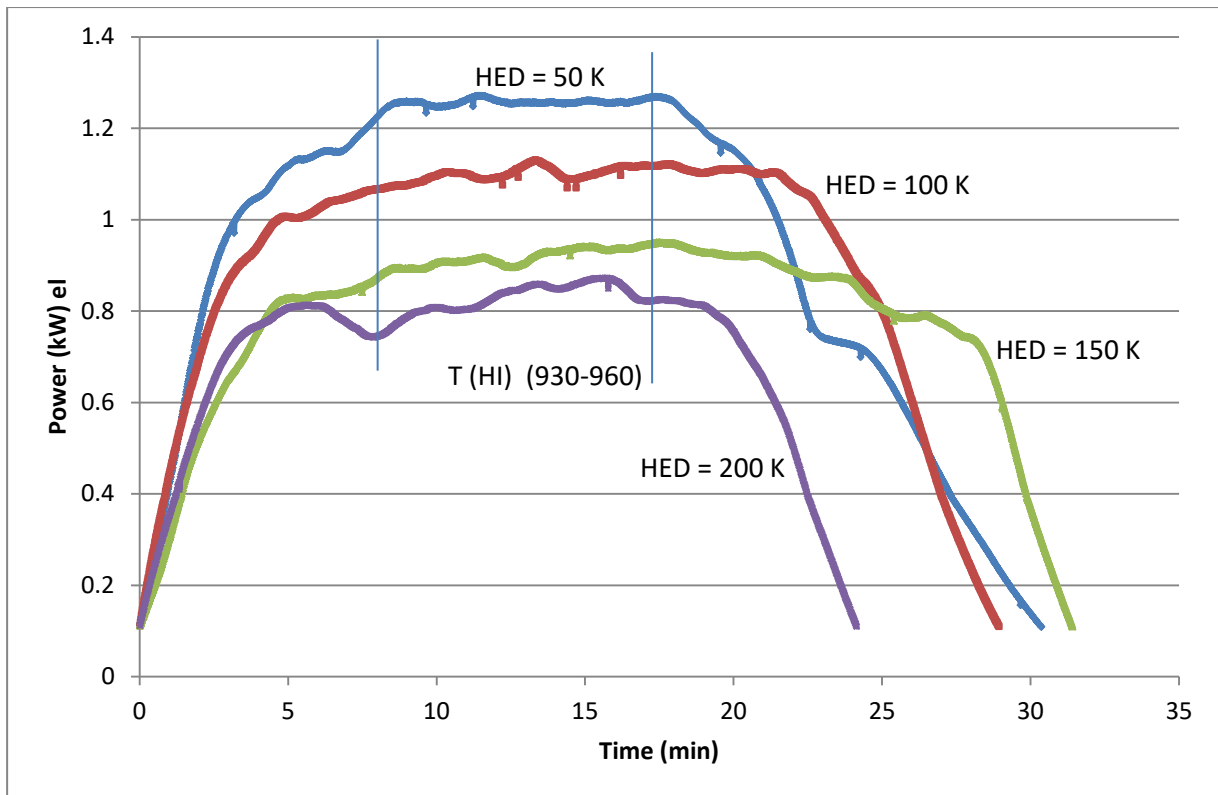
Figure 4-10. Electrical output power at different HED

Here it is clear that flame temperature is not in the maximum possible value, for instance 930-960 K, it appears that at HED 100 K registered even lower value than 1050 K in the previous section.

Both pressure and mass flow values in cold stream are adjusted to gain the maximum power (following mapping mentioned previously). But instead of depending on flame or flue gas temperature, the turbine inlet temperature is used to determine both optimum mass flow and pressure value as shown previously. It is important to note that mass flow map could be fixed for different compressor and turbine polytropic efficiencies, but pressure map should be

regenerated due to the dependency of isentropic efficiency on pressure ratio. Table 4-1 shows the steady state pressure and mass flow that should be adjusted.

Table 4-1. PR and $\dot{m}_{air}$ adjusted for different HED values

	HED 50 K	HED 100 K	HED 150 K	HED 200 K
$\dot{m}_{air}$ (kg/s)	0.0217	0.0237	0.0269	0.0288
PR	3.32	3.026	2.67	2.5

Referring again to Aspen results, large similarity is noticed between HiL and Aspen, the thing that also validates our results. In Aspen, flue gas temperature is around 950 K while in the real combustion is between 930-960 K.
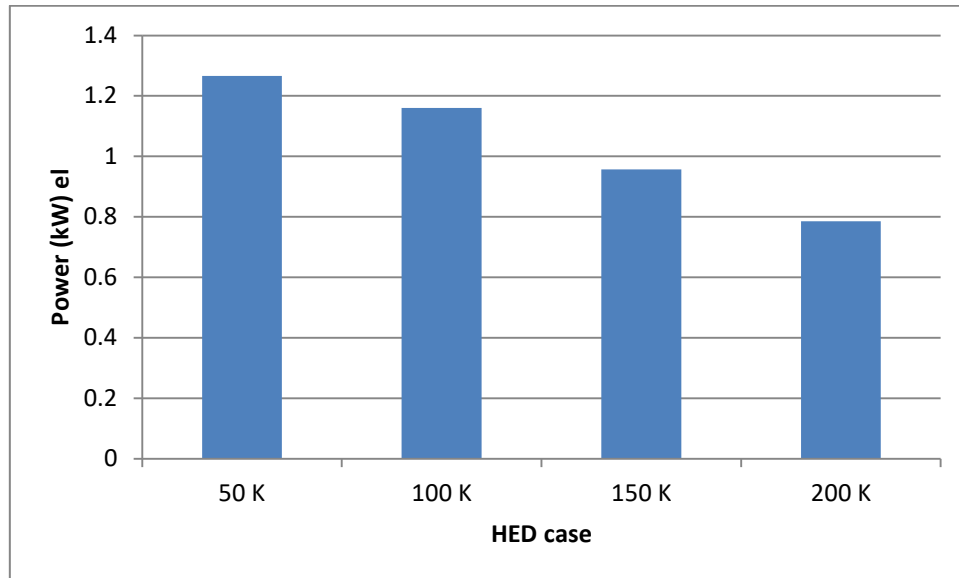
Figure 4-11. Electrical power at different HED values from Aspen [64]

The transferred heat is with an average of 10.0 kW_{th} as seen in figure 4-12. As a result, we can estimate that the exchanger efficiency to be around 66% taking into consideration the referenced parameters. This is a little bit higher than what mentioned in literature (i.e. 62% in [53]).
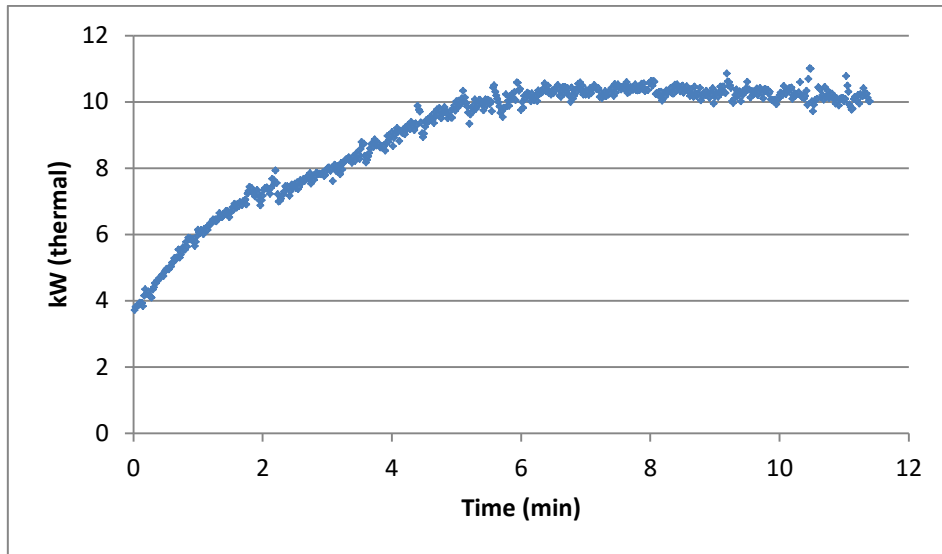
Figure 4-12. Heat transferred by the HE

HE efficiency is calculated depending on the input thermal power which is 15 kW$_{th}$, this is not a fixed value provided by the burner. By using balance data, we can easily find out the thermal power input. Slope of data feed in kg/s is shown in figure 4-13.
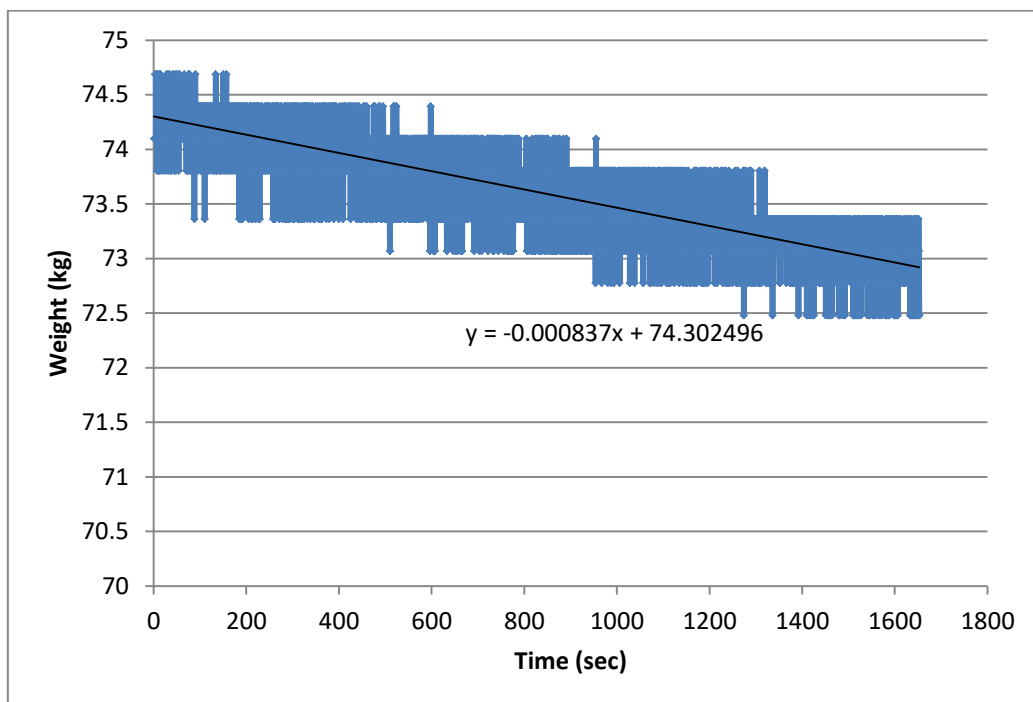
Figure 4-13. Pellets weight profile

Referring to the balance slope, plant needs around 3 kg to operate for one hour. This value is based on wood pellets as a fuel. However, consumption of other fuels could vary depending on the heat content.

4.1.3 Cold and warm starts

A small amount of pellets is used at the beginning to be heated and then burned. It needs from 10-15 min till the flame ignites. This period is followed by 20-30 min to heat up the equipment's. It is noticed that this period is the same to reach the maximum output power. Ignition devices should be periodically checked to avoid unsuccessful starting.

A relatively fast increase during the next 5 minutes is seen until about $1\ kW_{el}$. The approximate time needed until maximum power is 30 min, this is due to heat dissipated on boiler material itself.
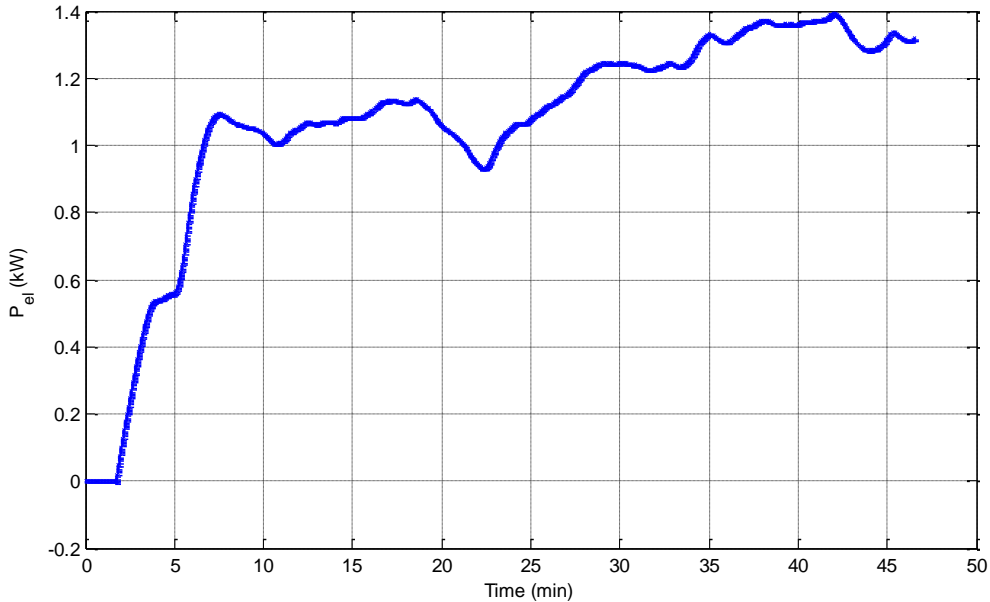
Figure 4-14. Cold start

Comparing this to the warm starting (e.g. in figure 4-10, 14), we can see a time of 5-6 min starting time needed to reach the maximum or steady state. We can see here one of the solid biomass combustion backwards, that is relatively slow starting compared with other oil or gas dependent.

4.1.4   Compressor and turbine performance

A natural temperature rise is accompanied with pressurizing air due to compressor isentropic operation. In the scope of our study, ambient temperature is considered constant (298 K) and pressure is 1 bar. Returning to the reference case, compressor consumes around 3.3 kW$_m$ for pressure ration of 3.4 approximately, air leaves the compressor with a temperature between 450-460 K (see figure 4-15).
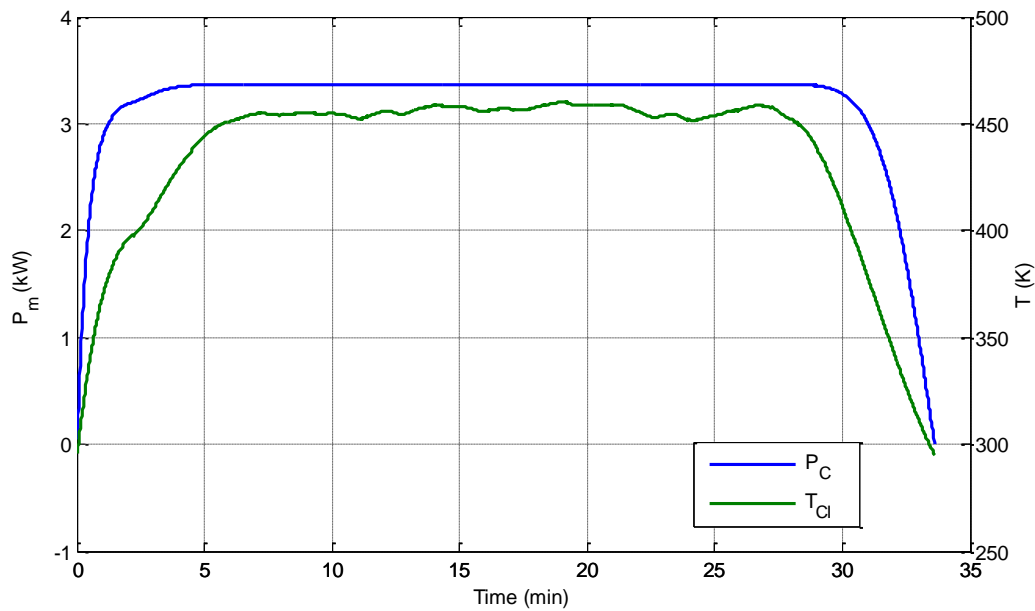
Figure 4-15. Compressor power and temperature.

On the other hand, turbine extracts around 4.9 kW$_m$ from the compressed air heated from the combustion (figure 4-16). Noting that this value is for 0.83 isentropic efficiency. Air leaves the turbine with around 750 K which is relatively high. Heat rejected from the turbine could be exploited in domestic heating or pellets preheating where higher efficiency could be gained.

It is possible that the turbine and compressor have different values of efficiencies, the thing that affects directly the generated power. After running the plant for each value separately, it is seen that for T$_{HI}$ of 920-945 K, the electrical output power is 1.48 kW at polytropic efficiency of 0.85. Noting that, this efficiency is considered for both compressor and turbine. At 0.81 the output power is 1.1 kW, and it decreases significantly for lower values like 0.75 where the output power is not more than 0.5 kW (figure 4-17).
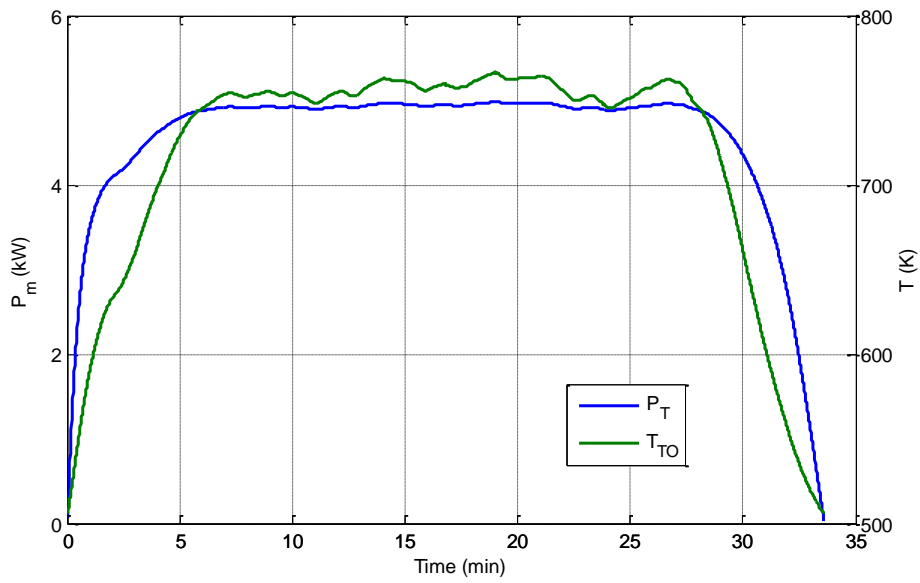
Figure 4-16. Turbine power and turbine outlet temperature
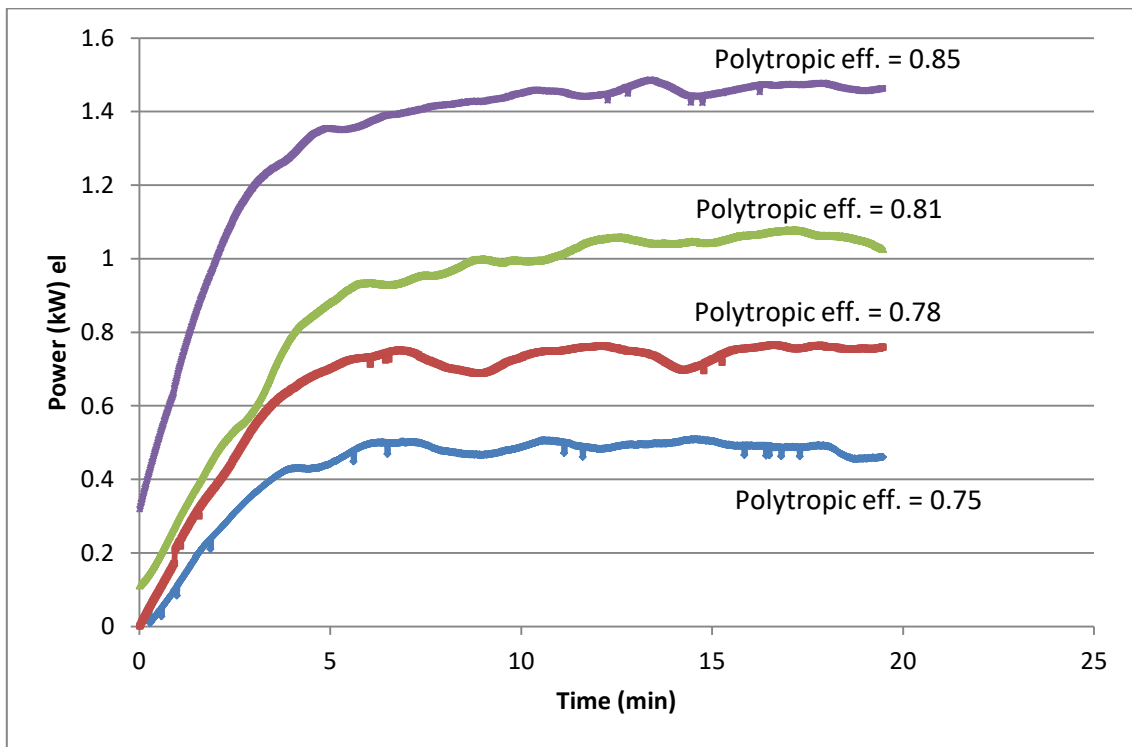
Figure 4-17. Electrical output power for different polytropic efficiencies, T_{HI} (920-945 K).

For the normal operation, turbine rotates at 155000 rpm approximately (figure 4-18). Take into consideration, that the flame temperature value for this graph is around 1050 K. It is

relatively connected to the power generated from turbine, which reaches approximately 4.5 kW
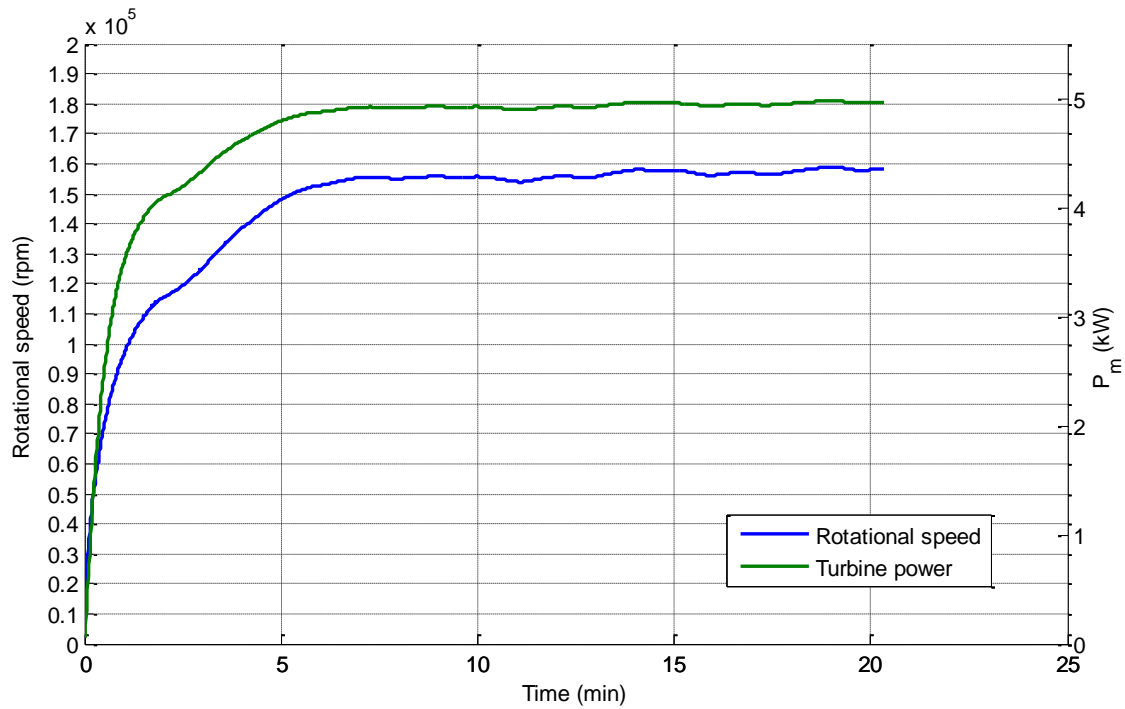
Figure 4-18. Turbine rotational speed and turbine mechanical power

High rotational speed needs in practical some considerations as mentioned previously like vibration, gearbox, and an electrical generator that can handle such value. Further cycloconverter is needed to change the high frequency current to lower one (e.g. 50 Hz). Gearbox could be another option by reducing the high rotational speed to the normal generators speed (e.g. 3000 rpm). This option should be carefully handled specially in coupling stages where high rpm could result in vibration that causes damage later.

4.2   Combustion

Burner fan is automatically adjusted with pellets amount or in other words the thermal power input. Unfortunately, parameters regarding fan operation have very restricted limits to be changed, and according to the manufacturer it is supposed to keep them as manufactured (this note is after contacting manufacturer).

Under pressure which is caused by air fan installed on the lab roof should be kept as mentioned previously between 10-20 Pa, lower or higher values could cause problems in extinguishing air or bringing smoke inside lab.

As we see, the total combustion air has many restrictions for the proper operation. This leads us to assume constant combustion air. λ as a result has a value ranges between 2-3. It becomes more stable at 2.3. (figure 4-19).
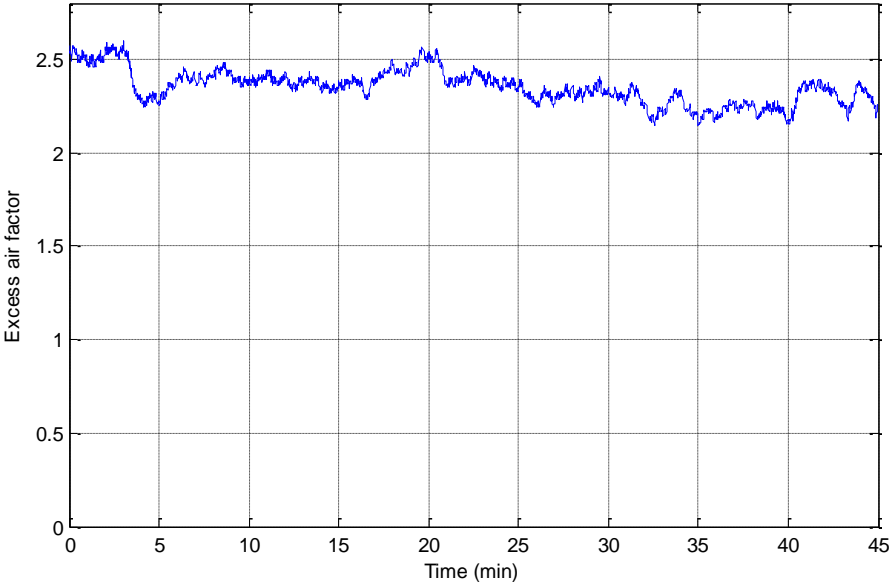
Figure 4-19. Combustion excess air factor (λ)

Wood pellets combustion shows 15 ppm approximately CO emissions in the steady state operation, on the other hand, NO_x is emitted with around 85 ppm. Those values are at oxygen content between 11-12.5 % in the flue gas.

Flue gas temperature is registered to have a maximum value of 1050 K, burner design can't go much further even if full fuel is provided. Reducing combustion air mass fuel could increase flame temperature (i.e. reducing λ). But for safety operation, under pressure is necessary as discussed previously. As a result, ash melting temperatures are not reachable (referring to ash melting section), this keeps us in the safe side of preventing ash melting. Cleaning becomes easier, and no hard slags expected to accumulate on the heat exchanger.

4.3   Other biomass types tests

Wood pellets are good example to be as a reference material in this plant. However, it is important to show the performance of this plant when using other types. This enhances the study on fuel type variation, which is important to acclimate with several places with different

biomass types. Considering many biomass types becomes too much for this study, thus we will interview two more types rather than wood, which are straw and torrefied.

4.3.1   Straw pellets

Figure 4-20. Straw pellets

Straw combustion performs the bad type of pellets to be used, this is due to low heating value shown in its analysis, and high ash content. Unfortunately, flue gas flame can't reach high values, this appears from TIT values that varies around 800 K at maximum burner feeding.

It is also clearly seen that the net electrical power is around 1 kW, which means an efficiency of around 6.7 % considering 15 kW_{th} entered the cycle (figure 4-21). A considerable ash amounts accumulated in a short time, this straiten the path for combustion air, which results in combustion problems.
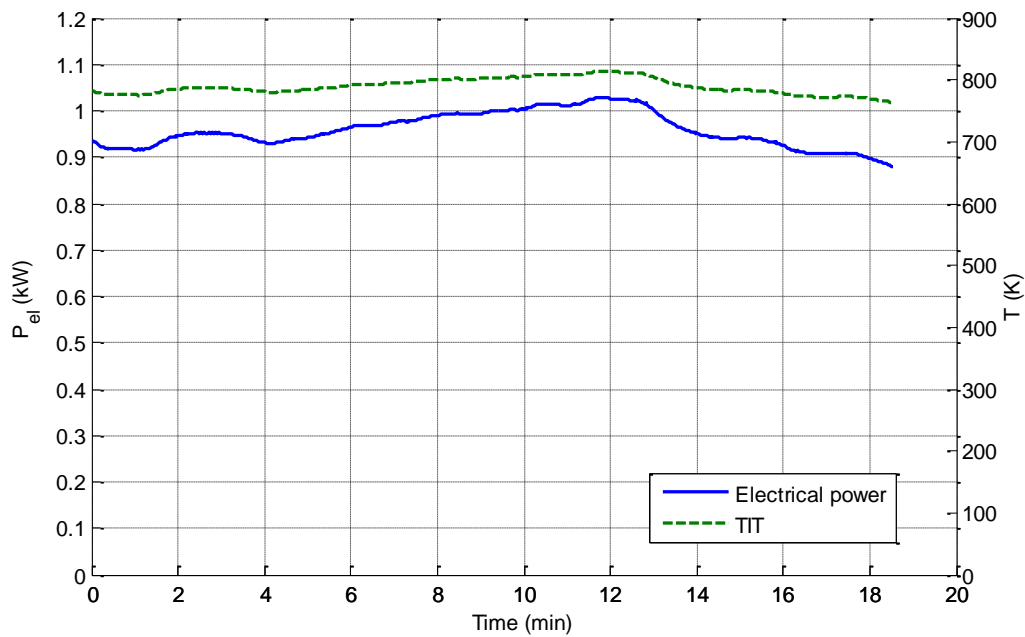
Figure 4-21. Electrical power and TIT data from straw pellets combustion

The direct combustion of straw pellets emits 13 ppm CO, a noticeable amount of NO_x which reaches 350 ppm.

4.3.2 Torrefied pellets

Figure 4-22. Torrefied pellets

In general, biomass could be pre-treated in the absence of oxygen and in temperature range between 200-300 °C. This is called torrefaction of biomass, which results in a complete

drying of biomass, increasing the calorific value, and grindability improvement. By those improvements we gain better combustible material and higher energy density [112].

Here we have tested the torrefied wood pellets at 275°C, the achieved flame temperature is around 950 K, while electrical power produced is 1.1 kW maximum (figure 4-23).
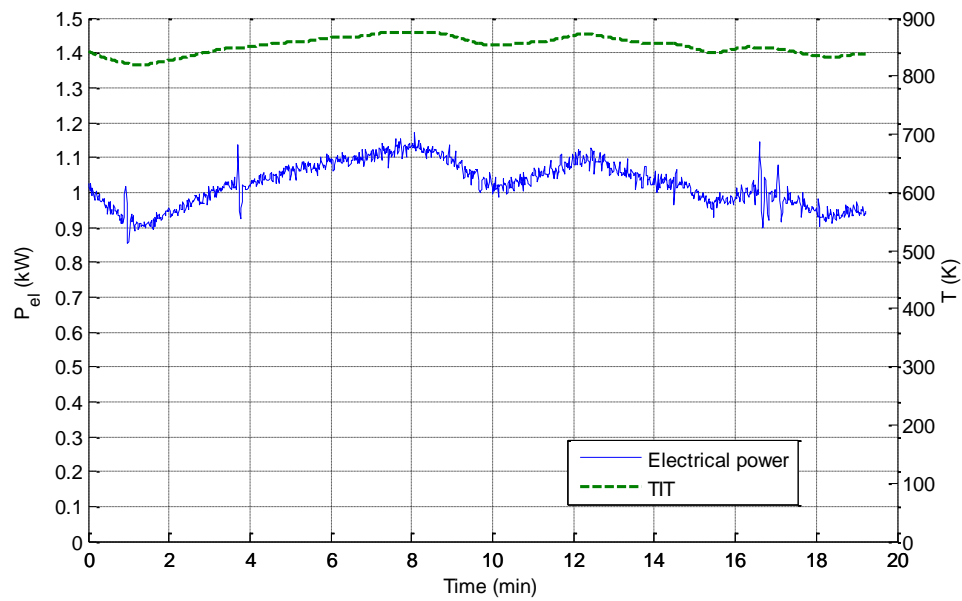
Figure 4-23. Electrical power and TIT for torrefied wood pellets

We can see clearly temperature and lower power than expected from torrefied pellets, it could be explained by having lower volatile matter (75.6%) compared with wood (84.2%) as an example, the thing that restrict the flame from the burner output tube. Higher values could be achieved by another burner design, but meanwhile, Pyro-Man shows this performance. However, lower flame temperature could be compensated by the heating content, torrefied pellets have higher heating value, and this leads to lower pellets consumption than normal wood pellets.

Combusting torrefied wood pellets show relatively lower CO emissions, around 6 ppm in the steady state operation. NO emission is around 200 ppm in the flue gas, which is lower than straw pellets combustion.

It is noticed that the average emitted CO from torrefied pellets is registered to be the lowest one. Where wood pellets combustion has the highest value, a summarized comparison between all types is shown in figure 24 and figure 25 noting that oxygen content in the flue gas is with an average of 12 %.
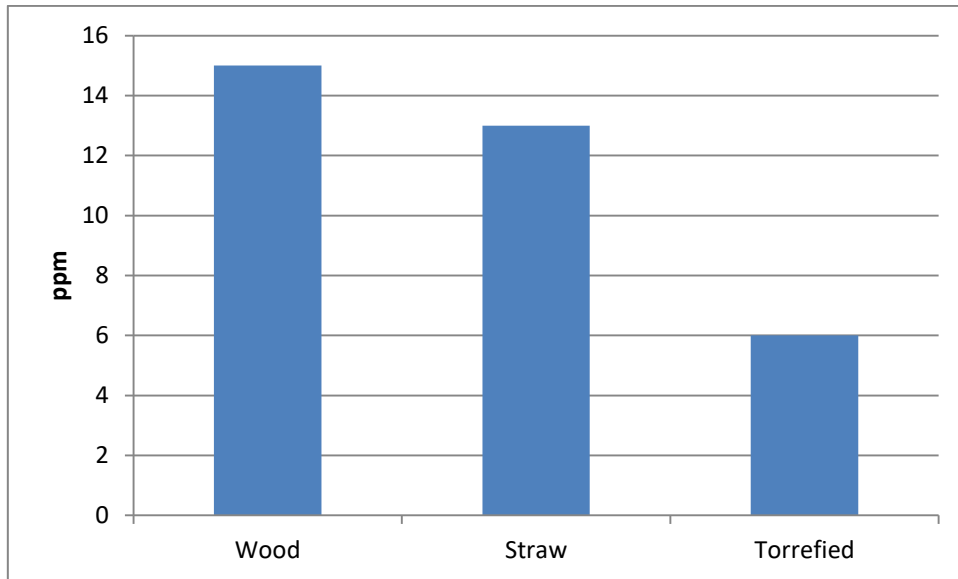
Figure 4-24. Fuels combustion CO emissions
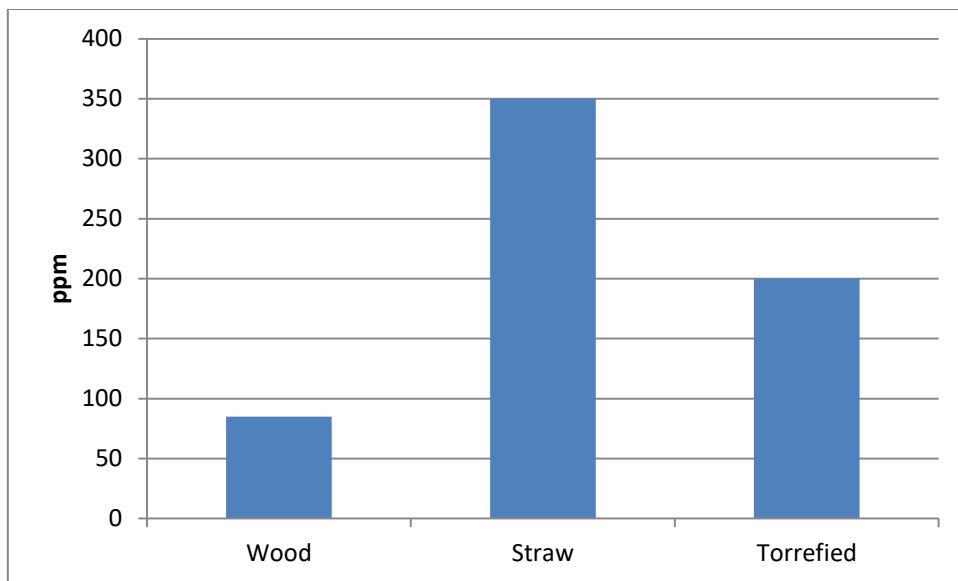
Figure 4-25. Fuels combustion NO_x emissions

4.4 Transient behavior

System components behavior performs the complete system response in transient case. But the slowest device is the dominant in this case. By returning to the system structure, compressor, gas turbine, heat exchanger, and combustion system are related components in this section.

4.4.1 Heat exchanger Transient

The discussion about heat exchanger transient operation is confined even it is important in plants modeling. Mainly, lumped parameter or finite volume approaches are used for this purpose as stated in [113]. In which the authors discussed a third criterion by using moving boundary approach. Evaporator simulation was conducted and it shows the temperature responses in a time of 10's seconds for various cases. Another control study in [114] is applied on shell tube heat exchanger to verify the response due to step input cold stream fluid temperature. All used methods in this research shows that the steady state (SS) is reached after 100 seconds in spite of the system controlled or not. In addition to further researches handle another types or configurations like co-flow heat exchanger transient response in [115], it also shows a step response for both hot and cold streams of lower than 30 seconds.

As a summary, David J. Bunce [116] explored the transient response of heat exchangers done in several researches. He claimed that there no general solution is completely accepted because of the complex operation. One of the discussed solutions is the finite difference method presented by F. E. Romie [117]. He provided the formulas in eq. 4-1 as a simple empirical relation to perform the transient behavior of the outlet temperatures with respect to inlet variations (modified by Bunce to start from any temperature since Romie considers zero as starting temperature in his solution).

$$\frac{T_1(t) - T_1(0)}{T_1(\infty) - T_1(0)} = 1 - Ae^{\frac{-a\theta_1}{1+V}} - Be^{\frac{-b\theta_1}{1+V}}$$

$$\frac{T_2(t) - T_2(0)}{T_2(\infty) - T_2(0)} = 1 - Ce^{\frac{-c\theta_2}{1+V}} - De^{\frac{-d\theta_2}{1+V}}$$

(4-1)

$$\theta_1 = \left[t - \frac{L}{v_1}\right]\left[\frac{C_{min}}{\bar{\bar{C}}_{wall}}\right]$$

(4-2)

$$\theta_2 = t\left[\frac{C_{min}}{\bar{\bar{C}}_{wall}}\right]$$

(4-3)

$$V = \left[\frac{C_{min}}{\bar{\bar{C}}_{wall}}\right]\left[\frac{L}{v_2} + \frac{L}{v_1}\right]$$

(4-4)

v: $Velocity$, 1 $for\ stepped$, 2 $for\ unstepped$

L: $Fluid\ flow\ Length\ of\ exchanger\ (m)$

C: $Heat\ capacity$

t: $Time\ (s)$

A, B, C, D, a, b, c, d: $Coefficients\ from\ table$ [117]

Equation 4.1 is examined for the suggested heat exchanger in this research with its parameters. If the hot fluid or the flue gas temperature is stepped from 300-900 K, air inside tubes (i.e. second stream) require around 60 seconds to reach the final value, see figure 4-26.
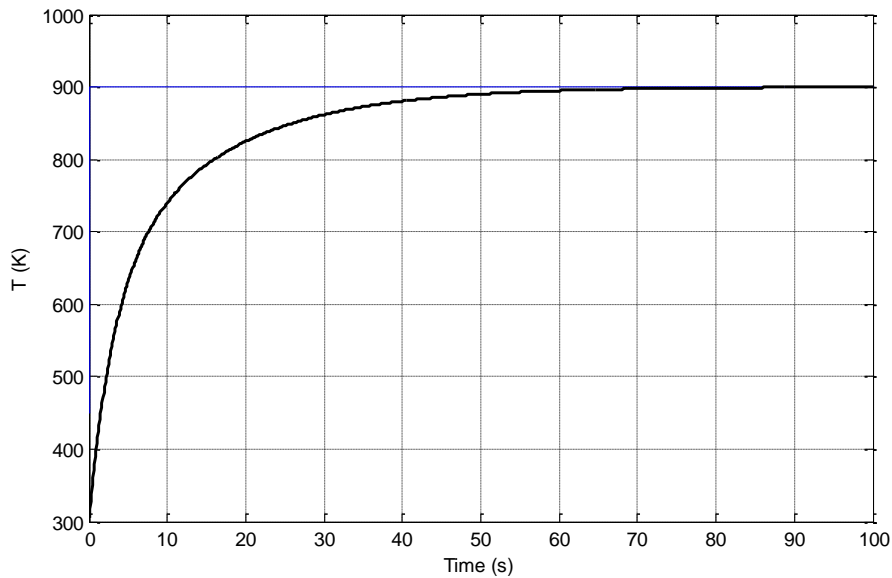
Figure 4-26. Heat exchanger temperature response

4.4.2 Turbine and Compressor transient

Compressor and turbine are both existed in many facilities, the closest application is the gas turbine (which is the concept of combination between both devices and combustion system). So the transient behavior could be approximated from the researches on gas turbine, separate researches on either compressor or turbine, or turbocharger configuration.

R.D. Burke et al. [118] analyzed the transient response of heat transfer in turbo charger. Results show that 95% of the input and output transient conditions need time varies between 4-20 seconds.

A detailed transient behavior for gas turbine cycle shown in [119]. Load step response functions of 30, 22.5, 15, and 7.5 kW are shown. For our purposes, we would consider the

lowest load value. Compressor reaches its final value when stepping to 7.5 kW after 35 seconds. The same thing applied on the turbine power response. Further step response values of speed, efficiency, turbine inlet pressure, and temperature require approximately the same time period

A research is provided on modeling compressor and gas turbine by P. Aaslid in [120], the system is much larger than presented here, it is about 8570 kW, but it worth to have a look on the transient analysis provided, the compressor up stream pressure change in the transient needs around 100 seconds as well as well as other parameters. Power response due to stepped fuel input requires around 10 seconds, fuel mass flow is changer from 0.8 to 1 (i.e. 80% to 100%).

Many other researches and experiments show that compressor and turbine have a relatively fast response compared with heat exchanger [121][122][123][124][125][126][127].

4.4.3 Combustion process transient

The related components (burner and boiler) determine the transient behavior of the combustion or heat addition to the cycle. From tests, burner can rises the temperature of the inlet hot stream from 620 K to 1050 K in around 6 min.
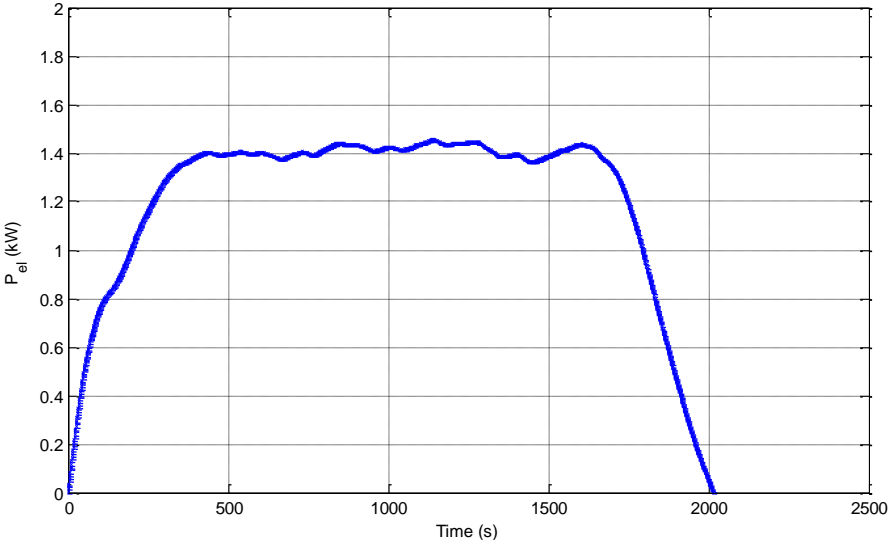
(a)
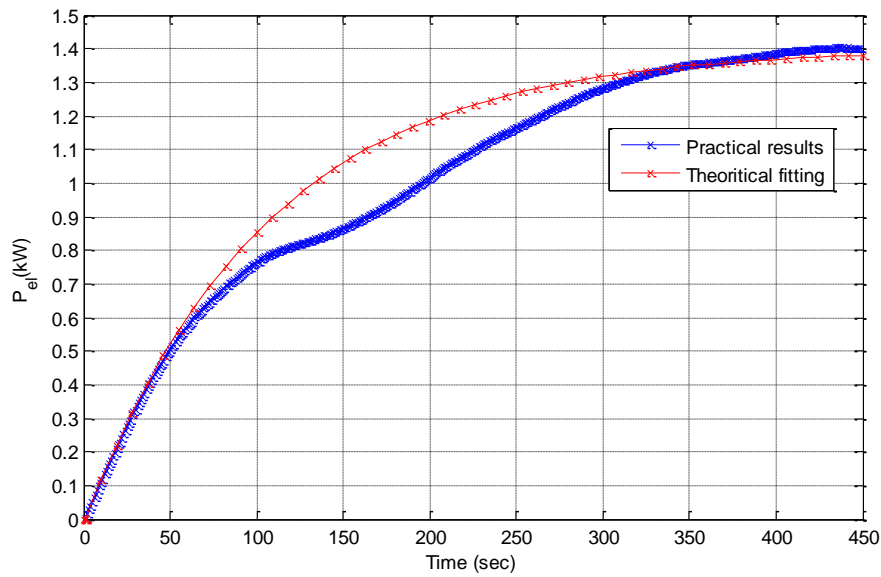
(b)

Figure 4-27. (a) Complete and (b) starting transient behavior

Curve shown in figure 4-27 is a first order system, the transfer function could be given in the general formula shown in eq. 4-2 referring to the basics of control systems in [128]:

$$G(s) = \frac{1.33 \times 10^{-2}}{s + 0.95 \times 10^{-2}} = \frac{Y(s)}{X(s)} \tag{4-5}$$

$Y(s)$ is the required electrical power (output) and its maximum value is around 1.4 kW, while $X(s)$ is the fuel mass flow as a percentage up to 100%.

4.5 Control process

It is clarified in literature that direct combustion is hard to control due to the system nature and fuel. However, Pyro-Man burner is designed to meet the heating demand (since it is for normal heating proposes), this advantage is exploited to perform control process on power generated amount.

For the transient modeling, combustion (e.g. burner) behavior is proved to be the dominant part as seen in the previous section (4.7). All other components will be modeled dynamically as in steady state situation, their transient have no effect on the process.

Before moving to the control details, there should be a consideration for mapped parameters. Firstly, air mass flow from the compressor along with input thermal power, three cases are

taken, at 133%, 100%, and 50% of the input power as shown in figure 4-28. There is a proportional relation noticed from the graph, this leads to easier modeling by taking 100% as a reference curve, and then take the rest as percentage multiples of the reference, see also figure 4-29 (a) and (b).
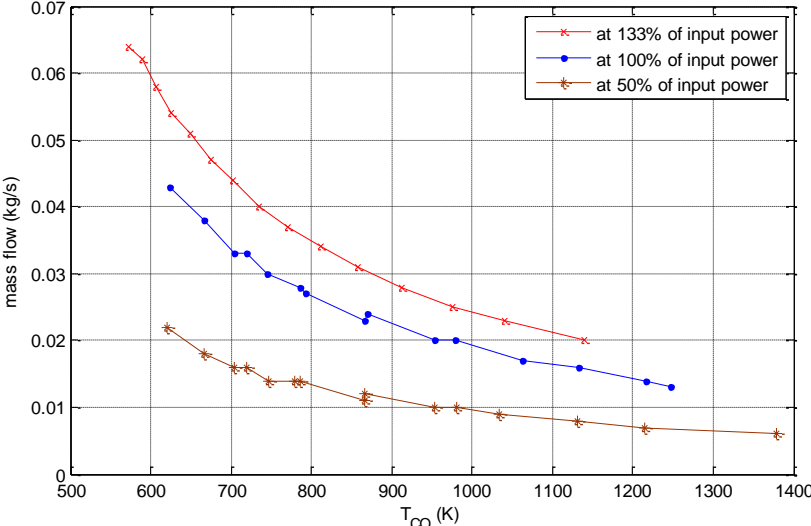
Figure 4-28. $\dot{m}_{air}$ mapping at different power levels

Air mass flow mapping is restricted to a certain range, for instance, 600 K is the minimum value. Where for the maximum value it is preferred to keep lower than 1200 K for more precise results.
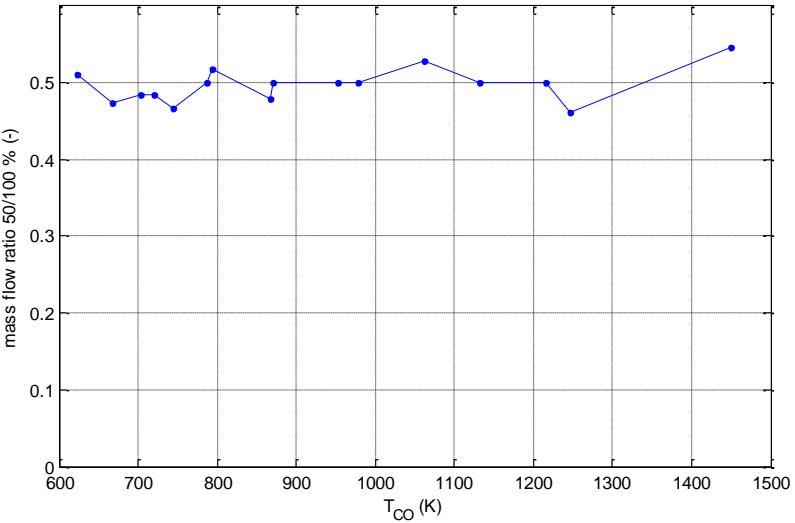
(a) 50% to 100% thermal power mass flow ratios
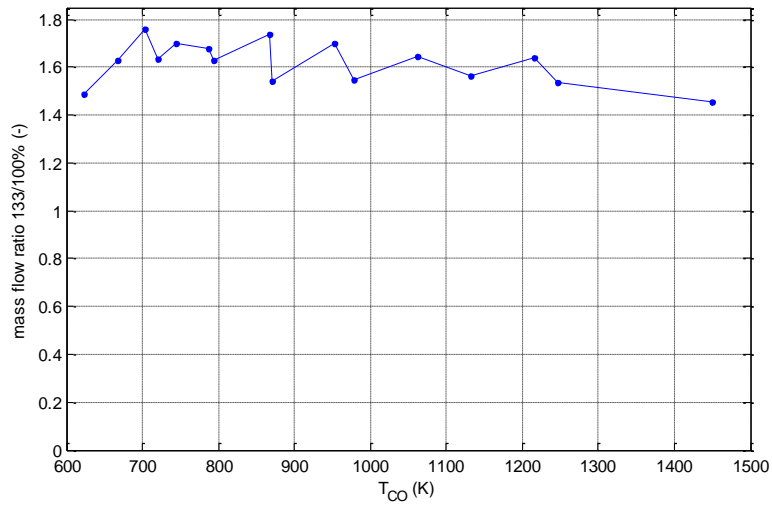
(b) 133% to 100% thermal power mass flow ratios

Figure 4-29. $\dot{m}_{air}$ mapping proportionality

The reference (100%) case is implemented by the exponential relation in equation 3-14

On the other hand, pressure seems to be fairly unaffected by the input thermal power. This is clearly seen in figure 4-30.
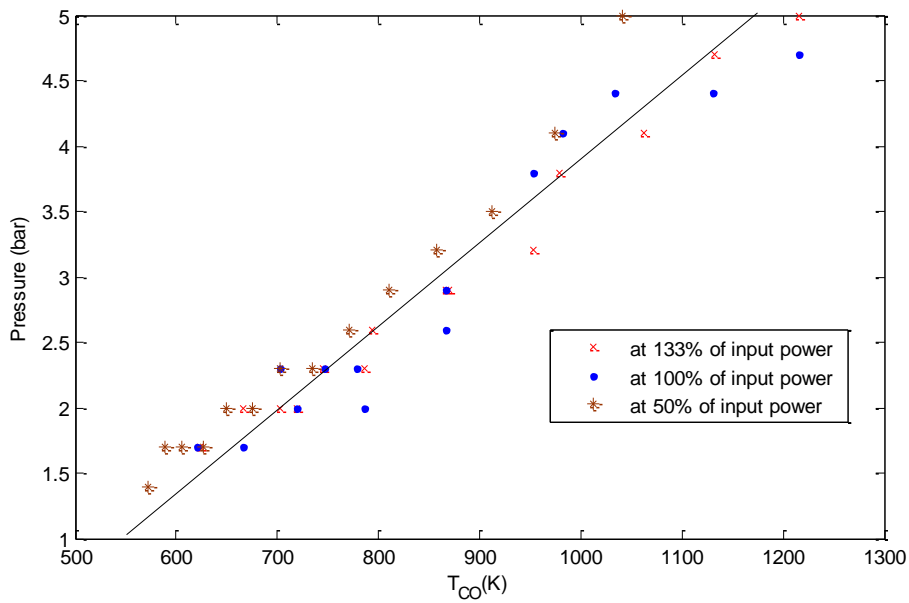
Figure 4-30. Pressure with TIT and at several power levels

As a result, air mass flow map should be tuned with both turbine inlet temperature and the supplied thermal power. This explained by the following, thermal power is controlled by pellets feeding amount, this means changing flue gas mass flow as a result. And since heat relations for heat exchanger are dependable on fluids mass flow, air mass flow through the compressor should be changed to a different curve of its relation with turbine inlet temperature. This curve is assigned by the thermal input power. On the other hand, pressure value can be adjusted to one curve with one parameter (e.g. turbine inlet temperature) neglecting the variation in thermal input power.

Electrical power is controlled by adjusting the thermal input power, this means controlling the amount of heat transferred as well. A better overview could be presented by having the relation between both electrical power produced and the transferred thermal power. The maximum P_{el} is achieved when thermal power is 10 kW or a little bit more. Thermal power values lower than 5 kW are not sufficient for electrical generation. This is due to the reason that the turbine can't provide power more than what is needed by the compressor (figure 4-31). We can notice a linear relationship between thermal heat and electrical power, this linearity is exploited in mapping $\dot{m}_{air}$ by multiplying its curve with a factor (Q_{act}/Q_{max}). By this step we guarantee that $\dot{m}_{air}$ is tuned to the amount of heat beside the TIT.
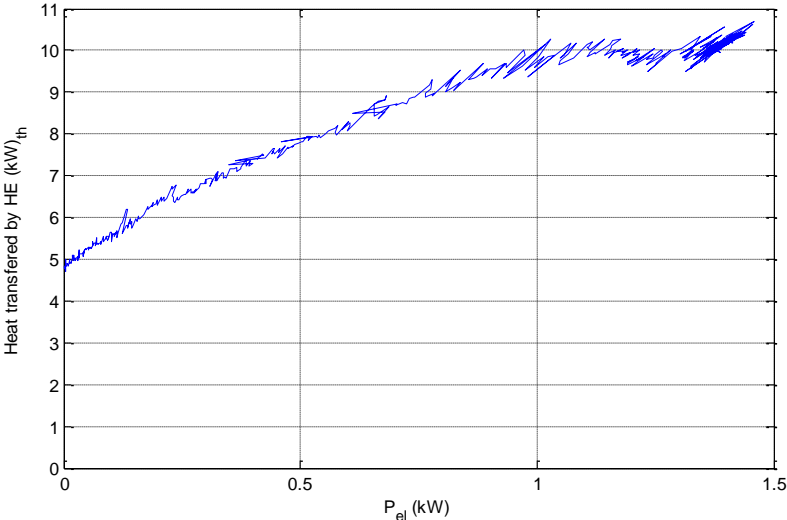
Figure 4-31. Thermal power control

After solving the problem of both $\dot{m}_{air}$ and p, now comes the next and important part of plant control. As stated previously, pellets feeding consist of periodic pulses of ON states, flowed

with OFF period. Maximum power is achieved when adjusting 2 min 40 sec OFF and 20 sec ON, it is possible to move to lower thermal power values by decreasing the ON period, see figure 4-33.
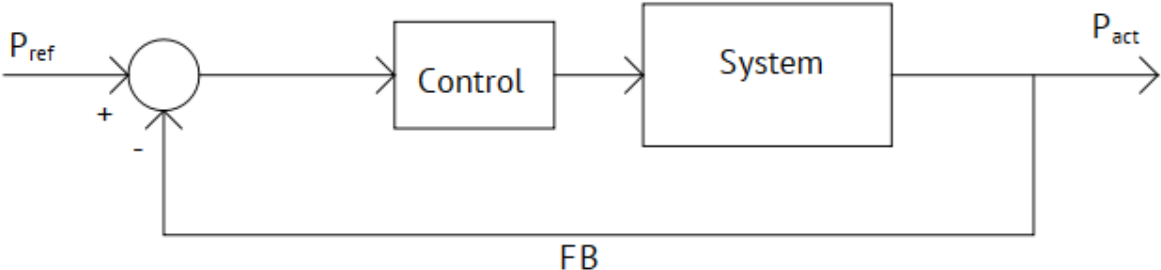
Figure 4-32. Control loop

Due to the long response of the burner as stated previously in transient section, control process could be implemented easily by measuring the error between the actual output power and the reference one. This error is multiplied by 10 for better control range, after that 11 cases are designed for ON periods of 6,7,8,9,10,12,14,16,18,20,21 seconds. Lower than 6 seconds will cause burner to turn OFF in some cases, and going further 21 will cause in pellets accumulation, see figure 4-34.
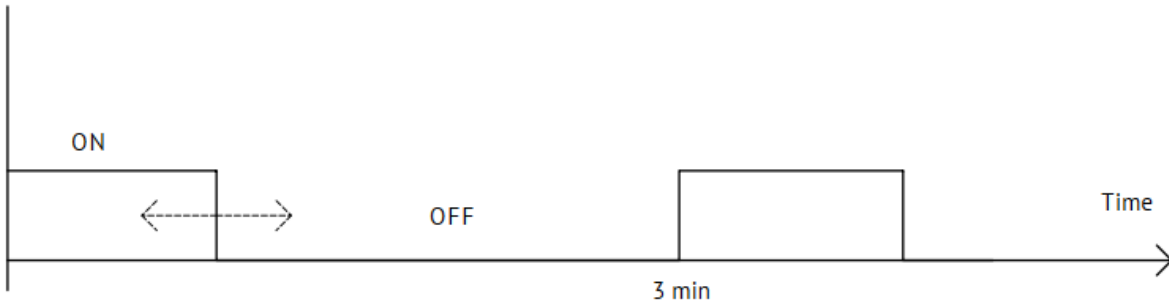
Figure 4-33. ON period control

At the end of each period the actual value of the electrical power will be picked up, the error signal from 1-10 enters a group of if statements where then the pellets feed is decided to stepped up or down by one to six steps.
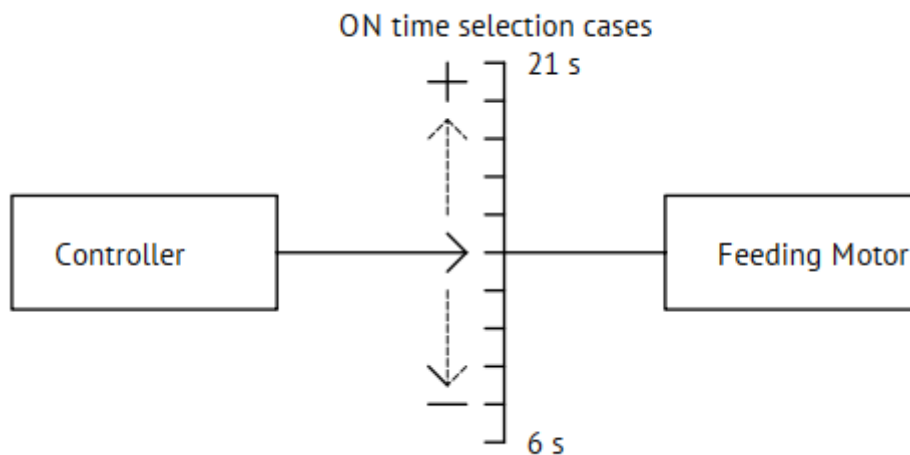
Figure 4-34. Cases selectivity

Delay periods are caused mainly by the long pellets combustion time, and the accumulated pellets consumption in feeding pipe. In moving from high to low value of power, pellets in the feed pipe add extra time for the response, sometimes a constant value stays for around 3 min without changing. The same thing is applied when moving from lower power values to higher ones, added pellets will be in higher amounts the thing that means more preheating till starting combustion.

In spite of that the burner can provide thermal power from 30-100%, we noticed sometimes unstable operation when adjusting for lower than 50% electrical power, for safe operation we recommend a range of 50-100% of electrical power providing.

Combustion of biomass is unstable in general, this is noticed by zooming in the power when adjusting on 1.3 kW_{el}, and fluctuations appear clearly in figure 4-35, where the response for load variations is presented. Those fluctuations are expected to be smoother if an experimental heat exchanger is installed. The transient model of the heat exchanger is not included because the main study is related to the general behavior rather than heat exchanger details.
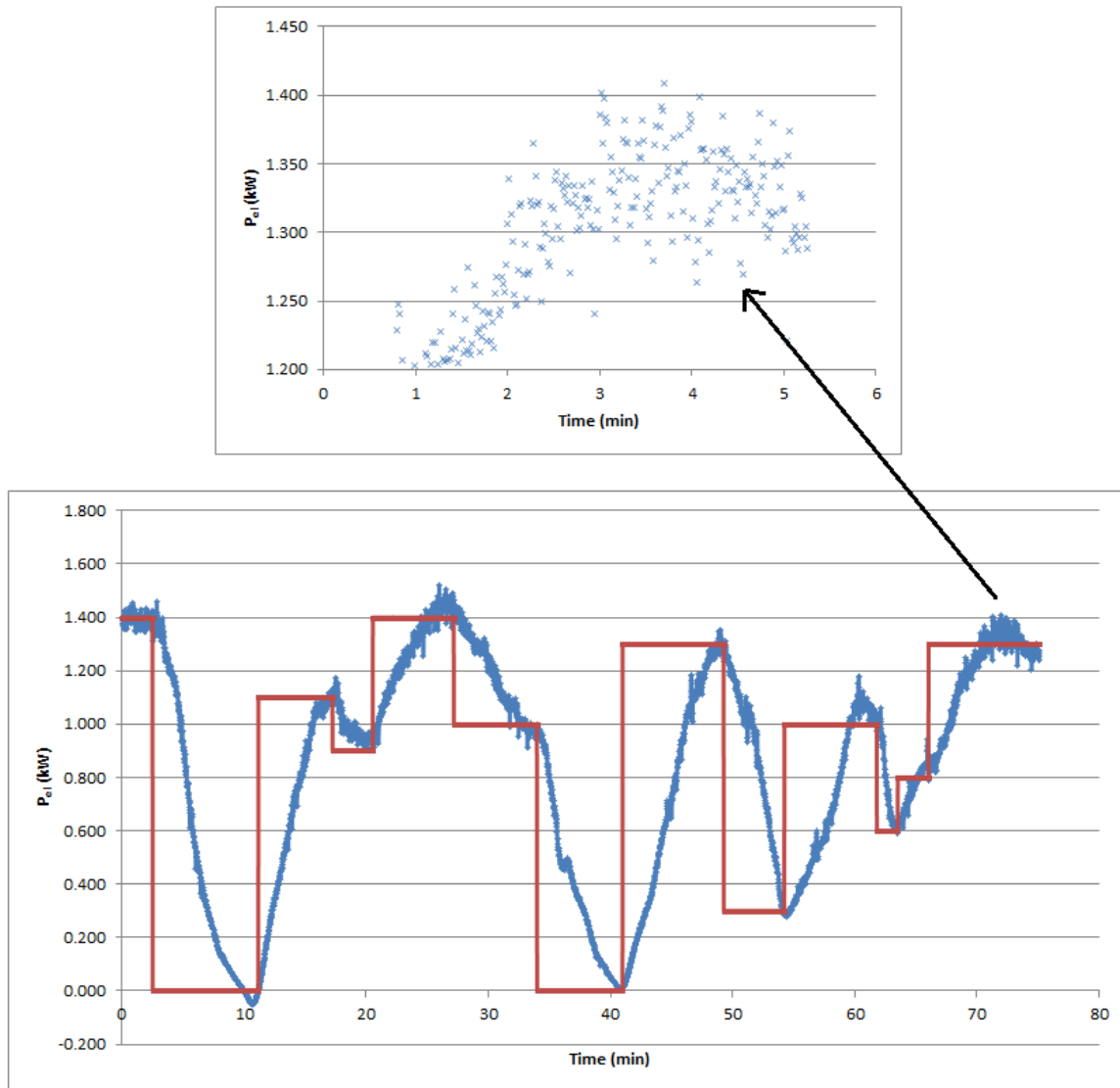
Figure 4-35. Response to load variations

Transient periods could not exactly follow the transfer function mentioned previously, some delays or faster operation could happen at different experiments.

Rotational speed is also varied with electrical power level, a maximum value of 155000 rpm is seen where the electrical power is also on maximum point (figure 4-36). A linear behavior is shown of the rotational speed with electrical power from 60000 rpm till the maximum, and an exponential one for values lower than 0.2 kW$_{el}$.
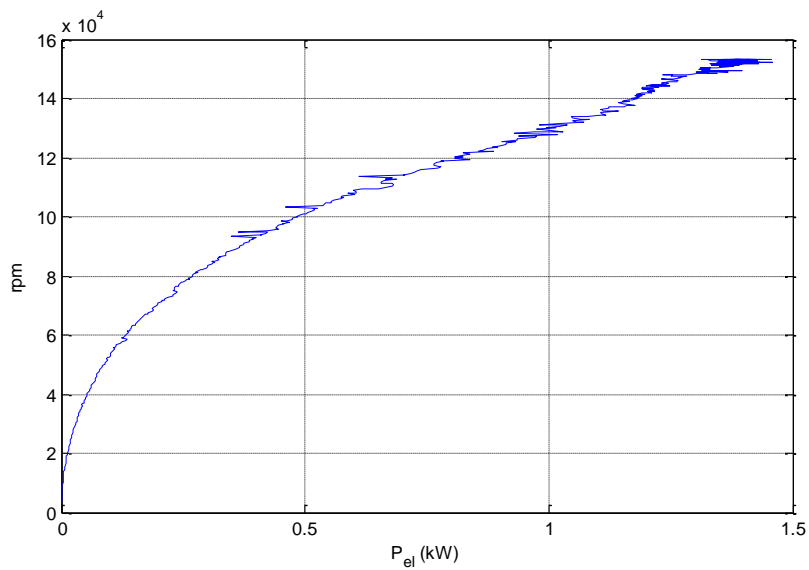
Figure 4-36. Rotational speed with electrical power

4.6   Emitted CO_2

Gases emitted from combustion process are a natural aspect accompanied with the study of EFGT system based on biomass combustion. The design of the burner itself plays the major rule in CO production in flue gas, well designed burners can achieve a very low values. Pyro-Man burner registered an average value of 15 ppm for wood pellets combustion as shown previously, which is relatively good. Starting process emits large values as seen from the same figure, it reaches more than 4000 ppm for wood pellets as an example.
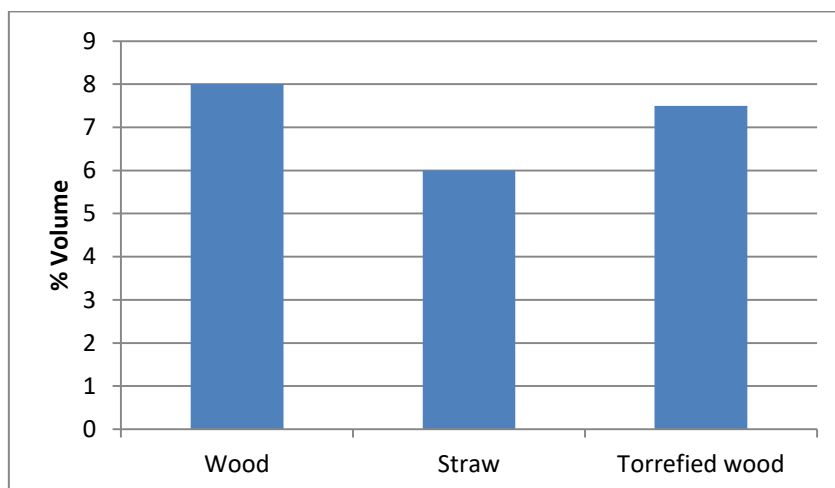
Figure 4-37. CO_2 emissions

Having a look on CO_2 percentage in the flue gas (figure 4-37), it is seen that emissions are nearly equal for the all types. Taking wood pellets as an example of CO_2 emissions, an average density of the flue gas of 0.75 kg/m^3 at 500 K, and flue gas mass flow of 0.016 kg/s. We get a volume flow of 0.0213 m^3/s total flue gas flow, which results in 0.0017 m^3/s of CO_2 produced from combustion process.

4.7   Operation scenarios and economics

Biomass can't cover the complete energy demands. However, its sharing is of a great benefit for domestic consumption. Thus, we would consider that the plant can cover 8000 working hours per year, lower values like 7000 and 4000 hours are considered to satisfy the controlled mode. And beside what discussed in this research about electrical generation, heat energy achievement improves the total efficiency for higher values like 80% (i.e. Combined Heat and Power - CHP) [60].

A general energy sharing estimation could be presented from the previous data, but before that, biomass type is important for such study. For instance, energy achieved from wood pellets needs lower amounts than straw, this is due to higher heating content in wood biomass. So separate calculations of produced energy would be presented, and it is related to the used types.

Take Jordan as one of countries that suffer from energy problem, normal customer consumption is 8124 kWh$_{el}$ per year (in the northern area of Jordan) [129]. Considering an EFGT plant with nominal electrical power of 1.2 kW$_{el}$, this value is estimated as an average electrical production from different types of biomass pellets, customer can cover his complete consumption if the plant operates 8000 hour (9600 kWh produced) as a maximum operational case. Take an operational range of 50-100% (0.6-1.2 kW$_{el}$), with 7000 and 4000 working hours. Then the resulting energy production is 4200 – 8400 kWh for 7000 hour mode, and 2400-4800 kWh for 4000 hour mode. As seen, plant can provide from 30-100 % of customer needs. Plant can also be adjusted to meet variations in power consumption during the day. Electrical grid ability to handle distributed generation is important as well as electricity provider regulations for cost considerations.

To calculate the overall energy potential, take olive residues in Jordan. Referring to the statistics, the average production of olive waste is 38804 tons per year [27]. This means 781.9 GJ per year thermal available from only olive processing.

It should be noted, that the actual potential for power production might be somewhat lower considering alternative uses of the olive waste e.g. for domestic heating purposes. On the other hand, by using combined heat and power technology, the introduction of sorption cooling technology could be used to further reduce electrical power consumption.

Complete economic study of EFGT plant in the range of 15 kW$_{th}$ will not be addressed. Current research handle more technical and design aspects of micro scale externally fired gas turbine plant. In addition, some components in the cycle are still not well commercialized. This section provides a general overview on plant cost, along with some examples from literature.

Starting with larger sizes, a plant of 1 MW$_{el}$ can reach a specific cost of 540 £ (ca. 632 euro) per kW$_{el}$, 15.3 £ (17.9 Euro) specific fixed operation and maintenance costs per MWh, and 7.11 £ (8.32 Euro) for specific variable operation and maintenance costs per MWh [130].

Cordiner et al. [131] has introduced a recent study on EFGT technology based on woody biomass, the plant is supposed to work with a utilization factor of 0.8 (7000 h/year). It is seen that the electrical cost is 0.33 Euro/kWh, this is for a plant size of 60 kW$_{el}$. The thermo economic analysis is also performed by Pantaleo et al. [72]. The study handles EFGT technology with two firing schemes, natural gas and biomass. Each scheme can be varied from 0-100%, at the same time the total sharing should be 100% to provide electrical power of around 100 kW$_{el}$. The capital cost is calculated to be 471000 Euro. Further operating cost which includes biomass supply, ash discharge, and maintenance are said to be 69,750 Euro/year when the biomass quota is 100%.

As we see, literature on EFGT cycle economics concentrates on relatively higher ranges than what is discussed in this study, 15 kW$_{th}$ or in the range of 1.5 kW$_{el}$. However, it is possible to estimate the total capital cost for such range, taking into consideration capital scaling effect for different installations [132]. Capital cost could be calculated from eq.

$$\frac{CC}{CC_0} = \left(\frac{PC}{PC_0}\right)^s \tag{4-6}$$

where CC is the capital cost of a plant of a capacity PC, CC_0, PC_0 are the base capital cost and capacity (consider [72]), and s is the dimensionless scale factor ($0.6 \leq s \leq 0.8$). Due to the low number of installed systems for externally fired gas turbines, the scaling factor cannot be estimated at a higher precision currently. Thus, the estimated capital cost of a 15 kW$_{th}$ power

plant with about 1.6 kW_{el} net output (including generator efficiency) is between 33800–65300 Euro, considering the reference data from [72] (CC_0 = 471000 Euro, PC_0 = 404 kW_{th}). Noting that, the capital cost is expected to be reduced with installing more installations referring to the learning curve effect.

5   Conclusions and outlook

Micro scale externally fired gas turbine technology is a promising biomass utilization method. It can provide relatively good energy percentage for residential needs, however, it is not commercialized as distributed plants. Improvements and developments still on the way of optimizing the biomass based externally fired gas turbine technology.

In this research, a technical study is provided in the scope of micro scale externally fired gas turbine technology (i.e. 15 kW$_{th}$). Integrating hardware in the loop improves the study by adding the flexibility of operation, as well as providing a complete control. Hardware in the loop can be easily used as a real time simulation to model part of gas turbine cycle. This merit is used for modeling the dynamics with more reality than static simulations.

Concept development of biomass utilization in externally fired gas turbine technology is important in the envelope of renewables investigation. It is seen that solid biomass direct combustion can be effectively used in electrical production. Take into consideration that the plant design should meet fuel combustion aspects, like solid type handling, instability in heat production, and ash processing. In spite of solid biomass combustion disadvantages, it is possible to modify the plant for better performance.

It is seen that the working pressure and air mass flow through the compressor-heat exchanger-turbine are important factors in plant design. Thus, mapping diagrams for both parameters are generated to be a function of the turbine inlet temperature. If the pressure is fixed and mass flow is changed, a maximum peak appears where the mass flow should be adjusted. The same thing is applied if the mass flow is fixed and pressure is changed. This criterion is used for mapping generation. The reference case (wood pellets combustion) shows an adjusted pressure and air mass flow of 3.4 bar and 0.021 kg/s respectively, the turbine inlet temperature for the steady state was around 950 K.

The turbine inlet temperature is an important factor for the turbine operation. Higher temperature means higher mechanical power achieved. However, turbine material firmness should be considered to avoid deterioration. Fuel type is a dominant factor in temperature values, for instance, wood pellets provided higher temperatures compared with straw and torrefied pellets.

Heat exchanger is the thermal connection part between combustion and clean air. Its properties like thermal connectivity, high temperature, and pressure firmness are important for increasing the total efficiency. Heat exchanger can be modeled by using the heat balance and the difference between hot inlet stream and cold outlet stream, which is proven from the literature with a maximum value of 300 K. A fair value of 100 K is taken in discussing the results, however, the model can deal with different range, but reality should be applied as well.

Both compressor and temperature efficiencies are main factors in the total efficiency. Compressor shows a decreasing isentropic efficiency compared with turbine for constant polytropic efficiency with pressure increase. Thus, one of the benefits of mapping is choosing the optimum pressure value. It is seen also that the air mass flow is relatively low, so the geometric design should be suitable for such values. Also as a result of small size, the rotational speed is relatively high, which has been calculated to be more than 150000 rpm.

Plant control is applied where the fuel flow is controlled depending on the needed power. A modified proportional controller is used for this purpose. The response to load variations is relatively slow, which is related to the combustion behavior. An unstable steady state (i.e. small fluctuations) in power providing is also noticed, take into account that the instantaneous heat exchanger model is considered. For the control requirements, pressure should be varied with the turbine inlet temperature. On the other hand, air mass flow should be varied with both turbine inlet temperature and the thermal power percentage.

6 References

[1] McKendry, P.: Energy production from biomass (part 1): overview of biomass; *Bioresource Technology*, vol. 83 (2002), no. 1, pp. 37–46, (doi:10.1016/S0960-8524(01)00118-3)

[2] Buratti, C. et al.: Thermal behaviour and kinetic study of the olive oil production chain residues and their mixtures during co-combustion; *Bioresource Technology*, vol. 214 (2016), pp. 266–275, (doi:10.1016/j.biortech.2016.04.097)

[3] Reilly, J.; Paltsev, S.: *Biomass Energy and Competition for Land*; MIT Joint Program on the Science and Policy of Global Change, Cambridge, MA, April 2007, (http://web.mit.edu/globalchange/www/MITJPSPGC_Rpt145.pdf)

[4] Brown, R.C.: *Thermochemical processing of biomass: conversion into fuels, chemicals and power*; John Wiley & Sons, Hoboken, NJ, 2011, Wiley Series in Renewable Resource, (ISBN: 978-0-470-72111-7)

[5] Lackner, M., (ed.): *Handbook of combustion*; Wiley-VCH, Weinheim, 2010, (ISBN: 978-3-527-32449-1)

[6] CEN (European Committee for standarization).: solid biofuels - fuel specification and classes, Part 1 - General requirments, EN14961-1; 2010

[7] Klass, D.L.: *Biomass for renewable energy, fuels, and chemicals*; Academic Press, San Diego, 1998, (ISBN: 978-0-12-410950-6)

[8] McGowan, T.: *Biomass and alternate fuel systems: an engineering and economic guide*; John Wiley, Hoboken, N.J, 2009, (ISBN: 978-0-470-41028-8)

[9] El-Mahallawy, F.M.; Habik, S.E.-D.: *Fundamentals and technology of combustion*; Elsevier, Amsterdam ; Boston, 2002, 1st ed, (ISBN: 978-0-08-044106-1)

[10] Van Loo, S.: *The handbook of biomass combustion and co-firing*; Earthscan, London ; Sterling, VA, 2008, (ISBN: 978-1-84407-249-1)

[11] Barbanera, M. et al.: Characterization of pellets from mixing olive pomace and olive tree pruning; *Renewable Energy*, vol. 88 (2016), pp. 185–191, (doi:10.1016/j.renene.2015.11.037)

[12] Garcia-Maraver, A. et al.: Factors affecting the quality of pellets made from residual biomass of olive trees; *Fuel Processing Technology*, vol. 129 (2015), pp. 1–7

[13] Kalnacs, J.; Lazdinsh, A.: Biomass for energy production characteristics,amount and distribution in Latvia; International Conference on Renewable Energies and Power Quality (ICREPQ'10), 2010

[14] Sims, R.E.H.: *Bioenergy options for a cleaner environment in developed and developing countries*; Elsevier, Amsterdam ; Boston, 2004, 1st ed, (ISBN: 0-08-044351-6)

[15] Grammelis, P.: *Solid biofuels for energy: a lower greenhouse gas alternative*; Springer, London ; New York, 2011, Green energy and technology, (ISBN: 978-1-84996-392-3)

[16] Spliethoff, H.: *Power generation from solid fuels*; Springer, Heidelberg ; New York, 2010, Power systems, (ISBN: 978-3-642-02855-7)

[17] Tortosa Masiá, A.A. et al.: Characterising ash of biomass and waste; *Fuel Processing Technology*, vol. 88 (2007), no. 11–12, pp. 1071–1081, (doi:10.1016/j.fuproc.2007.06.011)

[18] Miles, T.R. et al.: Boiler deposits from firing biomass fuels; *Biomass and Bioenergy*, vol. 10 (1996), no. 2–3, pp. 125–138, (doi:10.1016/0961-9534(95)00067-4)

[19] Fernández Llorente, M.J.; Carrasco García, J.E.: Comparing methods for predicting the sintering of biomass ash in combustion; *Fuel*, vol. 84 (2005), no. 14–15, pp. 1893–1900, (doi:10.1016/j.fuel.2005.04.010)

[20] Christoforou, E.; Fokaides, P.A.: A review of olive mill solid wastes to energy utilization techniques; *Waste Management*, vol. 49 (2016), pp. 346–363, (doi:10.1016/j.wasman.2016.01.012)

[21] Pagnanelli, F.; Toro, L.; Vegliò, F.: Olive mill solid residues as heavy metal sorbent material: a preliminary study; *Waste Management*, vol. 22 (2002), no. 8, pp. 901–907, (doi:10.1016/S0956-053X(02)00086-7)

[22] International Olive Council, http://www.internationaloliveoil.org/estaticos/view/132-world-table-olive-figures; accessed 07.07.2016

[23] Khalsa, J.; Döhling, F.; Berger, F.: Foliage and Grass as Fuel Pellets–Small Scale Combustion of Washed and Mechanically Leached Biomass; *Energies*, vol. 9 (2016), no. 5, p. 361, (doi:10.3390/en9050361)

[24] Azbar, N. et al.: A Review of Waste Management Options in Olive Oil Production; *Critical Reviews in Environmental Science and Technology*, vol. 34 (2004), no. 3, pp. 209–247, (doi:10.1080/10643380490279932)

[25] Caputo, A.C.; Scacchia, F.; Pelagagge, P.M.: Disposal of by-products in olive oil industry: waste-to-energy solutions; *Applied Thermal Engineering*, vol. 23 (2003), no. 2, pp. 197–214, (doi:10.1016/S1359-4311(02)00173-4)

[26] Toscano, P.; Montemurro, F.: Olive Mill By-Products Management; in: Muzzalupo, I., (ed.): : *Olive Germplasm - The Olive Cultivation, Table Olive and Olive Oil Industry in Italy*, InTech, 2012, (ISBN: 978-953-51-0883-2)

[27] *Annual Report*; Ministry of Agriculture - Jordan, 2012, (http://www.moa.gov.jo/ar-jo/agriinformationar.aspx)

[28] Vlyssides, A. et al.: Sustainable cultivation of olive trees by reusing olive mill wastes after effective co-composting treatment processes; 4th ISOFAR Scientific Conference, 2014

[29] Dahlquist, E.: *Technologies for converting biomass to useful energy*; CRC Press, Boca Raton, 2013, (ISBN: 978-0-203-12026-2)

[30] Jenkins, B.. et al.: Combustion properties of biomass; *Fuel Processing Technology*, vol. 54 (1998), no. 1–3, pp. 17–46, (doi:10.1016/S0378-3820(97)00059-3)

[31] Fang, X.; Jia, L.; Yin, L.: A weighted average global process model based on two−stage kinetic scheme for biomass combustion; *Biomass and Bioenergy*, vol. 48 (2013), pp. 43–50, (doi:10.1016/j.biombioe.2012.11.011)

[32] Miller, B.G.; Tillman, D.A., (eds.): *Combustion engineering issues for solid fuel systems*; Academic Press, Boston, MA, 2008, (ISBN: 978-0-12-373611-6)

[33] Soltani, S. et al.: Thermodynamic analyses of an externally fired gas turbine combined cycle integrated with a biomass gasification plant; *Energy Conversion and Management*, vol. 70 (2013), pp. 107–115, (doi:10.1016/j.enconman.2013.03.002)

[34] Pantaleo, A.M.; Camporeale, S.M.; Shah, N.: Thermo-economic assessment of externally fired micro-gas turbine fired by natural gas and biomass: Applications in Italy; *Energy Conversion and Management*, vol. 75 (2013), pp. 202–213, (doi:10.1016/j.enconman.2013.06.017)

[35] Demirbas, A.: Combustion characteristics of different biomass fuels; *Progress in Energy and Combustion Science*, vol. 30 (2004), no. 2, pp. 219–230, (doi:10.1016/j.pecs.2003.10.004)

[36] International Energy Agency, https://www.iea.org/topics/renewables/subtopics/bioenergy/, Accessed at 2016-11-25;

[37] Lewis, C.W.: Biomass through the ages; *Biomass*, vol. 1 (1981), no. 1, pp. 5–15, (doi:10.1016/0144-4565(81)90011-1)

[38] *WBA Global Bioenergy Statistics 2015*; World Bioenergy Association, Stockholm, Sweden, June 2015, (http://www.worldbioenergy.org/)

[39] Blair, L.: The Outlook For Wood Pellets: Demand, Supply, Costs and Prices – Q3 2016; Hawkins Wright

[40] http://biomassa.de/news-wood-pellet-prices-in-the-european-union-18.html, Accessed at 2016-11-25;

[41] *EU Biofuels Annual 2013*; USDA Foreign Agricultural Service, (https://gain.fas.usda.gov/Recent%20GAIN%20Publications/Biofuels%20Annual_The%20Hague_EU-27_8-13-2013.pdf)

[42] Munson, B.R.; Okiishi, T.H.; Huebsch, W.W.: *Fundamentals of fluid mechanics*; J. Wiley & Sons, Hoboken, NJ, 2009, 6th ed, (ISBN: 978-0-470-26284-9)

[43] Moran, M.J., (ed.): *Fundamentals of engineering thermodynamics*; Wiley, Hoboken, N.J., 2011, 7th ed, (ISBN: 978-0-470-91768-8)

[44] Simões-Moreira, J.R.: Fundamentals of Thermodynamics Applied to Thermal Power Plants; in: de Souza, G.F.M., (ed.): : *Thermal Power Plant Performance Analysis*, pp. 7–39, Springer London, London, 2012, (ISBN: 978-1-4471-2308-8)

[45] Anheden, M.: Analysis of gas turbine system for sustainable energy conversion; Doctoral thesis, KTH, Stockholm, Sweden; 2000 [ISSN 1104-3466 ISRN KTH/KET/R-112-SE]

[46] Ferreira, S.B.; Pilidis, P.: Comparison of Externally Fired and Internal Combustion Gas Turbines Using Biomass Fuel; *Journal of Energy Resources Technology*, vol. 123 (2001), no. 4, p. 291, (doi:10.1115/1.1413468)

[47] McDonald, C.F.: Helium turbomachinery operating experience from gas turbine power plants and test facilities; *Applied Thermal Engineering*, vol. 44 (2012), pp. 108–142, (doi:10.1016/j.applthermaleng.2012.02.041)

[48] Al-attab, K.A.; Zainal, Z.A.: Externally fired gas turbine technology: A review; *Applied Energy*, vol. 138 (2015), pp. 474–487, (doi:10.1016/j.apenergy.2014.10.049)

[49] Pritchard, D.: *Biomass fuelled indirect fired micro turbine*; Talbott's heading Ltd, 2005, (http://ukerc.rl.ac.uk/pdf/DTI_BT1008090000_file14923.pdf)

[50] McDonald, C.F.: The Nuclear Gas Turbine: Towards Realization After Half a Century of Evolution; p. V003T08A001, 1995, (ISBN: 978-0-7918-7880-4)

[51] Vera, D. et al.: Comparison between externally fired gas turbine and gasifier-gas turbine system for the olive oil industry; *Energy*, vol. 36 (2011), no. 12, pp. 6720–6730, (doi:10.1016/j.energy.2011.10.036)

[52] Karl, J.: *Dezentrale Energiesysteme: neue Technologien im liberalisierten Energiemarkt*; Oldenbourg, München, 2006, 2., Aufl, (ISBN: 978-3-486-57722-8)

[53] Al-attab, K.A.; Zainal, Z.A.: Turbine startup methods for externally fired micro gas turbine (EFMGT) system using biomass fuels; *Applied Energy*, vol. 87 (2010), no. 4, pp. 1336–1341, (doi:10.1016/j.apenergy.2009.08.022)

[54] Loeser, M.; Redfem, M.: Micro-Scale Biomass Generation Plant Technology: Stand-Alone Designs for Remote Customers; 16th European Biomass Conference and Exhibition, Valencia, Spain, 2008

[55] Cocco, D.; Deiana, P.; Cau, G.: Performance evaluation of small size externally fired gas turbine (EFGT) power plants integrated with direct biomass dryers; *Energy*, vol. 31 (2006), no. 10–11, pp. 1459–1471, (doi:10.1016/j.energy.2005.05.014)

[56] Anheden, M.: *Analysis of Gas Turbine Systems for Sustainable Energy Conversion*; Doctoral Thesis, Stockholm, Sweden, 2000

[57] Kautz, M.; Hansen, U.: The externally-fired gas-turbine (EFGT-Cycle) for decentralized use of biomass; *Applied Energy*, vol. 84 (2007), no. 7–8, pp. 795–805, (doi:10.1016/j.apenergy.2007.01.010)

[58] Al-attab, K.A.; Zainal, Z.A.: Performance of high-temperature heat exchangers in biomass fuel powered externally fired gas turbine systems; *Renewable Energy*, vol. 35 (2010), no. 5, pp. 913–920, (doi:10.1016/j.renene.2009.11.038)

[59] Schmid, M.: Dezentrale Stromerzeugung mit Feststoffbiomasse; Ökozentrum Langenbruck, 2007

[60] Pilavachi, P.A.: Mini- and micro-gas turbines for combined heat and power; *Applied Thermal Engineering*, vol. 22 (2002), no. 18, pp. 2003–2014, (doi:10.1016/S1359-4311(02)00132-1)

[61] do Nascimento, M.A.R. et al.: Micro Gas Turbine Engine: A Review; in: Benini, E., (ed.): : *Progress in Gas Turbine Performance*, InTech, 2013, (ISBN: 978-953-51-1166-5)

[62] Costamagna, P.; Magistri, L.; Massardo, A.F.: Design and part-load performance of a hybrid system based on a solid oxide fuel cell reactor and a micro gas turbine; *Journal of Power Sources*, vol. 96 (2001), no. 2, pp. 352–368, (doi:10.1016/S0378-7753(00)00668-6)

[63] Karl, J.: *Dezentrale Energiesysteme: neue Technologien im liberalisierten Energiemarkt*; Oldenbourg, München, 2006, 2., Aufl, (ISBN: 978-3-486-57722-8)

[64] Bdour, M. et al.: Determination of Optimized Parameters for the Flexible Operation of a Biomass-Fueled, Microscale Externally Fired Gas Turbine (EFGT); *Energies*, vol. 9 (2016), no. 10, p. 856, (doi:10.3390/en9100856)

[65] Pritchard, D.: *Biomass combustion gas turbine CHP*; Talbott's heading Ltd, 2002, (http://collection.europarchive.org/tna/20000607122935/http:/www.berr.gov.uk/files/file14922.pdf)

[66] A fluidized bed air biomass gasification CHP plant with an externally fired evaporative gas turbine cycle, BM/367/92-BE project; Vrije Universiteit Brussel, Belgium; 1992

[67] Traverso, A.; Massardo, A.F.; Scarpellini, R.: Externally Fired micro-Gas Turbine: Modelling and experimental performance; *Applied Thermal Engineering*, vol. 26 (2006), no. 16, pp. 1935–1941, (doi:10.1016/j.applthermaleng.2006.01.013)

[68] Vera, D. et al.: Comparison between externally fired gas turbine and gasifier-gas turbine system for the olive oil industry; *Energy*, vol. 36 (2011), no. 12, pp. 6720–6730, (doi:10.1016/j.energy.2011.10.036)

[69] Datta, A.; Ganguly, R.; Sarkar, L.: Energy and exergy analyses of an externally fired gas turbine (EFGT) cycle integrated with biomass gasifier for distributed power generation; *Energy*, vol. 35 (2010), no. 1, pp. 341–350, (doi:10.1016/j.energy.2009.09.031)

[70] de Mello, P.E.B.; Monteiro, D.B.: Thermodynamic study of an EFGT (externally fired gas turbine) cycle with one detailed model for the ceramic heat exchanger; *Energy*, vol. 45 (2012), no. 1, pp. 497–502, (doi:10.1016/j.energy.2012.01.003)

[71] Stefano Cordiner; Vincenzo Mulone.: Biomass energy conversion in EFGT (Externally Fired Gas Turbine): an experimental-numerical analysis; 2012

[72] Pantaleo, A.M.; Camporeale, S.M.; Shah, N.: Thermo-economic assessment of externally fired micro-gas turbine fired by natural gas and biomass: Applications in Italy; *Energy Conversion and Management*, vol. 75 (2013), pp. 202–213, (doi:10.1016/j.enconman.2013.06.017)

[73] Pilavachi, P..: Power generation with gas turbine systems and combined heat and power; *Applied Thermal Engineering*, vol. 20 (2000), no. 15–16, pp. 1421–1429, (doi:10.1016/S1359-4311(00)00016-8)

[74] do Nascimento, M.A.R. et al.: Micro Gas Turbine Engine: A Review; in: Benini, E., (ed.): : *Progress in Gas Turbine Performance*, InTech, 2013, (ISBN: 978-953-51-1166-5)

[75] Borgnakke, C.: *Fundamentals of thermodynamics*; Wiley, Hoboken, NJ, 2013, 8th ed., (ISBN: 978-1-118-13199-2)

[76] Cziesla, F.; Tsatsaronis, G.; Gao, Z.: Avoidable thermodynamic inefficiencies and costs in an externally fired combined cycle power plant; *Energy*, vol. 31 (2006), no. 10–11, pp. 1472–1489, (doi:10.1016/j.energy.2005.08.001)

[77] Schulte-Fischedick, J.; Dreißigacker, V.; Tamme, R.: An innovative ceramic high temperature plate-fin heat exchanger for EFCC processes; *Applied Thermal Engineering*, vol. 27 (2007), no. 8–9, pp. 1285–1294, (doi:10.1016/j.applthermaleng.2006.11.007)

[78] Sunden, B.: High temperature heat exchanger (hthe). In: Shah RK, Ishizuka M, Rudy TM, Wadekar VV, editors.; *Proceeding of 5th international conference on enhanced, compact and ultra-compact heat exchangers: science, engineering and technology.*, vol. (2005), no. Hoboken, NJ, USA: Engineering Conferences International, pp. 226–38

[79] Shah, R.K.: *Fundamentals of heat exchanger design*; John Wiley & Sons, Hoboken, NJ, 2003, (ISBN: 0-471-32171-0)

[80] Aquaro, D.; Pieve, M.: High temperature heat exchangers for power plants: Performance of advanced metallic recuperators; *Applied Thermal Engineering*, vol. 27 (2007), no. 2–3, pp. 389–400, (doi:10.1016/j.applthermaleng.2006.07.030)

[81] Cao, E.: *Heat transfer in process engineering*; McGraw-Hill, New York, 2010, (ISBN: 978-0-07-162408-4)

[82] Incropera, F.P.; Incropera, F.P., (eds.): *Fundamentals of heat and mass transfer*; John Wiley, Hoboken, NJ, 2007, 6th ed, (ISBN: 978-0-471-45728-2)

[83] Korpela, S.A.: *Principles of turbomachinery*; Wiley, Hoboken, N.J, 2011, (ISBN: 978-0-470-53672-8)

[84] Betsch, M.: Umbau einer μ-Turbine zu einer extern befeuerten Maschine mit Ankopplung an eine Stationäre-Wirbelschichtfeuerung; Fakultät für Maschinenbau und Schffstechnik, Universität Rostock, 2009

[85] Baina, F. et al.: Effect of the fuel type on the performance of an externally fired micro gas turbine cycle; *Applied Thermal Engineering*, vol. 87 (2015), pp. 150–160, (doi:10.1016/j.applthermaleng.2015.04.042)

[86] Vera, D.; Jurado, F.; Carpio, J.: Study of a downdraft gasifier and externally fired gas turbine for olive industry wastes; *Fuel Processing Technology*, vol. 92 (2011), no. 10, pp. 1970–1979, (doi:10.1016/j.fuproc.2011.05.017)

[87] Vidal, A. et al.: Performance characteristics and modelling of a micro gas turbine for their integration with thermally activated cooling technologies; *International Journal of Energy Research*, vol. 31 (2007), no. 2, pp. 119–134, (doi:10.1002/er.1231)

[88] Tahmasebi, A. et al.: Performance assessment of a hybrid fuel cell and micro gas turbine power system; Energy Equipment and System, 2013

[89] Nguyen-Schäfer, H.: Thermodynamics of Turbochargers; *Rotordynamics of Automotive Turbochargers*, pp. 21–36, Springer International Publishing, Cham, 2015, (ISBN: 978-3-319-17643-7)

[90] Dixon, S.L.; Hall, C.A.: *Fluid mechanics and thermodynamics of turbomachinery*; Butterworth-Heinemann/Elsevier, Burlington, MA, 2010, 6th ed, (ISBN: 978-1-85617-793-1)

[91] Romagnoli, A.; Martinez-Botas, R.: Heat transfer analysis in a turbocharger turbine: An experimental and computational evaluation; *Applied Thermal Engineering*, vol. 38 (2012), pp. 58–77, (doi:10.1016/j.applthermaleng.2011.12.022)

[92] Katsanos, C.O.; Hountalas, D.T.; Zannis, T.C.: Simulation of a heavy-duty diesel engine with electrical turbocompounding system using operating charts for turbocharger components and power turbine; *Energy Conversion and Management*, vol. 76 (2013), pp. 712–724, (doi:10.1016/j.enconman.2013.08.022)

[93] Miller, J.K.: *Turbo: real world high-performance turbocharger systems*; CarTech, North Branch, MN, 2008, S-A design, (ISBN: 978-1-932494-29-7)

[94] Chen, W.J.: Rotordynamics and bearing design of turbochargers; *Mechanical Systems and Signal Processing*, vol. 29 (2012), pp. 77–89, (doi:10.1016/j.ymssp.2011.07.025)

[95] Halvorsen, H.-P.: Hardware-in-the-Loop Simulation; Telemark University College, Department of Electrical Engineering, Information Technology and Cybernetics, N-3918 Porsgrunn, Norway, 2016

[96] Lu, B. et al.: A Low-Cost Real-Time Hardware-in-the-Loop Testing Approach of Power Electronics Controls; *IEEE Transactions on Industrial Electronics*, vol. 54 (2007), no. 2, pp. 919–931, (doi:10.1109/TIE.2007.892253)

[97] Rönsch, S.: *Anlagenbilanzierung in der Energietechnik: Grundlagen, Gleichungen und Modelle für die Ingenieurpraxis*; Springer Vieweg, Wiesbaden, 2015, Lehrbuch / Springer, (ISBN: 978-3-658-07824-9)

[98] Zheng, L.; Furimsky, E.: ASPEN simulation of cogeneration plants; *Energy Conversion and Management*, vol. 44 (2003), no. 11, pp. 1845–1851, (doi:10.1016/S0196-8904(02)00190-5)

[99] Li, B.-H.; Zhang, N.; Smith, R.: Process Simulation of a 420MW Gas-fired Power Plant using Aspen Plus; *Computer Aided Chemical Engineering*, pp. 209–214, Elsevier, 2015, Vol. 37, (ISBN: 978-0-444-63429-0)

[100] McAllister, S.; Chen, J.-Y.; Fernandez-Pello, A.C.: *Fundamentals of combustion processes*; Springer, New York, 2011, Mechanical engineering series, (ISBN: 978-1-4419-7942-1)

[101] Hurt, R.H.; Calo, J.M.: Semi-global intrinsic kinetics for char combustion modeling; *Combustion and Flame*, vol. 125 (2001), no. 3, pp. 1138–1149, (doi:10.1016/S0010-2180(01)00234-6)

[102] Haseli, Y.; van Oijen, J.A.; de Goey, L.P.H.: A detailed one-dimensional model of combustion of a woody biomass particle; *Bioresource Technology*, vol. 102 (2011), no. 20, pp. 9772–9782, (doi:10.1016/j.biortech.2011.07.075)

[103] Bates, R.B.; Altantzis, C.; Ghoniem, A.F.: Modeling of Biomass Char Gasification, Combustion, and Attrition Kinetics in Fluidized Beds; *Energy & Fuels*, vol. 30 (2016), no. 1, pp. 360–376, (doi:10.1021/acs.energyfuels.5b02120)

[104] SERI; Golden; Colorado.: Generator Gas – The Swedish Experience from 1939-1945; Solar Energy Research Institute (SERI), 1979

[105] Wünning, J.: Flameless oxidation to reduce thermal No-formation; *Progress in Energy and Combustion Science*, vol. 23 (1997), no. 1, pp. 81–94, (doi:10.1016/S0360-1285(97)00006-3)

[106] *Aspen Plus, Getting Started Modeling Processes with Solids*; April 2016, (http://docs.chejunkie.com/wp-content/uploads/sites/2/2014/11/AspenPlusSolidsV8_4-Start.pdf)

[107] User Manual for PLC Programming with CoDeSys 2.3; 3S - Smart Software Solutions GmbH, 2010

[108] VDI-Gesellschaft Verfahrenstechnik und Chemieingenieurwesen, (ed.): *VDI heat atlas*; Springer, Berlin ; New York, 2010, 2nd ed, VDI-buch, (ISBN: 978-3-540-77876-9)

[109] Incropera, F.P., (ed.): *Fundamentals of heat and mass transfer*; John Wiley, Hoboken, NJ, 2007, 6th ed, (ISBN: 978-0-471-45728-2)

[110] Reader-Harris, M.: Orifice Design; *Orifice Plates and Venturi Tubes*, pp. 33–76, Springer International Publishing, Cham, 2015, (ISBN: 978-3-319-16879-1)

[111] *https://neutrium.net/fluid_flow/discharge-coefficient-for-nozzles-and-orifices/*; August 2016

[112] Bergman, P.; Kiel, J.: Torrefaction for Biomass Upgrading; 14th European Biomass Conference & Exhibition, Paris, France, 2005

[113] Bendapudi, S.; Braun, J.E.; Eckhard, G.: Dynamic Modeling of Shell-and-Tube Heat Exchangers: Moving Boundary vs. Finite Volume; International Refrigeration and Air conditioning Conference, p. 649, Purdue, 2004

[114] International Conference on Computer and Communication Devices; Yang, L., (eds.): *Proceedings of 2011 International Conference on Computer and Communication Devices, 1-3 April, 2011, Bali Island, Indonesia (ICCCD 2011)*; Institute of Electrical and Electronics Engineers, Danver, MA, 2011, (ISBN: 978-1-4244-9829-1)

[115] Bagui, F.; Chafouk, H.: Transient heat transfert in coflow heat exchanger; *Heat and Mass Transfer*, vol. 42 (2006), no. 9, pp. 835–841, (doi:10.1007/s00231-005-0049-7)

[116] J. Bunce, D.: The Transient Response of Heat Exchangers; Master thesis. Rochester Institute of Technology, 1995

[117] Romie, F.E.: Transient Response of the Counterflow Heat Exchanger; *Journal of Heat Transfer*, vol. 106 (1984), no. 3, p. 620, (doi:10.1115/1.3246725)

[118] Burke, R.D. et al.: Heat transfer in turbocharger turbines under steady, pulsating and transient conditions; *International Journal of Heat and Fluid Flow*, vol. 52 (2015), pp. 185–197, (doi:10.1016/j.ijheatfluidflow.2015.01.004)

[119] Duan, J. et al.: Nonlinear modeling of regenerative cycle micro gas turbine; *Energy*, vol. 91 (2015), pp. 168–175, (doi:10.1016/j.energy.2015.07.134)

[120] Aaslid, P.: Modeling of variable speed centrifugal compressors for anti-surge control; Norwegian University of Science and Technology. Thesis, 2009

[121] van Helvoirt, J.; de Jager, B.: Dynamic model including piping acoustics of a centrifugal compression system; *Journal of Sound and Vibration*, vol. 302 (2007), no. 1–2, pp. 361–378, (doi:10.1016/j.jsv.2006.12.003)

[122] Dominic, S.; Maier, U.: Dynamic Modeling and Simulation of Compressor Trains for an Air Seperation Unit; The International Federation of Automatic Control, South Africa, 2014

[123] Shahin, I. et al.: Large eddy simulation of surge inception and active surge control in a high speed centrifugal compressor with a vaned diffuser; *Applied Mathematical Modelling*, vol. (2016), , (doi:10.1016/j.apm.2016.07.030)

[124] Link, R.; Deschamps, C.J.: Numerical modeling of startup and shutdown transients in reciprocating compressors; *International Journal of Refrigeration*, vol. 34 (2011), no. 6, pp. 1398–1414, (doi:10.1016/j.ijrefrig.2011.04.005)

[125] Moore, J.J. et al.: Transient Surge Measurements of a Centrifugal Compressor Station During Emergency Shutdouns; Proceedings of the Thirty-eighth Turbomachinery Symposium, 2009

[126] Filho, F. et al.: Dynamic Modeling Nonlinear and Control System for a Turboshaft; 12th Pan-American Congress of Applied Mechanics, Port of Spain, Trinidad, 2012

[127] Bettocchi, R.; Spina, P.R.; Fabbri, F.: Dynamic Modeling of Single-Shaft Industrial Gas Turbine; p. V004T11A007, 1996, (ISBN: 978-0-7918-7875-0)

[128] Ogata, K.: *Modern control engineering*; Prentice-Hall, Boston, 2010, 5th ed, Prentice-Hall electrical engineering series. Instrumentation and controls series, (ISBN: 978-0-13-615673-4)

[129] Irbid District Electricity Company: *Annual Report*; 2015

[130] Ilett, T.; Lawn, C.J.: Thermodynamic and economic analysis of advanced and externally fired gas turbine cycles; *Proceedings of the Institution of Mechanical Engineers, Part A: Journal of Power and Energy*, vol. 224 (2010), no. 7, pp. 901–915, (doi:10.1243/09576509JPE967)

[131] Cordiner, S.; Mulone, V.: Experimental–numerical analysis of a biomass fueled microgeneration power-plant based on microturbine; *Applied Thermal Engineering*, vol. 71 (2014), no. 2, pp. 905–912, (doi:10.1016/j.applthermaleng.2014.02.015)

[132] Jenkins, B.M.: A comment on the optimal sizing of a biomass utilization facility under constant and variable cost scaling; *Biomass and Bioenergy*, vol. 13 (1997), no. 1–2, pp. 1–9, (doi:10.1016/S0961-9534(97)00085-8)

Thesen

1- A modern micro scale externally fired gas turbine technology is discussed for electrical power production. This concept concentrates on processing solid biomass residues for energy utilization. This step becomes in the envelope of improving renewables investigation. The designed plant is capable to provide 15 kW$_{th}$ based on biomass pellets combustion, this size superficially discussed in literature.

2- Gas turbine cycle follows the Brayton concept. The experimental part consists of pellets combustion burner as the heat source in gas turbine cycle. On the other hand, the rest of cycle components are modeled as real time simulation, this concept is described by hardware in the loop integration. Hardware in the loop can simulate the real components, and does the control process as well. This integration provided more flexibility in components parameters optimization. Also costly and technically effective for discussing the externally fired cycle with relatively accurate results.

3- The cycle is modeled for declaring the initial results, then, pressure and air mass flow are mapped as a function of the turbine inlet temperature. The procedure in mapping is by variating pressure from 1.4 – 8 bar, and air mass flow from 0.001 – 0.045 kg/s. the produced matrix includes both parameters optimum values at each turbine inlet temperature. This mapping is performed for both 50 and 100 % input power values, also for different heat exchanger difference values. It is seen that pressure map depends on only the turbine inlet temperature in a linear line. On the other hand, air mass flow is exponentially varied with turbine inlet temperature, the exponential line should also multiplied by a factor for different thermal power ranges.

4- Modeling methodology handled components main parameters like compressor and turbine efficiencies, heat exchanger thermal transfer and terminals temperatures, pressure drop, and rotational speed as well as rotor diameter. In addition to temperatures and power analysis.

5- Electrical power produced is highly dependable on the combustion temperature. It is possible to reach more than 2 kW$_{el}$ at 1500 K. The heat exchanger difference has influence on the electrical power at low temperatures, however, this influence decreases with high temperature values.

6- The produced electrical power is around 1.4 kW at 950 K turbine inlet temperature. Pressure and air mass flow are adjusted to 3.4 and 0.021 kg/s respectively. The electrical efficiency is 10 % at the previous conditions. Efficiency can be improved by decreasing the heat exchanger difference and the combustion temperature as well. Both values are linked to burner design and the materials ability of high temperatures firmness.

7- The dynamic model of both compressor and turbine is adjusted to work 0.81 polytropic efficiency. At 3.5 bar, compressor and turbine isentropic efficiencies are 0.78 and 0.83 respectively in the steady state. Higher devices efficiencies improve the electrical efficiency, it also can compensate the low combustion temperatures.

8- The heat exchanger temperature difference is tested for flue gas temperature values in the range of 930-960 K. It is seen that for 50 K, 100 K, 150 K, and 200 K the achieved electrical power is 1.25 kW, 1.5 kW, 0.9 kW, and 0.8 kW respectively. This clearly shows the rule of the heat exchanger on the total electrical generation, also shows the effect of accumulated dirt's with time.

9- Thermal heat transferred through the heat exchanger is calculated to be around 10 kW. Referring to the 15 kW$_{th}$ entered the cycle, the heat exchanger efficiency is about 66 % for the reference case. In order to have electrical power production, it is necessary to guarantee heat of more than 4.5 kW$_{th}$ to be transferred through the heat exchanger, meanwhile.

10- Compressor consumes 3.3 kW$_m$ for the reference case, which is necessary to increase the pressure to 3.4 bar. Air temperature after compression is between 450-460 K. On the other hand, turbine delivers 4.9 kW$_m$, the hot air leaves with a temperature of 750 K. The waste heat from the turbine can be exploited in further cycle for efficiency improvement.

11- The initial start of the plant requires around 30 min. This time is necessary to heat up all components for the steady state. The response to load variations is relatively slow, for example, the plant needs around 6 min to go from the minimum to maximum electrical power value. The slow behavior is proved to be due to the combustion process itself. All cycle components have faster response to transient cases than combustion, so it is assumed that the combustion process is the dominant one in the transient states.

12- Combustion is performed at under pressure around 16 Pa for all pellets types. It is seen that the resulting electrical power of straw is 0.9-1 kW at lower than 800 K turbine inlet temperature. This means an electrical efficiency of 6.7 %. Torrefied pellets can provide around $1.1 \, kW_{el}$ at around 850 K flame temperature. The reason of having lower electrical power from torrefied than wood is that volatile matter content in torrefied pellets is lower. This affects the flame length from the burner tube, which is in turn affects the entered flue gas temperature.

13- Based on oxygen content in the flue gas of 11-12.5 %, wood combustion emits higher CO in the flue gas compared to than straw and torrefied pellets. It is seen that NO_x is the lowest when wood is combusted. While straw combustion has relatively high NO_x emissions. CO_2 emissions are between 6-8 % of the volume of the flue gas for all fuel types.

14- It is seen that the rotational speed is calculated to be more than 155 thousand rpm as expected from literature, which is relatively high compared with other plants with higher thermal power range. This value could be reduced by increasing the turbine diameter or using a gear box, both solutions have constraints of pressure loss and vibration respectively.

15- Plant capital cost could be relatively higher than other renewables investigation, however, it is considered a reliable source due to the storage ability of the raw material. For instance, pelletizing is a good method of shaping and storing, torrefaction of biomass is further improvement on pellets properties. Currently, pellets are used in a commercial form for heating purposes.

7 Appendix

7.1 Compressor modeling in Codesys
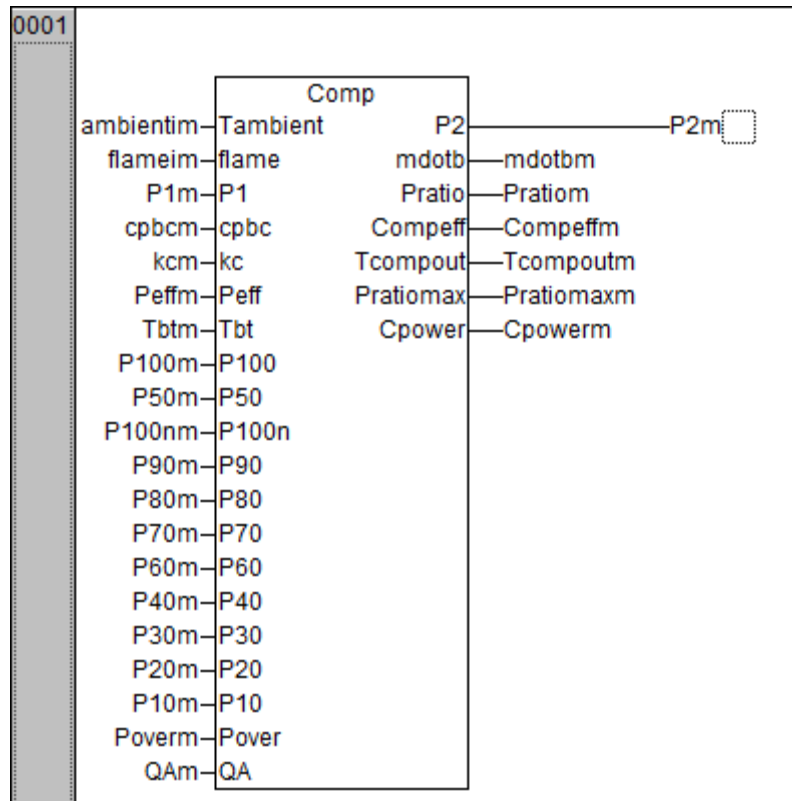
Figure 7-1. Compressor model block in Codesys

```
IF Peff > 0.8 AND Peff < 0.82 THEN
P2:=0.0057*Tbt - 1.8794;  (*f0 instead of Tbt*)
ELSIF Peff > 0.84 AND Peff < 0.86 THEN
P2:=0.0083*Tbt - 3.2163;
END_IF
(*-------------for the mass flow --------------*)
(*IF P100 = TRUE OR P100n = TRUE THEN*)    (* mass flow at 100 %
operation*)
f1:=EXP(-0.005971*Tbt);
f2:=EXP(-0.0009077*Tbt);
mdotb:=(0.7999*f1+0.04153*f2)*(QA/10);
(*------------------------------------*)
kf:=(kc-1)/kc;      (*  the formula to calculate the air constant at
the compressor side*)
kf1:=kf/Peff;        (* the formula to give the second exponential
in compressor efficiency calculation where Peff is the polytropic
efficiency*)

Pratio:=P2/P1;
```

```
Compeff:=(EXPT(Pratio,kf)-1)/(EXPT(Pratio,kf1)-1);

Cpower:=(1/Compeff)*mdotb*(cpbc*Tambient)*(EXPT(Pratio,kf)-1);
(*cpbc is the specific heat of the air on the compressor side*)

form1:=EXPT(Pratio,kf)-1;

form2:=Tambient*(1/Compeff)*form1;

Tcompout:=Tambient+form2;
```

7.2 Control Modeling in Codesys

```
(*to generate a signal at the end of 2m40s *)

IF ot6=TRUE THEN tperiod :=t6;

ELSIF ot8=TRUE THEN tperiod:= t8;

ELSIF ot12=TRUE THEN tperiod:=t12;

ELSIF ot14=TRUE THEN tperiod:=t14;

ELSIF ot16=TRUE THEN tperiod:=t16;

ELSIF ot10=TRUE THEN tperiod:=t10;

ELSIF ot18=TRUE THEN tperiod:=t18;

ELSIF ot20=TRUE THEN tperiod:=t20;

ELSIF ot22=TRUE THEN tperiod:=t222;

ELSIF ot24=TRUE THEN tperiod:=t24;

ELSIF ot26=TRUE THEN tperiod:=t26;

END_IF

tperiod1:= TIME_TO_REAL (tperiod);

IF tperiod1 >156000 AND tperiod1 <=156010 THEN

Yzadd:=Yzad;

picvalue:=TRUE;

ELSE

picvalue := FALSE;

END_IF
```

```
(*normal control*)

Dy:=10* (Yzadd-Y)/Yzadd; (*generate error signal from 0-10*)

IF Dy>=1 AND Dy<=2 THEN

step:=1;

ELSIF Dy>2 AND Dy<=3 THEN

step := 2;

ELSIF Dy>3 AND Dy<=4 THEN

step:=3;

ELSIF Dy>4 AND Dy<=5 THEN

step:=4;

ELSIF Dy>5 AND Dy<=6 THEN

step:=5;

ELSIF Dy>6 AND Dy<=10 THEN

step:=6;

ELSIF Dy<=-1 AND Dy>=-2 THEN

step := -1;

ELSIF Dy<-2 AND Dy>=-3 THEN

step:=-2;

ELSIF Dy<-3 AND Dy>= -10 THEN

step:=-3;

ELSIF Dy<-3 AND Dy>= -4 THEN

step:=-4;

ELSIF Dy<-4 AND Dy>= -5 THEN

step:=-5;

ELSIF Dy<-5 AND Dy>= -10 THEN

step:=-6;

ELSIF Dy>-1 AND Dy < 1THEN

step :=0;

END_IF
```

```
IF step <> 0 AND picvalue = TRUE THEN

U := Uold+ step;

Uold := U;

IF Uold>=11 THEN Uold :=11;

END_IF

IF Uold<= 0 THEN Uold := 0;

END_IF

END_IF

(*limitation on U*)

IF U> 11 THEN

U:=11;

ELSIF U<1

THEN U:=1;

END_IF

(*--------------------*)

(*this condition is for the starting period*)

IF Trs = TRUE THEN

(*control the power depending on the controller output*)

Pover := FALSE;

P100:=FALSE;

P90:=FALSE;

P80:=FALSE;

P70:=FALSE;

P60:=FALSE;

P50:=FALSE;

P40:=FALSE;

P30:=FALSE;

P20:=FALSE;

P10:=FALSE;

ELSE
```

```
(*over selection*)

IF U >10.5  THEN

 Pover := TRUE;

P100:=FALSE;

P90:=FALSE;

P80:=FALSE;

P70:=FALSE;

P60:=FALSE;

P50:=FALSE;

P40:=FALSE;

P30:=FALSE;

P20:=FALSE;

P10:=FALSE;

(*100 selection*)

ELSIF U >9.5 AND U<= 10.5 THEN

Pover := FALSE;

P100:=TRUE;

P90:=FALSE;

P80:=FALSE;

P70:=FALSE;

P60:=FALSE;

P50:=FALSE;

P40:=FALSE;

P30:=FALSE;

P20:=FALSE;

P10:=FALSE;

(*90% selection*)

ELSIF U >8.5 AND U<= 9.5 THEN

Pover := FALSE;

P100:=FALSE;
```

```
P90:=TRUE;

P80:=FALSE;

P70:=FALSE;

P60:=FALSE;

P50:=FALSE;

P40:=FALSE;

P30:=FALSE;

P20:=FALSE;

P10:=FALSE;

(*80% selection*)

ELSIF U >7.5 AND U<= 8.5 THEN

Pover := FALSE;

P100:=FALSE;

P90:=FALSE;

P80:=TRUE;

P70:=FALSE;

P60:=FALSE;

P50:=FALSE;

P40:=FALSE;

P30:=FALSE;

P20:=FALSE;

P10:=FALSE;

(*70 % selection*)

ELSIF U >6.5 AND U<= 7.5 THEN

Pover := FALSE;

P100:=FALSE;

P90:=FALSE;

P80:=FALSE;

P70:=TRUE;

P60:=FALSE;
```

```
P50:=FALSE;

P40:=FALSE;

P30:=FALSE;

P20:=FALSE;

P10:=FALSE;

(*60 % selection*)

ELSIF U >5.5 AND U<= 6.5 THEN

Pover := FALSE;

P100:=FALSE;

P90:=FALSE;

P80:=FALSE;

P70:=FALSE;

P60:=TRUE;

P50:=FALSE;

P40:=FALSE;

P30:=FALSE;

P20:=FALSE;

P10:=FALSE;

(*50 % selection*)

ELSIF U >4.5 AND U<= 5.5 THEN

Pover := FALSE;

P100:=FALSE;

P90:=FALSE;

P80:=FALSE;

P70:=FALSE;

P60:=FALSE;

P50:=TRUE;

P40:=FALSE;

P30:=FALSE;

P20:=FALSE;
```

```
P10:=FALSE;

(*40% selection*)

ELSIF U >3.5 AND U<= 4.5 THEN

Pover := FALSE;

P100:=FALSE;

P90:=FALSE;

P80:=FALSE;

P70:=FALSE;

P60:=FALSE;

P50:=FALSE;

P40:=TRUE;

P30:=FALSE;

P20:=FALSE;

P10:=FALSE;

(*30 %selection*)

ELSIF U >2.5 AND U<= 3.5 THEN

Pover := FALSE;

P100:=FALSE;

P90:=FALSE;

P80:=FALSE;

P70:=FALSE;

P60:=FALSE;

P50:=FALSE;

P40:=FALSE;

P30:=TRUE;

P20:=FALSE;

P10:=FALSE;

(*20 % selection*)

ELSIF U >1.5 AND U<= 2.5 THEN
```

```
Pover := FALSE;

P100:=FALSE;

P90:=FALSE;

P80:=FALSE;

P70:=FALSE;

P60:=FALSE;

P50:=FALSE;

P40:=FALSE;

P30:=FALSE;

P20:=TRUE;

P10:=FALSE;

(*10 % selection*)
ELSIF U<= 1.5 THEN

Pover := FALSE;

P100:=FALSE;

P90:=FALSE;

P80:=FALSE;

P70:=FALSE;

P60:=FALSE;

P50:=FALSE;

P40:=FALSE;

P30:=FALSE;

P20:=FALSE;

P10:=TRUE;

END_IF

END_IF
```

7.3 Pellets feed control

.(a)

(b)

115

(c)

116
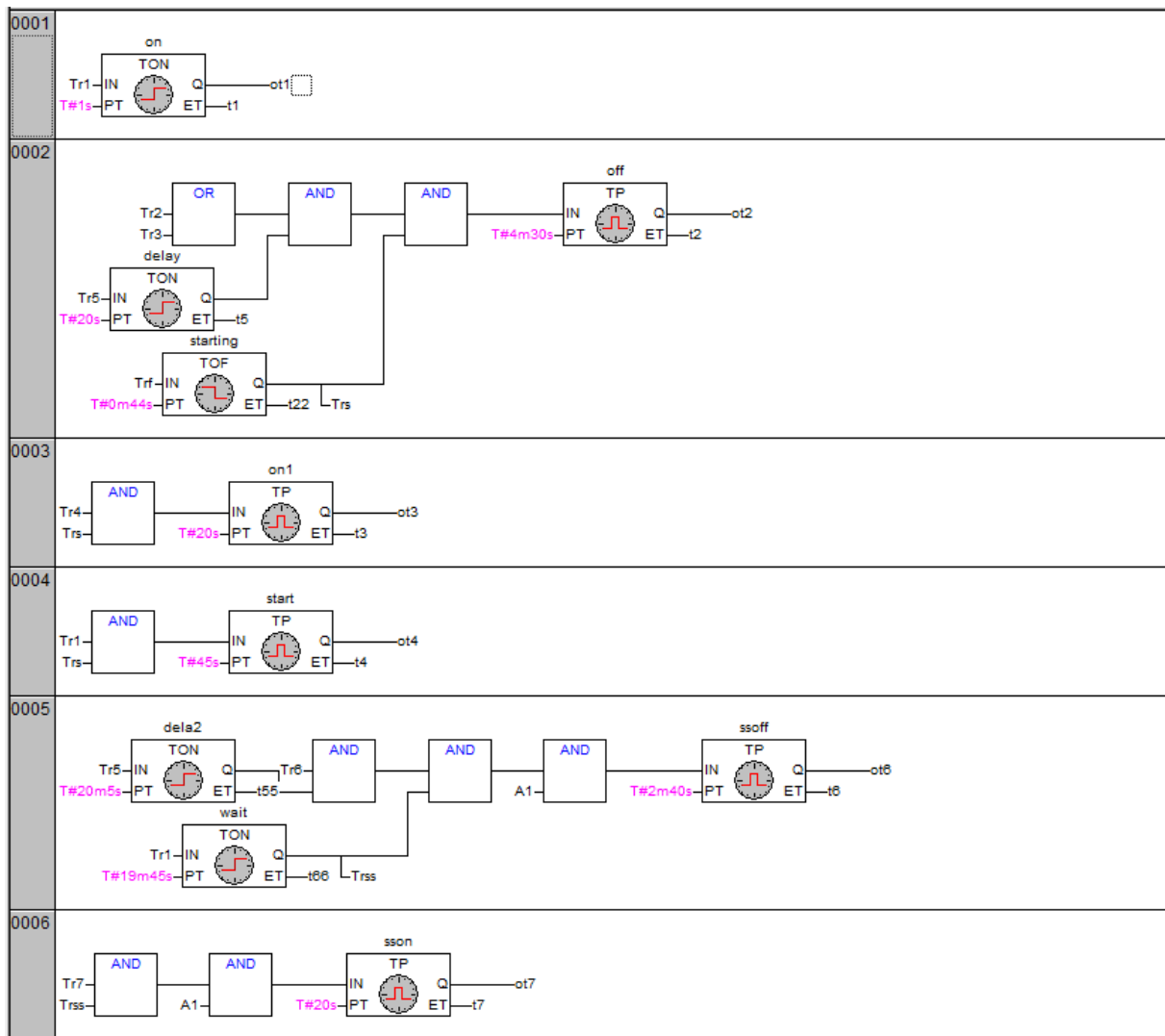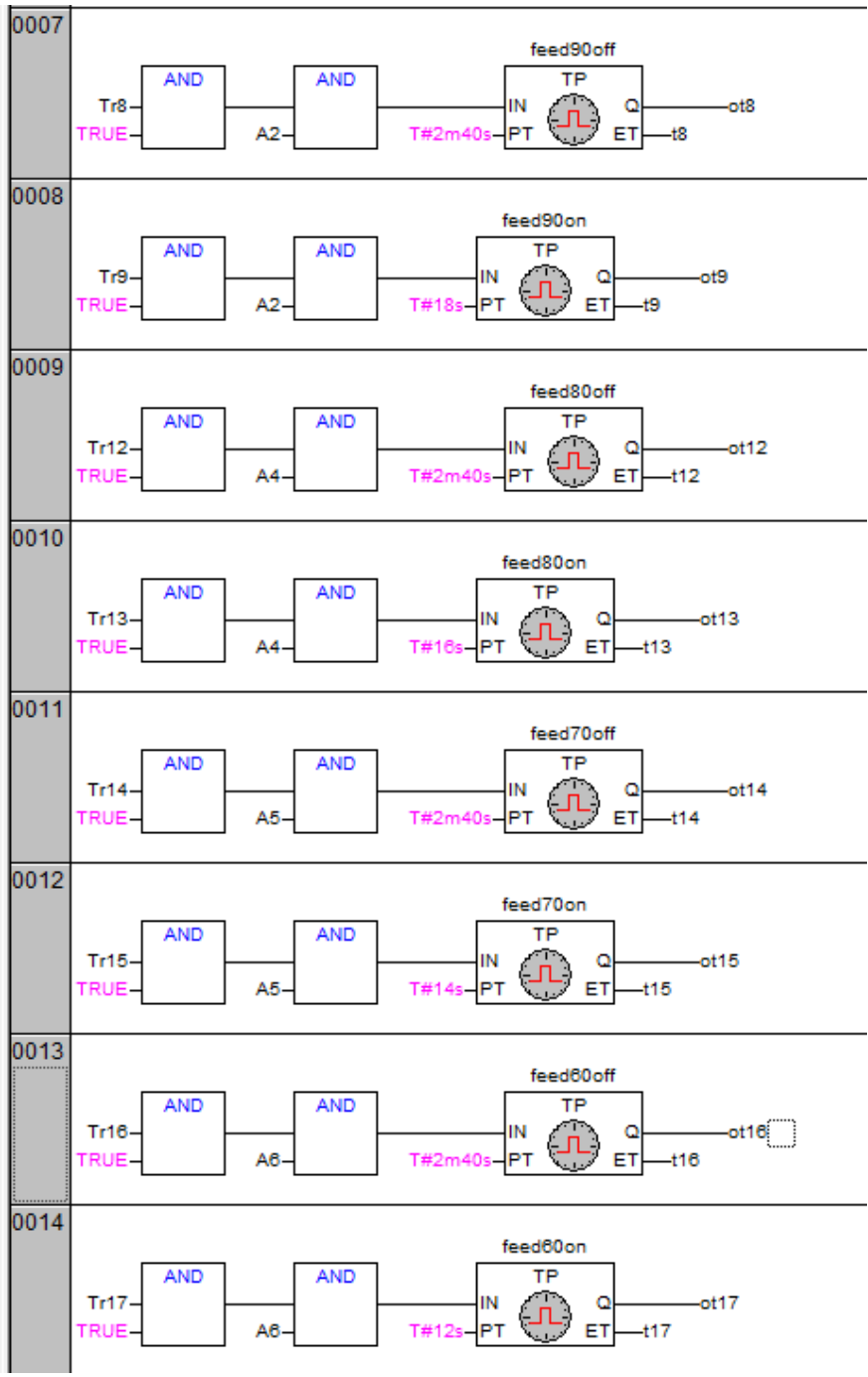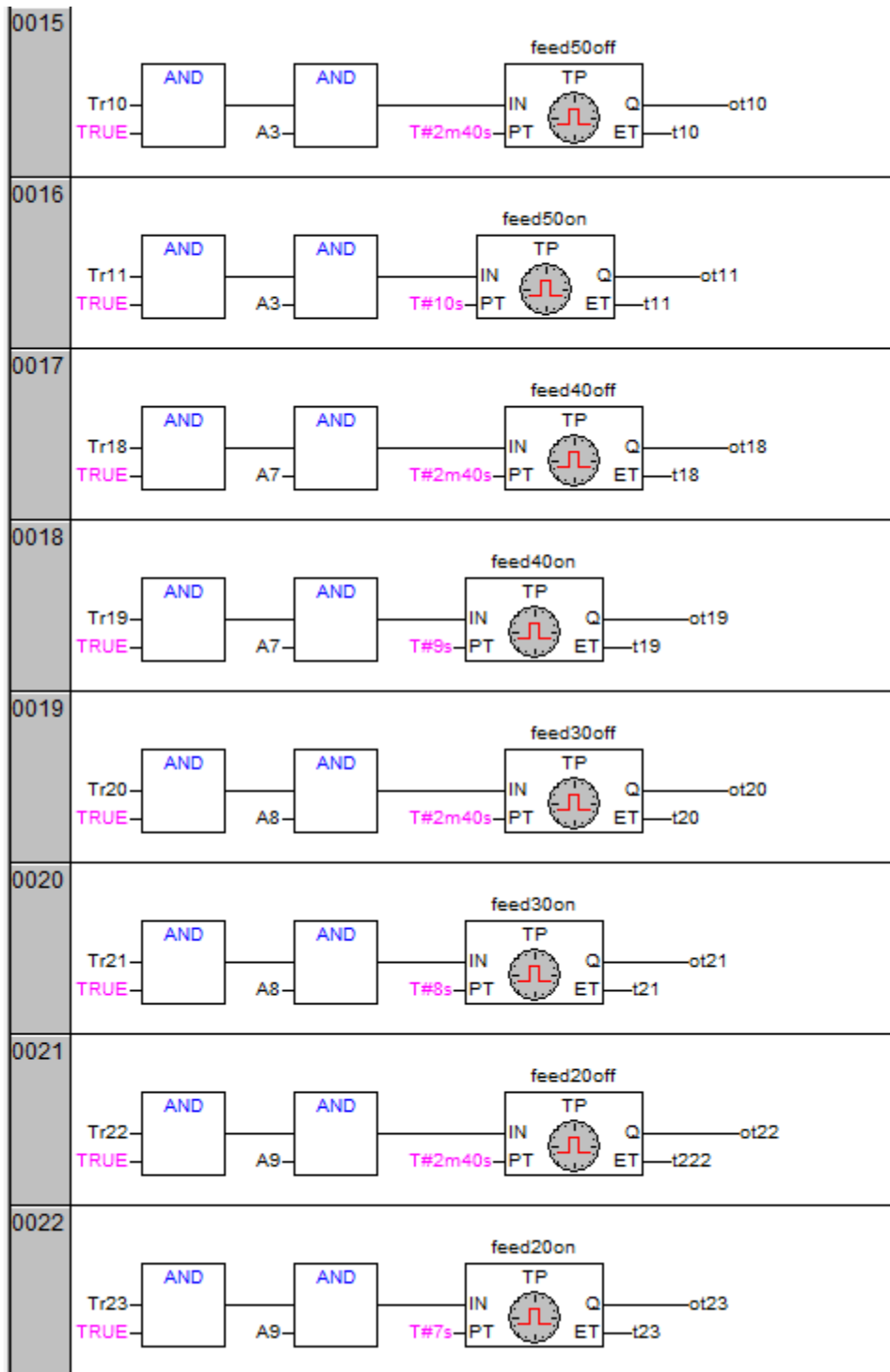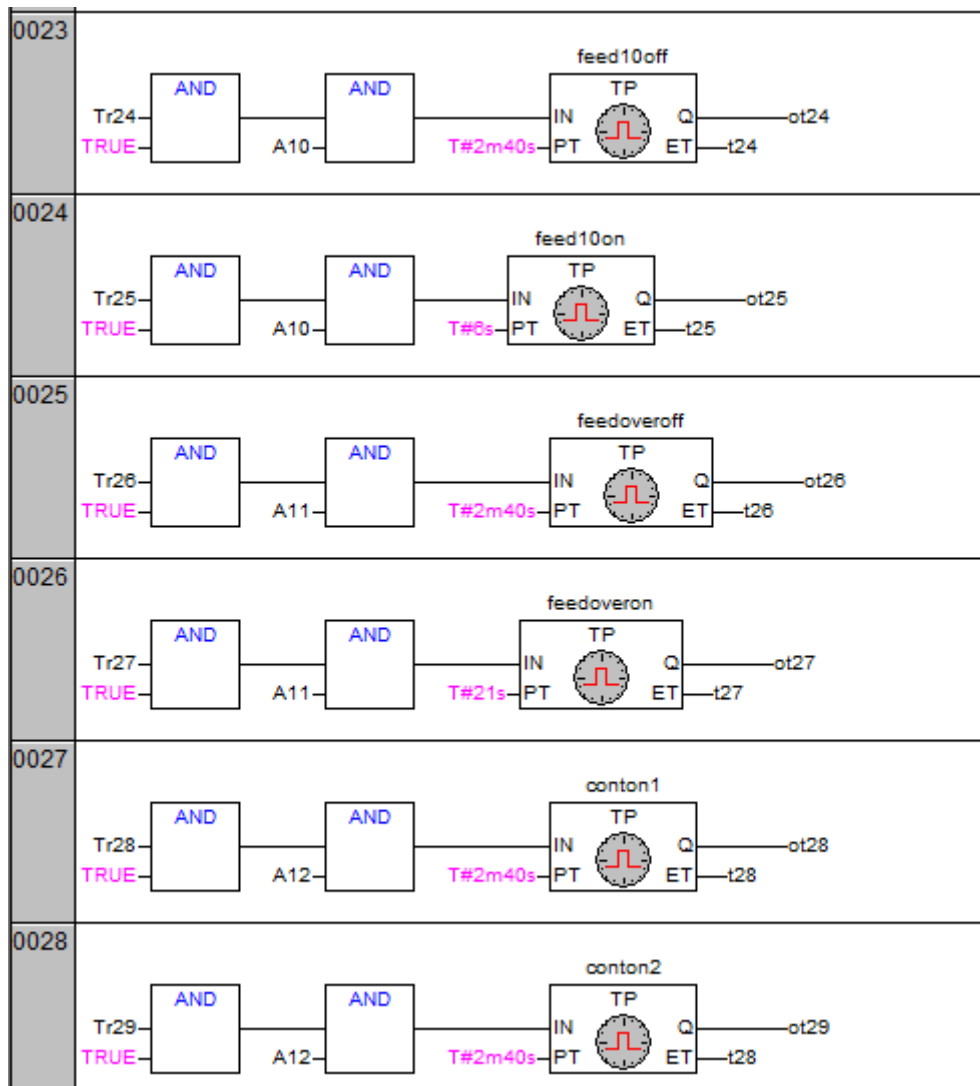
(d)

Figure 7-2. (a,b,c,d) Complete pellets control (FBD)

7.4 Heat exchanger model in Codesys
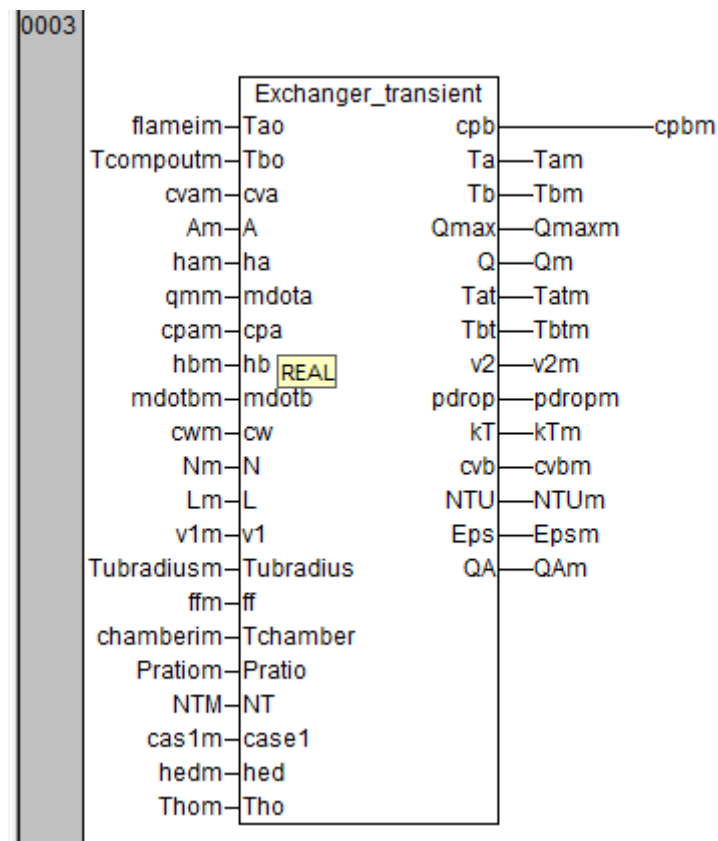
Figure 7-3. Heat exchanger model block

```
(* to calculate the cp and air constant for heat exchanger and gas
turbine (kt is output) at different temperaturs*)

Tchamber1:=Tchamber/1000;

Tchamber2:=EXPT(Tchamber1,2);

Tchamber3:=EXPT(Tchamber1,3);

cpb:=1.05-(0.365*Tchamber1)+(0.85*Tchamber2)-(0.39*Tchamber3);

cvb:=cpb-0.287;

KT:=cpb/cvb;

(*Time generation*)

b1m; (*Trigger controller*)

t:=b3m;

C:=TIME_TO_REAL(t) ;

Ci:=C;

CC:=c/1000; (* time in seconds*)
```

```
(*----------------------------------------*)
IF case1 = TRUE THEN
(*using NTU method*)
(*--------------------------------*)
Cb:=mdotb*cpb;
Ca:=mdota*cpa; (*mdota*)
IF Cb>Ca THEN
Cmax:=Cb;
Cmin:=Ca;
ELSE
Cmax:=Ca;
Cmin:=Cb;
END_IF
Cratio:=Cmin/Cmax;
Cratiow:=Cmin/cw;
NTU:=(ha*A)/(Cmin*1000);
Formula0:=EXPT(Cratio,2);
Formula00:=(1+Formula0);
Formula1:=EXPT(Formula00,0.5);
Formula11:=-1*(NTU)*Formula1;
Formula2:=1+EXP(Formula11);
Formula3:=1-EXP(Formula11);
Formula33:=Formula1*(Formula2/Formula3);
Eps1:=2*1/(1+Cratio+Formula33);
Formula4:=EXPT(((1-Eps1*Cratio)/(1-Eps1)),N);
Eps:=(Formula4-1)/(Formula4-Cratio);
Qmax:=Cmin*(Tao-Tbo);
(*Q:=Eps*Qmax;*)
f2:=mdota*cpa;
Ta:=Tao-Q/f2; (*Tao*)
```

```
f3:=mdotb*cpb;

Tb:=Tbo+Q/f3; (*Tbo*)

(*Transient operation*)

Tratio:=Tat/Ta;

IF Tratio > 1.51 OR Tratio < 0.59THEN

b1m:=TRUE;

Formula5:=L/v1;   (*L : length of the tubes , v1 velocity of fluid
a*)

Formula6:=CC-Formula5;

p1:=Formula6*Cratiow;

p2:=CC*Cratiow;

Formula7:=1/v2;

Formula8:=1/v1;

V:=(Cmin/Cw)*(Formula7+Formula8);

Formula9:=-afa*p1/(1+V);

Formula10:=-bfb*p1/(1+V);

Formula91:=Af*EXP(Formula9);

Formula101:=Bf*EXP(Formula10);

Formula92:=(1-Formula91-Formula101);

Tat:=Tao+(Ta-Tao)*Formula92;

Formula12:=-cfc*p2/(1+V);

Formula13:=-dfd*p2/(1+V);

Formula121:=Cf*EXP(Formula12);

Formula131:=Df*EXP(Formula13);

Formula122:=(1-Formula121-Formula131);

Tbt:=Tbo+(Tb-Tbo)*Formula122;

ELSE

b1m:=FALSE;

Tat:=Ta;

Tbt:=Tb;
```

```
END_IF

(*end using NTU method*)

ELSIF case1 = FALSE THEN

Ta:= Tao;

Tb:=Tbo;

Tbt:=Tao- hed;

Q:=mdotb*cpb*(Tbt- Tbo);

Eps:=0.9; (* could be changer *)

Qmax:=Q/Eps;

 form:= mdota*cpa;

Tat:=Tao - Q/form;

NTU := 00; (* changed later *)

QA:=cpa*mdota* (Tao-Tho);

END_IF

(*pressure drop*)

Tbaver:=(Tb+Tbo)/2;

Pratiopas:=Pratio*100000;

Airdensity:=(Pratiopas*28.97)/(8.31447*Tbaver); (*28.97 is the air
molicular wieght kg/kmol and 8.31447 is gas constant for all gases
Kj/kmol.k*)

drop0:=2*Tubradius;

drop1:=EXPT(drop0,2);

drop2:=Airdensity*3.14*drop1;

v2:=(4*mdotb)/(drop2);

drop3:=ff*Airdensity*EXPT(v2,2)*(L*NT);

drop4:=2*2*Tubradius;

pdrop:=((drop3)/(drop4))/100000;        (*ff       friction   factor,
2*2*Tubradius  is for diameter,  deltap in N/m2 so we divide by
100000 to get it in bar*)
```

7.5 Measured data conversions

```
(*Ambient*)

ambient;
```

```
amb:= INT_TO_REAL (ambient);

ambienti:=amb/10+273.15;

(*Flame*)

flame;

fla:=INT_TO_REAL (flame);

flamei:=  fla/10+273.15;

(*Chamber*)

chamber;

cha:=INT_TO_REAL(chamber);

chamberi:= cha/10+273.15;

(*exhaust*)

exhaust;

exh:=INT_TO_REAL(exhaust);

exhausti:=exh/10+273.15;

(*burner inside temp*)

burner1;

burn:=INT_TO_REAL(burner1);

burner:=burn/10+273.15;

(*ballance*)

pellets_kgr:=WORD_TO_REAL(ballance);

pell:=pellets_kgr/3273.282;

contwieght:=60.192*0.602-6.82222; (*0,602 is the voltage when the
container and tube are existed*)

pelletswight:=(60.192*pell-6.82222) - contwieght;

(*flew gas from exhaust*)

flewgas;

flewgas1:=WORD_TO_REAL(flewgas);

flewgas2:=flewgas1/3.27;

formula1:=(flewgas2-250)*(0.033333);

flewgas3:=formula1*1;
```

```
fluegas:=flewgas3;

cond:=20;

IF fluegas>cond OR fluegas<10 THEN

alarm1:=1;

ELSE

alarm1:=0;

END_IF

(*calculating mass flow*)

dp:=fluegas;   (*pressure difference in pa*)

(*Torfice*)

torfice;

Torf:=INT_TO_REAL(torfice);

Tor:=Torf/10+273.15;

Tho:=Tor;     (*for the exhaust temperature by using Tor*)

density:=366/Tor; (*(101000*30.13)/(8314.47*Tor)*)

formu:=2*dp*density;

fm1:=SQRT(formu);

qm:= (0.605/0.977)*1*0.7854*0.0036*fm1;(*0.6 is coefficient, 0.83666
is sqrt(1-0.3^4), 1 is epsilon, 0.7854 is pi/4, qm is kg/s*)

(*lambda calculations*)

lambda;

lambdav:=WORD_TO_REAL(lambda);

lam:=lambdav/3273.282;

o2:=2.84*lam;

IF o2 >= 15 THEN

Lambdaf := 00;

ELSE

lambdaf:=20.9/(20.9-o2);

END_IF
```

7.6 Signals provided to feeding motor code
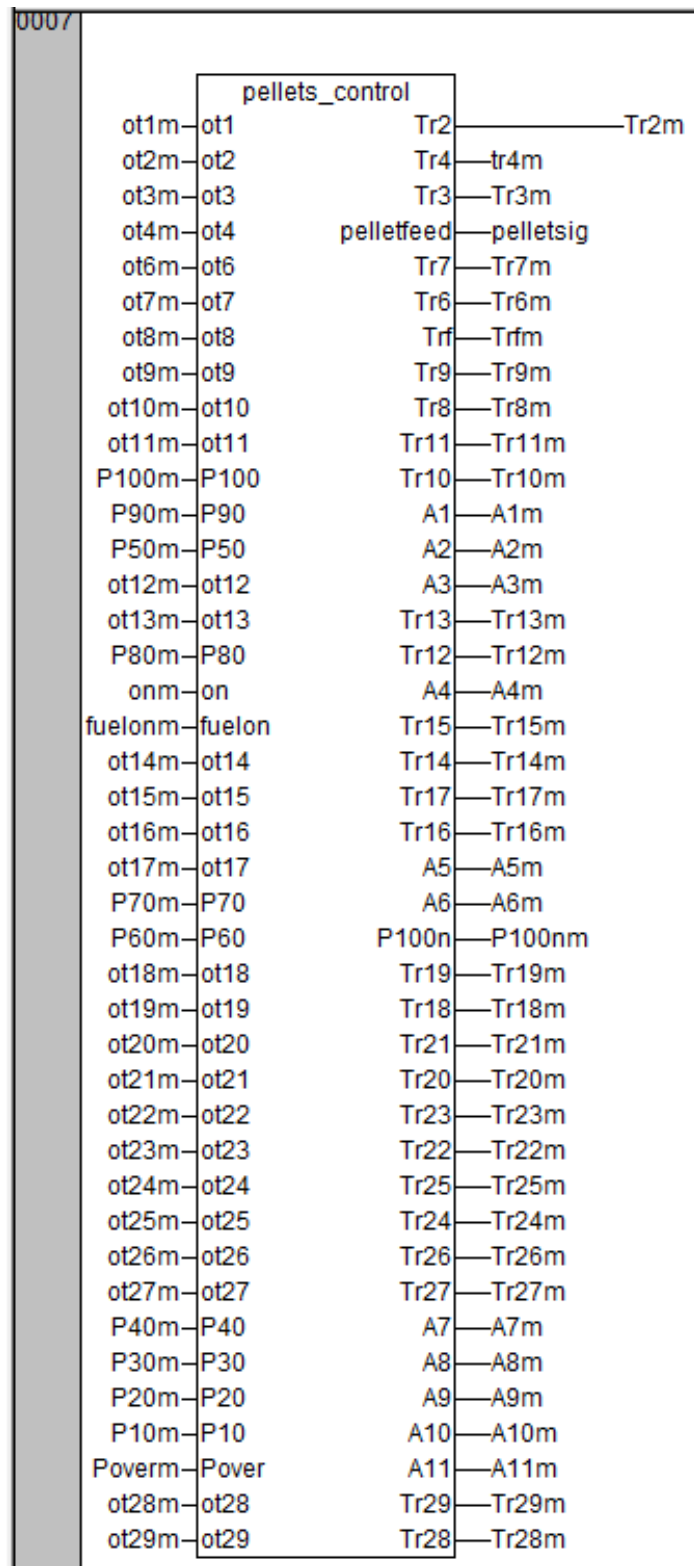
Figure 7-4. Trigger signals for the pellets feed motor

```
ot1;
```

```
IF ot1=TRUE THEN

Tr2:=FALSE;

Trf:=FALSE;

ELSE

Tr2:=TRUE;

Trf:=TRUE;

END_IF

IF ot2 = TRUE THEN

Tr4:=FALSE;

ELSE

Tr4:= TRUE;

END_IF

IF ot3=FALSE THEN

Tr3 := TRUE;

ELSE

Tr3:= FALSE;

END_IF

(*---------------   now for power control*)

(*100 % power*)

IF P100 = TRUE THEN

A1 := TRUE;

A2:= FALSE;

A3:=FALSE;

A4:=FALSE;

A5:=FALSE;

A6:=FALSE;

A7:=FALSE;

A8:=FALSE;

A9:=FALSE;

A10:=FALSE;
```

```
A11:=FALSE;

P100n:= FALSE;

IF ot6= TRUE THEN

Tr7 := FALSE;

ELSE

TR7:=TRUE;

END_IF

IF ot7 = FALSE THEN

Tr6 := TRUE;

ELSE

Tr6:= FALSE;

END_IF
(*-----------*)
(*90 % power*)
ELSIF P90= TRUE   THEN

A1:= FALSE;

A2:=TRUE;

A3:=FALSE;

A4:=FALSE;

A5:=FALSE;

A6:=FALSE;

A7:=FALSE;

A8:=FALSE;

A9:=FALSE;

A10:=FALSE;

A11:=FALSE;

P100n:= FALSE;

IF ot8= TRUE THEN

Tr9 := FALSE;

ELSE
```

```
TR9:=TRUE;

END_IF

IF ot9 = FALSE THEN

Tr8 := TRUE;

ELSE

Tr8:= FALSE;

END_IF

(*-------------*)

(*80% power*)

ELSIF P80= TRUE   THEN

A1:= FALSE;

A2:=FALSE;

A3:= FALSE;

A4:= TRUE;

A5:=FALSE;

A6:=FALSE;

A7:=FALSE;

A8:=FALSE;

A9:=FALSE;

A10:=FALSE;

A11:=FALSE;

P100n:= FALSE;

IF ot12= TRUE THEN

Tr13:= FALSE;

ELSE

Tr13:=TRUE;

END_IF

IF ot13= FALSE THEN

Tr12:= TRUE;

ELSE
```

```
Tr12:= FALSE;

END_IF

(*--------------------------*)

(*70 % power*)

ELSIF P70= TRUE   THEN

A1:= FALSE;

A2:=FALSE;

A3:= FALSE;

A4:= FALSE;

A5:=TRUE;

A6:=FALSE;

A7:=FALSE;

A8:=FALSE;

A9:=FALSE;

A10:=FALSE;

A11:=FALSE;

P100n:= FALSE;

IF ot14 = TRUE THEN

Tr15 := FALSE;

ELSE

Tr15:=TRUE;

END_IF

IF ot15= TRUE THEN

Tr14:= FALSE;

ELSE

Tr14:= TRUE;

END_IF

(*--------------------------*)

(*60 % power*)

ELSIF P60= TRUE   THEN
```

```
A1:= FALSE;

A2:=FALSE;

A3:= FALSE;

A4:= FALSE;

A5:=FALSE;

A6:=TRUE;

A7:=FALSE;

A8:=FALSE;

A9:=FALSE;

A10:=FALSE;

A11:=FALSE;

P100n:= FALSE;

IF ot16 = TRUE THEN

Tr17 := FALSE;

ELSE

Tr17:=TRUE;

END_IF

IF ot17= TRUE THEN

Tr16:= FALSE;

ELSE

Tr16:= TRUE;

END_IF

(*--*--------------------*)

(*50 % power*)

ELSIF P50 = TRUE THEN

A1:= FALSE;

A2:=FALSE;

A3:= TRUE;

A4:=FALSE;

A5:=FALSE;
```

```
A6:=FALSE;

A7:=FALSE;

A8:=FALSE;

A9:=FALSE;

A10:=FALSE;

A11:=FALSE;

P100n:= FALSE;

IF ot10 = TRUE THEN

Tr11 := FALSE;

ELSE

Tr11:=TRUE;

END_IF

IF ot11 = FALSE THEN

Tr10 := TRUE;

ELSE

Tr10:= FALSE;

END_IF

(*------------------------------*)

(*40 % power*)

ELSIF P40 = TRUE THEN

A1:= FALSE;

A2:=FALSE;

A3:= FALSE;

A4:=FALSE;

A5:=FALSE;

A6:=FALSE;

A7:=TRUE;

A8:=FALSE;

A9:=FALSE;

A10:=FALSE;
```

```
A11:=FALSE;

P100n:= FALSE;

IF ot18 = TRUE THEN

Tr19 := FALSE;

ELSE

Tr19:=TRUE;

END_IF

IF ot19= TRUE THEN

Tr18:= FALSE;

ELSE

Tr18:= TRUE;

END_IF

(*------------------------------------*)

(*30 % power*)

ELSIF P30 = TRUE THEN

A1:= FALSE;

A2:=FALSE;

A3:= FALSE;

A4:=FALSE;

A5:=FALSE;

A6:=FALSE;

A7:=FALSE;

A8:=TRUE;

A9:=FALSE;

A10:=FALSE;

A11:=FALSE;

P100n:= FALSE;

IF ot20 = TRUE THEN

Tr21 := FALSE;

ELSE
```

```
Tr21:=TRUE;

END_IF

IF ot21= TRUE THEN

Tr20:= FALSE;

ELSE

Tr20:= TRUE;

END_IF

(*-----------------------------*)

(*20 % power*)

ELSIF P20 = TRUE THEN

A1:= FALSE;

A2:=FALSE;

A3:= FALSE;

A4:=FALSE;

A5:=FALSE;

A6:=FALSE;

A7:=FALSE;

A8:=FALSE;

A9:=TRUE;

A10:=FALSE;

A11:=FALSE;

P100n:= FALSE;

IF ot22 = TRUE THEN

Tr23 := FALSE;

ELSE

Tr23:=TRUE;

END_IF

IF ot23= TRUE THEN

Tr22:= FALSE;

ELSE
```

```
Tr22:= TRUE;

END_IF

(*--------------------------------*)

(*10 % power*)

ELSIF P10 = TRUE THEN

A1:= FALSE;

A2:=FALSE;

A3:= FALSE;

A4:=FALSE;

A5:=FALSE;

A6:=FALSE;

A7:=FALSE;

A8:=FALSE;

A9:=FALSE;

A10:=TRUE;

A11:=FALSE;

P100n:= FALSE;

IF ot24 = TRUE THEN

Tr25 := FALSE;

ELSE

Tr25:=TRUE;

END_IF

IF ot25= TRUE THEN

Tr24:= FALSE;

ELSE

Tr24:= TRUE;

END_IF

(*-------------------------*)

(*over % power*)

ELSIF Pover = TRUE THEN
```

```
A1:= FALSE;

A2:=FALSE;

A3:= FALSE;

A4:=FALSE;

A5:=FALSE;

A6:=FALSE;

A7:=FALSE;

A8:=FALSE;

A9:=FALSE;

A10:=FALSE;

A11:=TRUE;

P100n:= FALSE;

IF ot26 = TRUE THEN

Tr27 := FALSE;

ELSE

Tr27:=TRUE;

END_IF

IF ot27= TRUE THEN

Tr26:= FALSE;

ELSE

Tr26:= TRUE;

END_IF

(*-----------------------*)

ELSE

P100n:= TRUE;

A1 := TRUE;

A2:= FALSE;

A3:=FALSE;

A4:=FALSE;

A5:=FALSE;
```

```
A6:=FALSE;

A7:=FALSE;

A8:=FALSE;

A9:=FALSE;

A10:=FALSE;

A11:=FALSE;

END_IF

(*pellets feed*)

IF on=TRUE THEN

     IF ot4=TRUE OR ot3=TRUE OR ot7=TRUE OR ot9=TRUE OR ot11=TRUE OR
ot13=TRUE OR ot15= TRUE OR ot17 = TRUE OR ot19 = TRUE OR ot21 = TRUE
OR ot23 = TRUE OR ot25 = TRUE OR ot27 = TRUE OR fuelon=TRUE THEN

     nr:=32500;

(*Tperiod:=TRUE;*)

   pelletfeed:=REAL_TO_WORD(nr);

    ELSE

   nr:=0;

(*Tperiod:= FALSE;*)

   pelletfeed:=REAL_TO_WORD(nr);

   END_IF

ELSE

nr:=0;

END_IF

(*for control of the periodic signal*)

IF ot28 = TRUE THEN

Tr29 := FALSE;

ELSE

Tr29:=TRUE;

END_IF

IF ot29= TRUE THEN

Tr28:= FALSE;
```

```
ELSE

Tr28:= TRUE;

END_IF
```

7.7   Turbine model in Codesys
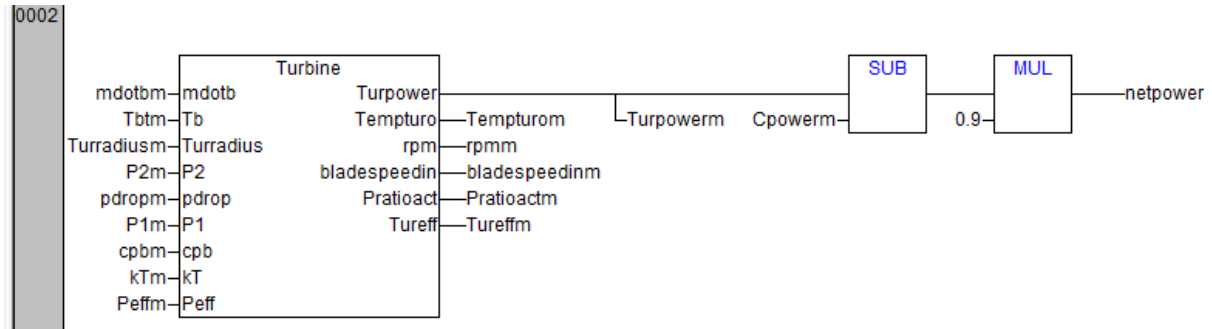
Figure 7-5. Turbine model block

```
Pratioact:=(P2-pdrop)/P1;      (*real pressure ratio after drop*)

kTf:=(kT-1)/kT;  (*k-1/k  formula  but  with  the  value  change  with
temperature from the heat exchanger*)

kTf1:=Peff*kTf;

Formula0:=1/Pratioact;

Formula1:=EXPT(Formula0,kTf1);

formula11:=(1-EXPT(Formula0,kTf));

Tureff:=(1-Formula1)/formula11;

f1:=(1-EXPT(Formula0,kTf));

Turpower:=(Tureff*mdotb*(cpb*Tb)*f1);

form1:=Tb*Tureff;

form2:=1-Formula1;

Tempturo:=Tb-form1*form2;

(*calculating rpm*)

Formula2:=(Turpower*1000)/mdotb;

Formula3:=SQRT(Formula2);

rpm:=  (Formula3/Turradius)*9.5493;         (*9.5493  is  60/2*pi,  to
convert from m/s to rpm*)

bladespeedin:=Formula3;
```

7.8   Aspen simulation

- Sensitivity tool
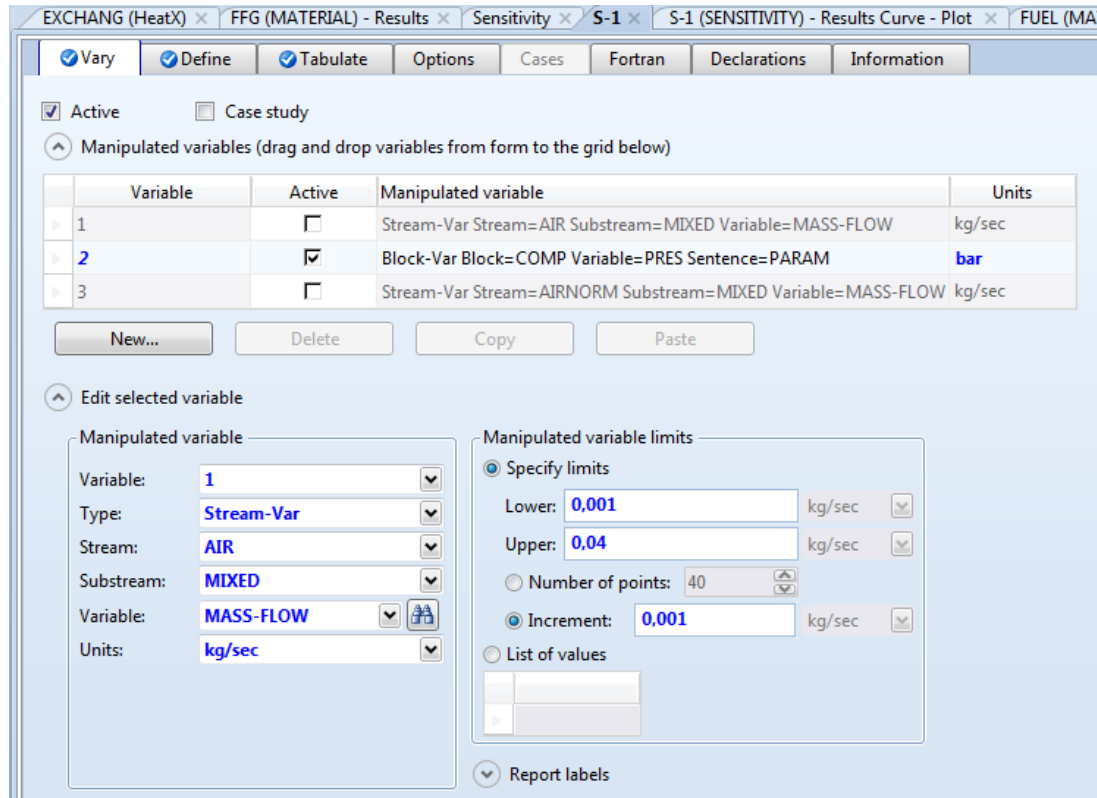
Figure 7-6. Variables to be changed settings
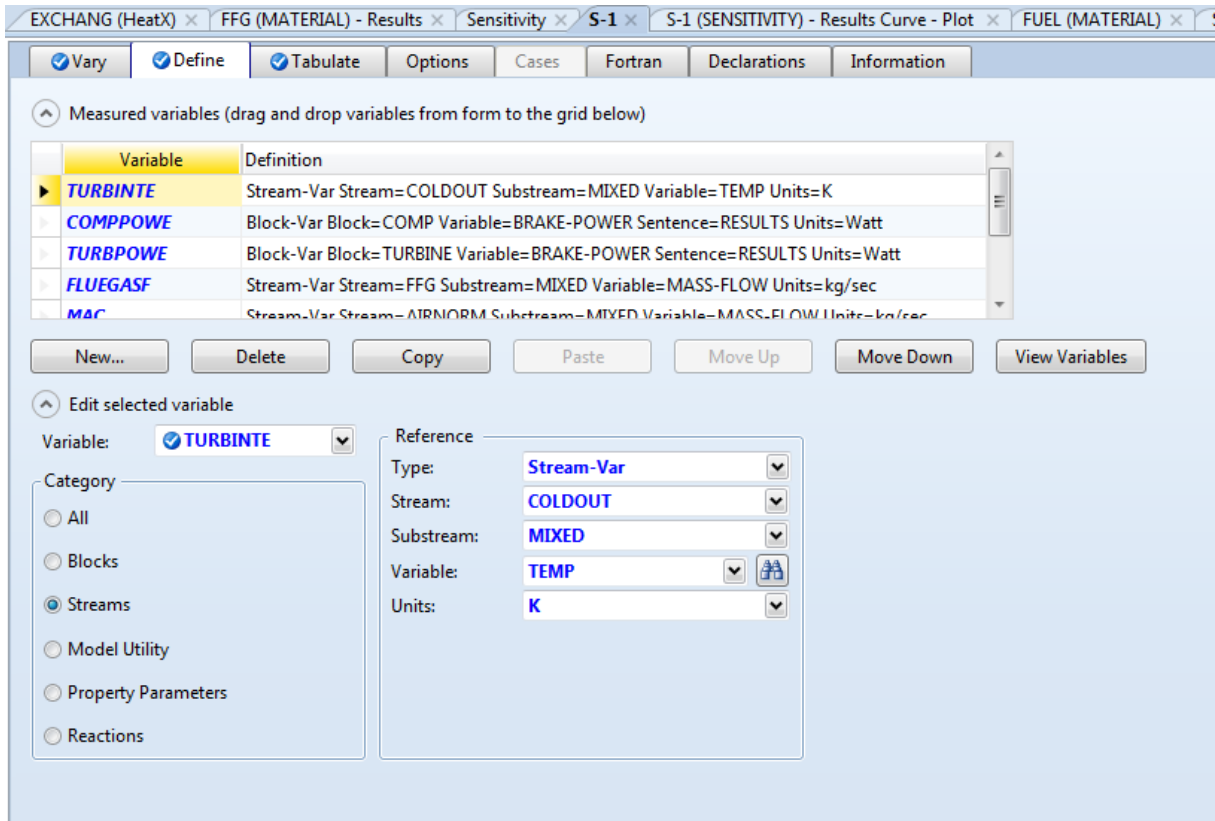
Figure 7-7. Defining the calculated variables to be presented

- Heat exchanger definition

Figure 7-8. Heat exchanger definition

- RGIBBS reactor

Figure 7-9. RGIBBS products definition

Figure 7-10. Aspen results in Excel

Air to fuel Ratio S.	6,7265		
Airnorm mass flow	0,0415		
Fuel mass flow	0,00074331		
Air to fuel Ratio	20,18000565		
Lambda	3,000075173		

Flame temp (k)	in turbine temp (K)
1088,207187	938,2071733

FFG density			Ex density			Desnsities			
mass flow (kg/s)	vol flow cum/s		mass flow (kg	vol flow cum/s		co2	h2o	o2	N2
0,0115655	0,0398209	0,290437936	0,0115655	0,0247766	0,46679125	1,842	0,804	1,331	1,165
Coldin density			cold out density						
mass flow (kg/s)	vol flow cum/s		mass flow (kg	vol flow cum/s					
0,01	0,00429057	2,330692659	0,01	0,0101519	0,98503728				

comp/value	Pin(N/sqm)	Pout(N/sqm)	Tin(K)	Tout(K)
Compressor	100000	400000	300	489,5125291
Heat Ex.Cold	400000	399953,208	489,5125291	938,2071733
Heat Ex.Hot	100000	99905,9964	1088,207187	633,2753719
Turbine	399953,208	100000	938,2071733	934,4611872

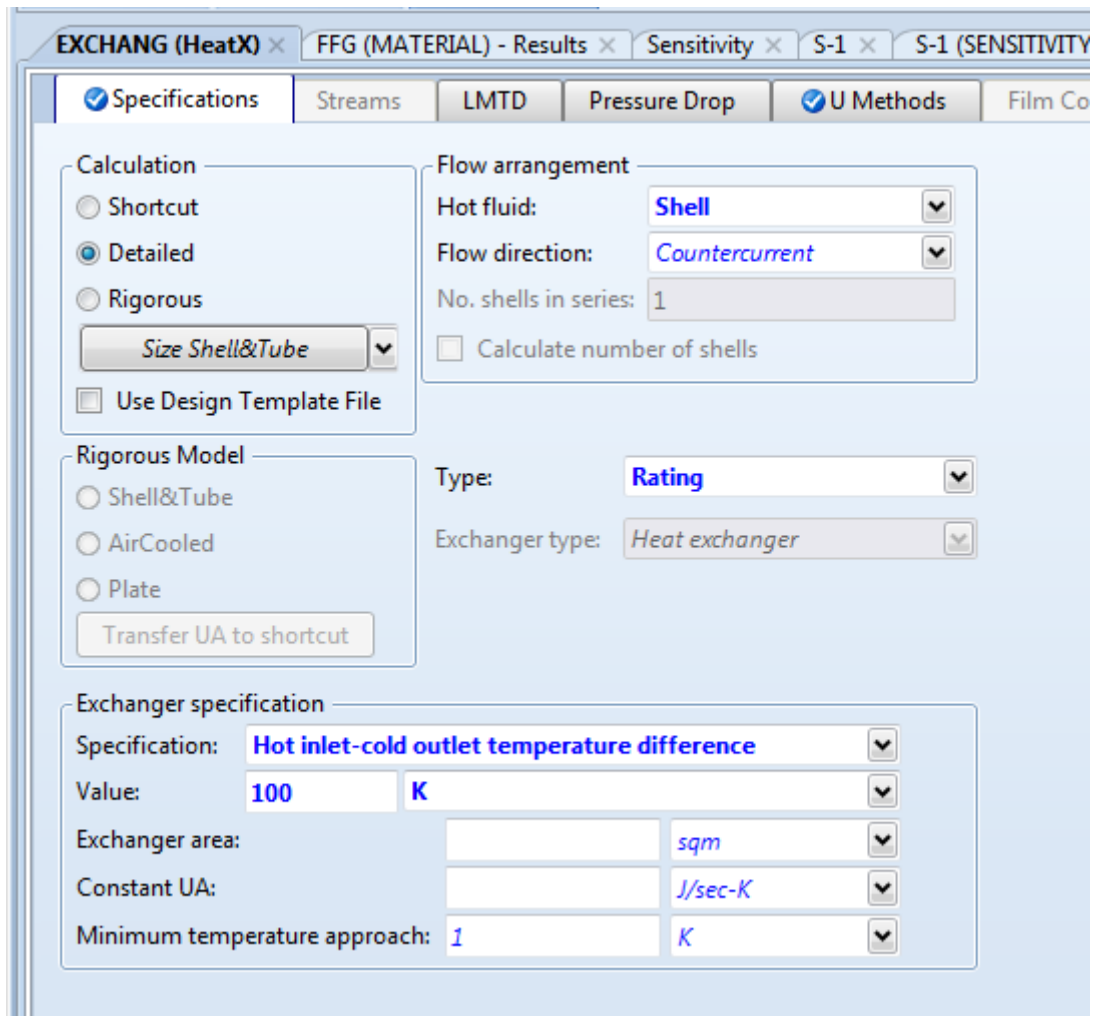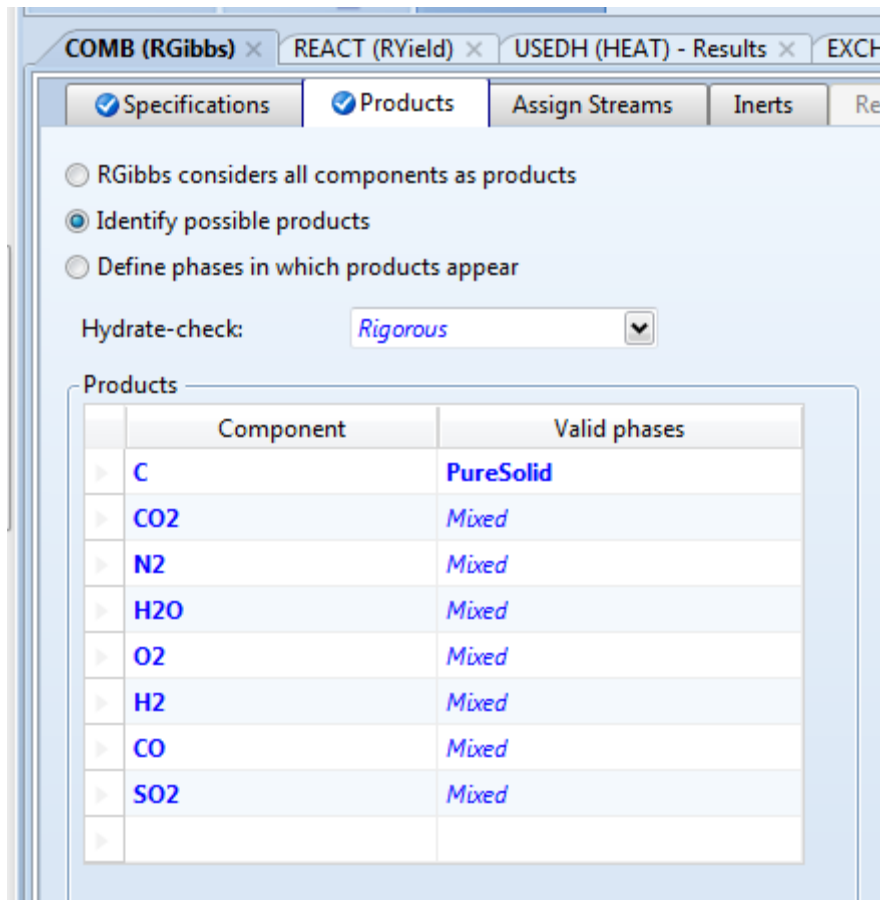| Heat Ex. Data		Hot				Cold			
		In		Out		In		Out	
Mass Flow (kg/h)	0,015706287	56,5426317			0,017	61,2	0,017	61,2	
Volume flow(m3/h)	0,015706287	194,6806003	0,015706287	121,1304456	0,017	26,2582884	0,017	62,129628	
Q flow (kW)	1E+35								
Temp (C)		815,2071874		360,2753719		216,512529		665,207173	
Pressure (bar)		1		0,999059964		4		0,99905996	
CO2 flow (m3/h)	0,001264957	2,472229428	0,001264957	2,472229428	0	0	0	0	
H2O flow (m3/h)	0,000461494	2,066391076	0,000461494	2,066391076	0	0	0	0	
O2 flow (m3/h)	0,002466156	6,670293123	0,002466156	6,670293123	0,003961	10,7134485	0,003961	10,7134485	
N2 Flow (m3/h)	0,011510626	35,56931778	0,011510626	35,56931778	0,013039	40,2921888	0,013039	40,2921888	

streams info			compositions											
streams / value	mass flow (kg/s)	press.	Stream/compo	olive	Ash	CO2	N2	H2O	O2	H2	CO	SO2	sum	
Fuel	0,00074331	100000	Fuel	1	0	0	0	0	0	0	0	0	1	
FFG	0,015706287	100000	FFG	0	0	0,08053829	0,732867466	0,029382757	0,157017102	8,53273E-12	1,29064E-10	0,00019439	1	
Air	0,017	#NAME?	Air	0	0	0	0,767	0	0,233	0	0	0	1	
Cold in	0,017	400000	Cold in	0	0	0	0,767	0	0,233	0	0	0	1	
Cold out	0,017	399953,208	Cold out	0	0	0	0,767	0	0,233	0	0	0	1	
Hot out	0,017	100000	Hot out	0	0	0,08053829	0,732867466	0,029382757	0,157017102	8,53273E-12	1,29064E-10	0,00019439	1	
Air norm	0,003495	100000	Air norm	0	0	0	0,767	0	0,233	0	0	0	1	
comp work	3287,584271													
Turb work	-4390,799573													

141

ultimate analysis	%	moles (at 1 g)	percentages refaring to total	values based on C =1	
C	0.545	0.045416667	0.353048117	1.000	n
H	0.0584	0.0584	0.453974533	1.286	m
O	0.39034	0.02439625	0.18964514	0.537	p
N	0.0058	0.000414286	0.003220465	0.009	q
S	0.00046	0.000014375	0.000111745	0.000	r
sum		0.128641577	1		

Heating	KJ/kg			
LHV	20350		λ =	2.5

Required thermal input	Kw
Po	15

Mass Flow Fuel	0.000737101	kg/s

C	H	O	N	S	O2+3.76N2	results	CO2	H2O	N2	SO2
1.0000	1.2859	0.5372	0.0091	0.0003	1.0530		1.0000	0.6429	3.9640	0.0002

Flows stoichiometry	Kg/s	g/s	mole/s					
Fuel flow	0.000737101	0.7371	0.033687542				calculating for flame temp	
C (fuel in)	0.00040172	0.4017	0.033476658				O2	1.579565367
H (fuel in)	4.30467E-05	0.0430	0.043046683				N2	9.910011992
O (fuel in)	0.00028772	0.2877	0.017982494					
N (Fuel in)	4.27518E-06	0.0043	0.00030537				fuel kj/km	924.2291667
S (fuel in)	3.39066E-07	0.0003	1.05958E-05				hfco2	-393520
O2 (from air)		1.1281	0.03525238				hfh2o	-241820
Air		4.8413	0.167868477				sum	636264.2292
N2 (from air)		3.7114	0.13254895					

Air/Fuel ratio stoich	6.568066806

O2 and air /kg fuel	kg
m O2	1.530
m Air	6.567

Total flow with λ	g/s	kg/s
Air	12.103	0.012103317
O2	2.820	0.00282019
N2 stoichiometry	3.716	0.003715646
O2 Excess	1.6921	0.001692114
N2 added with excess air	5.570	

Figure 7-11. Torrefied wood pellets Stoichiometric calculations

ultimate analysis	%	moles (at 1 g)	percentages refaring to total	values based on C =1	
C	0.525	0.04375	0.314172044	1.000	n
H	0.0702	0.0702	0.504111486	1.605	m
O	0.3939	0.02461875	0.176789098	0.563	p
N	0.0086	0.000614286	0.004411232	0.014	q
S	0.0023	0.000071875	0.00051614	0.002	r
sum	1	0.139254911	1		
Heating	KJ/kg				
LHV	20150		λ =	2	

Required thermal input	Kw
Po	15

Mass Flow Fuel	0.000744417	kg/s

C	H	O	N	S	O2+3.76N2	results	CO2	H2O	N2	SO2
1.0000	1.6046	0.5627	0.0140	0.0016	1.1206		1.0000	0.8023	4.2205	0.0008

Flows stoichiometry	Kg/s	g/s	mole/s					
Fuel flow	0.000744417	0.7444	0.032927144				calculating for flame temp	
C (fuel in)	0.000390819	0.3908	0.032568238				O2	1.120607143
H (fuel in)	5.22581E-05	0.0523	0.052258065				N2	8.441006531
O (fuel in)	0.000293226	0.2932	0.018326613					
N (Fuel in)	6.40199E-06	0.0064	0.000457285				fuel kj/km	881.5625
S (fuel in)	1.71216E-06	0.0017	5.3505E-05				hfco2	-393520
O2 (from air)		1.1679	0.0364962				hfh2o	-241820
Air		5.0121	0.17379143				sum	636221.5625
N2 (from air)		3.8423	0.137225713					

Air/Fuel ratio stoich	6.73298125

O2 and air /kg fuel	kg
m O2	1.568
m Air	6.728

Total flow with λ	g/s	kg/s
Air	10.024	0.01002429
O2	2.336	0.002335757
N2 stochiometry	3.849	0.003848722
O2 Excess	1.1679	0.001167878
N2 added with excess air	3.844	

Figure 7-12. Olive stoichiometric calculations

ultimate analysis	%	moles (at 1 g)	percentages refaring to total	values based on C =1	
C	0.512	0.042666667	0.323108695	1.000	n
H	0.0628	0.0628	0.475575611	1.472	m
O	0.42394	0.02649625	0.200652393	0.621	p
N	0.0012	8.57143E-05	0.000649102	0.002	q
S	0.00006	0.000001875	1.41991E-05	0.000	r
sum		0.132050506	1		
Heating	KJ/kg				
LHV	19060		λ =	2.5	
Required thermal input	Kw				
Po	15				
Mass Flow Fuel	0.000786988	kg/s			

C	H	O	N	S	O2+3.76N2	results	CO2	H2O	N2	SO2
1.0000	1.4719	0.6210	0.0020	0.0000	1.0575		1.0000	0.7359	3.9772	0.0000

Flows stoichiometry	Kg/s	g/s	mole/s		calculating for flame temp	
Fuel flow	0.000786988	0.7870	0.033620536			
C (fuel in)	0.000402938	0.4029	0.033578174		O2	1.586231689
H (fuel in)	4.94229E-05	0.0494	0.049422875		N2	9.942896415
O (fuel in)	0.000333636	0.3336	0.020852243			
N (Fuel in)	9.44386E-07	0.0009	6.74562E-05		fuel kj/km	813.2266667
S (fuel in)	4.72193E-08	0.0000	1.4756E-06		hfco2	-393520
O2 (from air)		1.1363	0.035508509		hfh2o	-241820
Air		4.8765	0.16908814		sum	636153.2267
N2 (from air)		3.7383	0.133511995			

Air/Fuel ratio stoich	6.196408472

O2 and air /kg fuel	kg
m O2	1.444
m Air	6.196

Total flow with λ	g/s	kg/s
Air	12.191	0.012191255
O2	2.841	0.002840681
N2 stochiometry	3.739	0.00373928
O2 Excess	1.7044	0.001704408
N2 added with excess air	5.610	

Figure 7-13. Wood stoichiometric calculations

ultimate analysis	%	moles (at 1 g)	percentages refaring to total	values based on C =1						
C	0.463	0.038583333	0.315969435	1.000	n					
H	0.0533	0.0533	0.43648823	1.381	m					
O	0.47407	0.029629375	0.242643029	0.768	p					
N	0.0074	0.000528571	0.004328616	0.014	q					
S	0.00223	6.96875E-05	0.00057069	0.002	r					
sum		0.122110967	1							
Heating	KJ/kg									
LHV	16620		λ =	2.5						
Required thermal input	Kw									
Po	15									
Mass Flow Fuel	0.000902527	kg/s								

C	H	O	N	S	O2+3.76N2	results	CO2	H2O	N2	SO2
1.0000	1.3814	0.7679	0.0137	0.0018	0.9623		1.0000	0.6907	3.6251	0.0009

Flows stoichiometry	Kg/s	g/s	mole/s							
Fuel flow	0.000902527	0.9025	0.035161104			calculating for flame temp				
C (fuel in)	0.00041787	0.4179	0.034822503			O2	1.4434402			
H (fuel in)	4.81047E-05	0.0481	0.048104693			N2	9.06268293			
O (fuel in)	0.000427861	0.4279	0.026741313							
N (Fuel in)	6.6787E-06	0.0067	0.00047705			fuel kj/km	641.255			
S (fuel in)	2.01264E-06	0.0020	6.28949E-05			hfco2	-393520			
O2 (from air)		1.0723	0.033509467			hfh2o	-241820			
Air		4.6020	0.159568891			sum	635981.255			
N2 (from air)		3.5279	0.125995596							

Air/Fuel ratio stoich	5.098979236									

O2 and air /kg fuel	kg									
m O2	1.187									
m Air	5.094									

Total flow with λ	g/s	kg/s								
Air	11.505	0.011504917								
O2	2.681	0.002680757								
N2 stochiometry	3.535	0.003534555								
O2 Excess	1.6085	0.001608454								
N2 added with excess air	5.294									

Figure 7-14. Straw stoichiometric calculations

Declaration of primary authorship

I declare, that I have written the submitted thesis for doctorate without foreign help. No other references were used except for the listed ones, and quoted results were always marked with the relevant reference. The present thesis was never submitted for examination in the present or similar version either abroad or in Germany.

Selbständigkeitserklärung

Hiermit erkläre ich, dass ich die vorliegende Dissertationsschrift selbständig und ohne fremde Hilfe erstellt habe, dass alle Hilfsmittel und sonstigen Hilfen angegeben und dass alle Stellen, die ich wörtlich oder dem Sinne nach aus anderen Veröffentlichungen entnommen habe, kenntlich gemacht worden sind. Die vorliegende Arbeit wurde in gleicher oder ähnlicher Form keiner anderen Prüfungskommission in oder außer Deutschland vorgelegt.

Leipzig, am 08.03.2017

Curriculum Vitae

Personal Data:

- Date of Birth : May 30, 1987
- Place of birth : Irbid – Jordan
- Nationality   : Jordanian
- Sex   : Male
- Marital Status : Married
- Current Address: Gerichtsweg.4, 04103, Leipzig

Current Position:

- PhD Student - Rostock University
- Guest researcher at DBFZ Deutsches Biomasseforschungszentrum gemeinnützige GmbH
- Work address: DBFZ Deutsches Biomasseforschungszentrum gemeinnützige GmbH

    Torgauer str. 116

    04347 Leipzig– Germany

    Telephone: +49-(0)341-2434-792

    Mobile: +49-176-72727914

    E-mail: Madher.bdour@gju.edu.jo

Education:

- **M.Sc.,** Electrical Power Engineering, 2012, **Yarmouk University**, Irbid, Jordan.

   Thesis topic: "Analysis of impact of large scale photovoltaic solar systems on the power quality in distribution networks".

- **B.Sc.**, Electrical Power Engineering, 2010, **Yarmouk University** , Irbid, Jordan.

- Primary Project : Rectifiers (single phase and three phase rectifiers, controlled , half controlled and fully controlled)

- Secondary Project: Speed Control of Induction Motors (Voltage and frequency controlled).

Professional Experience:

- Since April/2013 : Guest researcher at DBFZ Deutsches Biomasseforschungszentrum gemeinnützige GmbH
- June/2011 – April/2013: Research and teaching assistant at German Jordanian University.
- Sep/2010 - Jan/2011   : Research and teaching assistant at Yarmouk University.
- Oct/2009 – Dec/2009   : Training in Irbid District Electricity (IDECO).
- June/2009 – Oct/2009 : Training in National Electric Power Company (NEPCO).

Languages:

- Arabic (Native)
- English (Excellent)
- German (good)

Amman, 08.08.2017